Abteilung für Experimentelle Neurologie an der Klinik für Neurologie

der Medizinischen Fakultät Charité - Universitätsmedizin Berlin

DISSERTATION

SUMOylation is an endogenous neuroprotective mechanism in stroke

zur Erlangung des akademischen Grades

Doctor of Philosophy in Medical Neurosciences

(Ph.D in Medical Neurosciences)

im Rahmen des
International Graduate Program Medical Neurosciences

vorgelegt der Medizinischen Fakultät

Charité – Universitätsmedizin Berlin

von

Anna Lena Dätwyler

M.Sc in Biology, Neurosciences

aus Berlin, Deutschland

Gutachter:

1.: Prof. Dr. med. C. Harms

2.: Priv.-Doz. Dr. rer. nat. U. Schweizer

3.: Prof. Dr. N. Brose

Datum der Promotion: 01. 02. 2013

Acknowledgements

I would like to sincerely thank:

- my supervisors Prof. Dr. Christoph Harms and Prof. Dr. Matthias Endres for giving me the opportunity to work in their group on this exciting topic. I have learned a great deal from them and am much obliged for their support and advice.

- Prof. Dr. Ulrich Dirnagl for his precious continuous advice.

- Catherine Aubel for proofreading the manuscript.

- my collegues and friends Janet Lips, Anny Kretschmer, Nadine Weser, Dr. Gisela Lättig-Tünnemann, Denise Hübner, Sabrina Lin Lin Lee, Dr. Christian Hoffmann, Dr. Ulrike Harms, Dr. Shengbo Ji, Dr. Karen Gertz, Petra Loge, Dr. Martina Füchtemeier, Marco Foddis, Dr. Tracy Farr, Dr. Denise Harhausen, Uldus Kojasteh, Dr. Dorette Freyer, Sophie Schweizer and Ines Laginha, who at various stages have been supportive in technical and scientific matters and who made life in the lab easy and fun.

- Dr. Vincent Prinz, Susanne Müller and Dr. Mustafa Balkaya for introduction to the techniques of middle cerebral artery occlusion, magnetic resonance imaging and behavioural testing.

- Dr. Alexander Kunz for establishing the bicarotid artery occlusion model.

- the transgenic core facility of the Charité-Universitätsmedizin Berlin for embryonic stem cell culture, electroporation and blastocyst injections.

- our collaborators Prof. Dr. Wulf Paschen and Dr. Wei Yang from Duke University Medical Center in Durham, USA.

- the International Graduate Program of Medical Neurosciences of the Charité-Universitätsmedizin Berlin, Germany.

- my parents for their constant support, care and encouragement.

This list would grow much larger, if I were to include every single person who has been helpful during my Ph.D thesis project. Thanks to all of you.

Table of contents

1. Summary

The post-translational protein modification through SUMO (small ubiquitin-like modifiers) alters folding, distribution, stability, activity and function of target proteins. It has been implicated in the response to various stress conditions such as anoxic conditions, hypothermia, hypoxia, and hibernation torpor. This work shows induction of SUMO2/3ylation following ischemic stress, and evidences a causal involvement of SUMO2/3ylation in neuroprotection following neuronal ischaemic injury. Neuron-specific RNA interference directed against SUMO2/3 exacerbated loss of neuronal integrity and survival following oxygen-glucose deprivation (OGD) in embryonic neurons and glutamate excitotoxicity in adult neuronal cells. While the SUMOylation of given substrates can be specifically regulated, global levels of SUMOylation in neurons are modulated in an activity-dependent manner, potentially placing changes in protein SUMOylation central to the coordination of neuronal signalling and response to ischaemic stress. Protein synthesis is inhibited quickly after the onset of ischaemia, so stability, activity and interaction of the proteins already present at ischaemia onset are of significant importance. To unravel the neuroprotective role of SUMO2/3 *in vivo*, transgenic mice were generated as a tool for investigating inducible and cell type-specific alterations in SUMO2/3 levels in different tissues. Furthermore, specific and stringent screening for SUMO2- and SUMO3-target proteins is facilitated, and the effects on target proteins in other pathophysiological contexts can be investigated. We suggest that SUMO2/3ylation is an endogenous neuroprotective mechanism in response to ischaemic stress. Thus, enhancement of SUMOylation appears an attractive avenue for developing novel treatment strategies to reduce brain injury after cerebral ischemia. Given that currently there is no effective treatment for stroke, results of this work suggest that SUMO2/3ylation should be evaluated for potential use in clinical trials in stroke patients. Alternatively, small SENP7 inhibitors that enhance stabilization of SUMO2/3 might be promising neuroprotective drugs.

2. Introduction

2.1 Cerebral ischaemia

Stroke is the second cause of mortality worldwide after ischaemic heart disease. It is also the leading cause of disability in industrialized countries (Hoffmann, Zhu et al. 2012; Yilmaz and Reith 2012). According to the WHO, 15 million people worldwide suffer a stroke annually, 60% of those who suffer a stroke die or become dependent. The average lifespan in industrialized countries is increasing, and with age the risk for stroke becomes higher. Furthermore, recovery in motor function after stroke is more demanding in the elderly population (Merrett, Kirkland et al. 2010). Today, the only Food and Drug Administration (FDA)-approved stroke treatment is intravenous application of recombinant tissue plasminogen activator (rt-PA), which induces the thrombolysis of occluded vessels. This treatment was first described in 1995 in the NINS-study (The National Institute of Neurological Disorders and Stroke rt-PA Stroke Study Group (NINS 1995)) showing that despite a slightly increased incidence of symptomatic intracerebral hemorrhage, treatment with intravenous rt-PA within 3 h of the onset of ischaemic stroke improved clinical outcome at three months. The time window of application was extended to up to 4.5 h after acute stroke in 2008 (Hacke, Kaste et al. 2008) (ECASS III), (Wahlgren, Ahmed et al. 2008) (SITS-ISTR)). Following publication of ECASS III, there has been a significant increase in the use of tPA between 3 and 4.5 h without adverse effects for treatment of patients in the < 3 h window (Messe, Fonarow et al. 2012). More than one fourth of patients with ischaemic stroke arrive within the time window for rt-PA therapy; however, this percentage has remained unchanged over recent years (Tong, Reeves et al. 2012). Nevertheless, within this narrow time window, not only does the patient need to reach the hospital, but also a number of diagnostic procedures have to be carried out to exclude contraindications and facilitate appropriate therapeutic desicions (Yilmaz and Reith 2012). Intravenous rt-PA remains the only treatment shown in numerous studies to reduce disability 3 months after stroke with no increase in the risk of death and a relatively minor rate of symptomatic intracerebral hemorrhage complications. So far, none of the other neuroprotective interventions has exhibited a significant improvement of outcome in randomized double-blind class III trials (Hossmann 2009; Brethour, Nystrom et al. 2012). Furthermore, genetic variations and dispositions have been described that may influence response to certain

drugs, e.g. to antithrombotic drugs for stroke prevention in atrial fibrillation (FDA, 2007). Thus, to rescue neurons after an ischaemic insult and to extend the time window for treatment, research on endogenous neuroprotective systems is of high importance to better understand and be able to enhance the self-healing capacity of the body and the brain. Furthermore, given the dismal statistics and the high cost of stroke treatment, high priority should be accorded to preventive and curative strategies.

2.1.1 The pathophysiology of cerebral ischaemia

Occlusion of a brain artery results in alterations in the brain which highly depend on the severity, location and duration of the vessel occlusion. Neurons are the most sensitive brain cells and the first cell type prone to die during an ischaemic insult. Oligondendrocytes are the second cell type to die followed by astrocytes and vascular cells. The so-called core region of ischaemia is the area where blood flow acutely decreases below the threshold of energy metabolism, in this case the primary pathology is necrosis, which is irreversible. If the duration of the ischaemic insult is very short or the occlusion not complete, the status of energy failure is not reached or is reversed through reperfusion, respectively. In this case, two different types of delayed cell death may occur in the affected area, namely necrosis and apoptosis (Brainin and Heiss 2010). While reconstitution of blood flow is essential to save neurons, reperfusion on the other hand increases neuronal injury by increasing reactive oxygen species (ROS) and the inflammatory response. During the subacute and the chronic phase of cerebral ischaemia, a susceptible balance between inflammation and ROS must exist (Vangilder, Huber et al. 2012). The primary mechanism of neuron survival stems from mitochondrial function and signalling. Oxygen–glucose deprivation (OGD) and oxidative damage to mitochondria result in decreased Adenosine triphosphat (ATP) production, which contribute to the initiation of death signalling cascades. Mitochondrial signalling cascades regulating delayed ischaemic apoptosis are up regulated in the early and late phases of ischaemia (Mehta, Manhas et al. 2007).

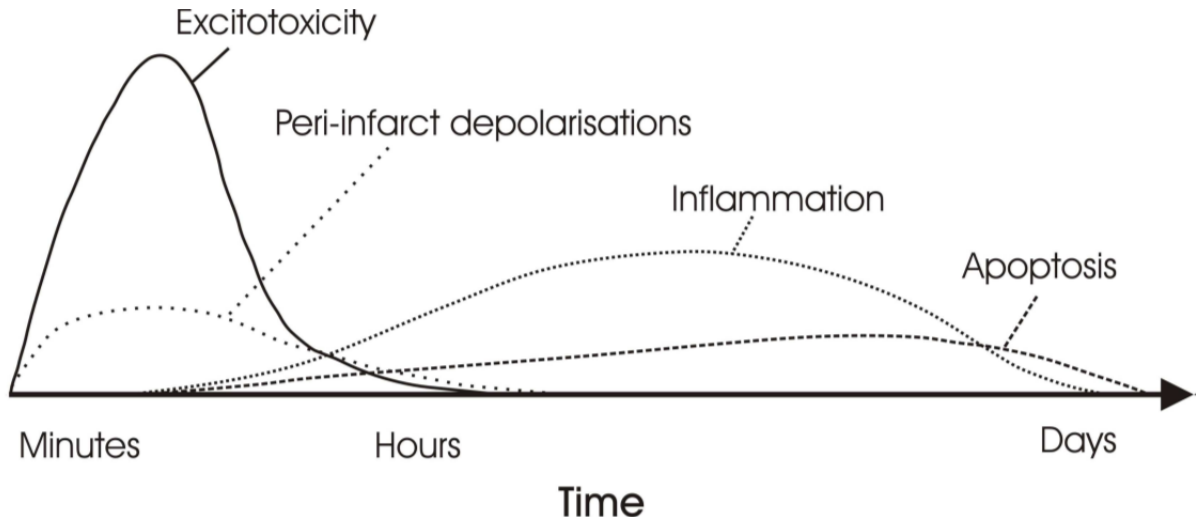

(Dirnagl, Iadecola et al. 1999)

Fig 1: Illustration of pathophysiological events after focal cerebral ischaemia. *Temporal evolution of the cascades and the impact of each pathological event on final outcome are reflected by the x- and y-axes, respectively.*

2.1.2 Primary and delayed ischaemic cell death and the penumbra concept

The first signs of cellular injury after occlusion of a brain artery are neuronal swelling or shrinkage; the cytoplasm characteristically shows microvacuolation which at the ultrastructural level has been identified mostly as swollen mitochondria, retaining their double membranes despite progressive disruption of their internal structure (McGee-Russell, Brown et al. 1970). These changes are potentially reversible if blood flow is restored through reperfusion before mitochondrial membranes begin to rupture. Oxygen–glucose deprivation (OGD) and oxidative damage to mitochondria result in decreased ATP production, which contribute to initiation of death signalling cascades. Mitochondrial signalling cascades regulating delayed ischaemic apoptosis are upregulated in the early and late phases of ischaemia (Mehta, Manhas et al. 2007). A few hours after the onset of the ischaemic insult, neurons undergo irreversible necrotic changes. In a timeframe up to 6h, acute changes take place including scalloping, shrinkage, and swelling. Delayed changes usually happen from 12 or more hours on and include eosinophilia and karyolysis (Garcia, Yoshida et al. 1993). Astrocytic responses include cytoplasmic disintegration, nuclear and cytoplasmic swelling within the first 24h after the insult and increased astrocytic glial fibrillary acidic protein

reactivity after 4 to 6 h at the interface between the lesion and the surrounding brain tissue. Delayed neuronal death includes the CA1 region of the hippocampus, the periphery of cortical infarcts, substantia nigra and thalamus. A consistent ultrastructural finding in neurons undergoing delayed cell death is disaggregation of ribosomes, which reflects the inhibition of protein synthesis at the initiation step of translation (Hossmann 1993).

Thus, upon blood flow reduction of usually more than 20%, a so called `core´ of the perfusion deficit develops. At declining flow rates, inhibition of protein synthesis occurs first (at a threshold of about 0.55 ml/gm/min), followed by a stimulation of anaerobic glycolysis (at 0.35 ml/gm/min), the release of neurotransmitters and the beginning disturbance of energy metabolism (at about 0.20 ml/min), and finally the anoxic depolarization (< 0.15 ml/gm/min, (Hossmann 1994). All this develops within minutes after the onset of ischaemia. Cells are killed rapidly by lipolysis, proteolysis, the disaggregation of microtubules that follows total bioenergetic failure and the subsequent breakdown of ion homeostasis (Dirnagl, Iadecola et al. 1999). The core region of ischaemia is irreversibly damaged very fast (5-10 min). Surrounding the core, there lies a region of silence in electrical activity, which has still preserved energy metabolism, the so called `penumbra´. The residual perfusion supplies sufficient oxygen to maintain a close to normal tissue concentration of ATP. Nevertheless, this tissue is at risk, as some degree of energy failure exists through disregulated levels of phosphocreatine, lactate, adenosine diposphat and adenosine monophosphat (Astrup et al., 1981). Without treatment, the penumbra can progress to infarction through excitotoxicity, spreading depolarizations, inflammation and apoptosis (Dirnagl, Iadecola et al. 1999). It is therefore obvious that the primary goal of neuroprotection should be to rescue the ischaemic penumbra and that the focus of further research should be on endogenous neuroprotective mechanisms and their targets for future drug development, or at least to facilitate an increase in cerebral tolerance to ischaemia for extension of the therapeutic window.

2.1.3 Models of cerebral ischaemia

According to the Framingham study, 65% of all strokes worldwide result from vascular occlusion affecting the middle cerebral artery (MCA) territory, 2% the anterior and 9% the posterior cerebral artery territories. The remaining 24% are located either in the brainstem or cerebellum or in multiple regions. In experimental stoke research, this situation is reflected in the preferential use of MCAo models (Brainin and Heiss 2010).

2.1.3.1 Animal models of focal ischaemia

Substantial research has lead to the generation of different animal models of focal cerebral ischaemia, which corresponds clinically to ischaemic stroke. A distinction is made between models of permanent and transient focal cerebral ischaemia, depending on the duration of blood-flow interruption. If cerebral blood flow (CBF) drops below 25% of normal, the probability of infarction in the target tissue area of the respective vessel is higher than 95%. This threshold has been validated in the clinics by quantitative PET- and MRI-imaging methods (Heiss, Kracht et al. 2001), and corresponds well with the data for experimental stroke (Ginsberg 2003). After the drop in CBF, depletion of oxygen and glucose in the brain as well as accumulation of toxic metabolites happens within minutes.

2.1.3.2 Transorbital middle cerebral artery occlusion

This model was first described in 1966 (Sundt and Waltz 1966) and further developed in monkeys (Hudgins and Garcia 1970). Later it was adapted for use in cats, dogs, rabbits and rats. Surgery is demanding and involves removal of the eyeball, which is invasive and may evoke functional side effects. Occlusion of the middle cerebral artery is carried out at its origin and therefore interrupts blood flow in the entire vascular territory. The basal ganglia are consistently part of the infarct core whereas the cerebral cortex exhibits a gradient of blood flow which decreases from the peripheral towards the central parts of the vascular territory (Brainin and Heiss 2010).

2.1.3.3 Transcranial middle cerebral artery occlusion

Transcranial approaches for occlusion of the middle cerebral artery are mainly used in rats and mice because in these species the main stem of the artery lies on the cortical surface close to its origin in the internal carotid artery. In these models the infarct area stretches mainly through the temporo-parietal cortex with a gradient of declining CBF from the peripheral to the central parts of the vascular territory. The basal ganglia are not affected (Brainin and Heiss 2010). Robust involvement of the frontal cortex as well as the lateral part of the neostriatum was reported, see e.g. (Tamura, Graham et al. 1981). However, in sham-operated animals, local lesions were seen at the surgical site.

2.1.3.4 Filament occlusion of the middle cerebral artery

The so called `filament model´ is currently the most widely used technique for middle cerebral artery occlusion in mice and rats. This model has the advantage of inducing reproducible transient or permanent ischaemia of the MCA territory in a relatively non-invasive manner. Intraluminal approaches interrupt the blood flow throughout the entire territory of the affected artery. Filament occlusion thus arrests flow proximal to the lenticulo-striate arteries which supply the basal ganglia. Filament occlusion of the MCA results in reproducible lesions in the cortex and striatum and can be either permanent or transient (Engel, Kolodziej et al. 2011). Using a transient 30 min-occlusion, the reproducible development of a penumbra can be achieved and methods that could rescue dying neurons of this tissue-at-risk can be investigated.

2.1.3.5 Models used in this study

In this study, the following models were used:

i*) In vitro*: Combined oxygen-glucose deprivation in dissociated embryonic primary mouse neurons.

A transient stress mimicks interruption of blood flow and supply of oxygen and glucose to primary cortical neurons, with subsequent restitution. For details see materials and methods 3.1.1.3

ii) *In vitro*: Organotypical model of adult retina and glutamate stress.

Glutamtate homeostastis is interrupted in retinal ganglion cells as an organotypical neuronal model with subsequent partial restitution. For details see materials and methods 3.2.1.1

iii) *In vivo* model: Middle cerebral artery occlusion.

Transient intraluminal filament occlusion of the middle cerebral artery in mice is applied, with development of a core and a penumbra zone within the brain. For details see materials and methods 3.3.1.2

2.2 Endogenous neuroprotection in stroke

Neurons are the most endangered cells after an ischaemic insult, and yet the hardest to rescue. Neuroprotective agents aim to rescue ischaemic tissue, limit infarct size, prolong the time window for thrombolytic therapy or minimize post-ischaemic reperfusion injury or inflammation. There are currently a number of ongoing trials for neuroprotective strategies including hypothermia, albumin, magnesium, minocycline, and statins as potential approaches to neuroprotection in the clinical setting, but the outcome of these approaches remains to be seen. There are also a number of neuroprotectants in preclinical development including haematopoietic growth factors, and inhibitors of the nicotinamide adenine dinucleotide phosphate oxidases (Sutherland, Minnerup et al. 2012). Nevertheless, criticism has been raised about the use of 'synthetic' compounds that intercept cascades of damage

in a potentially 'unphysiological' way (e.g. N-methyl-D-aspartate (NMDA)–receptor antagonists). This critique leads to further questions (Dirnagl and Meisel 2008). Exploiting endogenous neuroprotective mechanisms might overcome some of the problems encountered with conventional neuroprotection. So far, in clinical trials, drugs targeting only one key mechanism of cerebral ischaemia have failed to improve outcome. One plausible reason for this failure might be the multiplicity of mechanisms involved in causing neuronal damage following stroke. Therefore, a novel approach for the development of neuroprotective drugs includes evaluating compounds with a multimodal mode of action (Sutherland, Minnerup et al. 2012). To maximize outcome after stroke, the combined use or reperfusion and neuroprotection will likely be needed (Minnerup and Schabitz 2009; Fisher 2011). It is possible that many of the neuroprotective effects of treatment strategies observed could be due to a manifestation of physiological/pathophysiological changes following ischaemia, which means endogenous neuroprotective effects of the body itself. These changes could include modulating temperature (hypothermia), CBF (hyperperfusion), inflammation (anti-inflammatory effects), and blood-brain barrier (BBB) damage (reducing BBB disruption and vascular permeability (Sutherland, Minnerup et al. 2012). It is therefore crucial to investigate these endogenous mechanisms which facilitate neuroprotection in many different contexts to understand how these findings could then be translated into more specific treatment strategies.

2.3 Hypothermia in stroke treatment and the putative role of SUMO

In early stages of ischaemic stroke, metabolic alterations and an inflammatory response take place locally at the ischaemic penumbra, inducing an increase in brain temperature within that region. This augmentation of the metabolic rate in the peri-infarct zone results in a faster exhaustion of limited energy and oxygen supplies, thereby increasing conversion of ischaemic but viable tissue to infarction (Karaszewski, Wardlaw et al. 2009). Such hyperthermia can also be accompanied by the increase of intracranial pressure and CBF (Childs, Wieloch et al. 2010). Protein restitution by chaperones requires ATP and other energetic sources, compromised to a higher degree by hyperthermia (White, Luca et al. 2007). Hyperthermia has also been associated with oxidative stress, alteration of the

cytoskeleton and alteration of transduction kinases (Wang, Stroink et al. 2009). Such hyperthermia is an independent predictor of mortality and morbidity, as determined using the Barthel index at 6 months. The relationship between body and cerebral temperature, and the evolution of acute cerebral infarct is robust. There are several mechanisms involved in hyperthermia and hypothermia, but neurotoxicity and neuroinflammation play a predominant role. Treatment of hyperthermia in ischaemic stroke patients, regardless of the origin of disease, improves patient comfort and outcome, both in the short- and the long-term. But further work needs to be done to gain definitive clinical evidence to prove its benefits (Campos, Blanco et al. 2012). Inversion of the stroke-induced temperature rise has opened new possibilities in stroke treatment. Hypothermia is one of the most promising neuroprotective approaches; it has consistently shown benefit in animal models of cerebral ischaemia and reducing infarct volume by more than 40% (van der Worp, Sena et al. 2007). A major phase III clinical trial of mild hypothermia to treat stroke patients by cooling the brain will be launched later this year (2012). The five year trial known as EUROHYP-1, will begin in November, when 60 hospitals in 25 countries use the technique to treat 1500 patients who have had an acute ischaemic stroke (Watson 2012). It is estimated that the metabolic rate of the brain is reduced 6% to 10% for each 1 °C reduction of the brain temperature (Erecinska, Thoresen et al. 2003), reaching a reduction of 50% at 32 °C (Polderman and Herold 2009). The duration of hypothermia may be more important than the cooling intensity, and the feasibility of very prolonged hypothermia beyond 3 weeks using gamma-hydroxybutyrate (GHB) sedation in severe hemispheric infarcts has recently proven to be successful (Mourand, Escuret et al. 2012). Hypothermia is thought to work neuroprotectively through several mechanisms which include decreasing excitatory amino acid release, reducing free radical formation, attenuating protein kinase C activity, and slowing cellular metabolism (Globus, Alonso et al. 1995; Berger, Schabitz et al. 2002; Yenari, Kitagawa et al. 2008). It is now essential to investigate these mechanisms to understand how this neuroprotection is achieved and how it could further be enhanced. The SUMOylation pathway has also been implicated in diverse aspects in the attenuation of stress-induced ROS generation by inhibiting NADPH oxidases (Kim, Yun et al. 2011; Pandey, Chen et al. 2011). Thus, SUMOylation is a promising target to be investigated in the context of neuroprotection in the early stages of an ischaemic insult as well as in combination with other treatment strategies. During hyperthermia for example, the brain needs additional protection and it is

desirable to enhance the existing endogenous systems which could be responsible for protection of the brain. Since rewarming the patients after hyperthermia is a crucial step and involves the danger of increasing intracranial pressure, bleedings and recurring stroke, additional protection especially during this phase would be of great benefit. Many of the mechanisms involved in the neuroprotective effect of hypothermia in ischaemia are also involved in other neurological disorders. It is well known that pathologies such as traumatic brain injury (TBI), spinal cord injury (SCI) and intracerebral hemorrhage (ICH) are associated with processes of glutamate excitotoxicity, BBB disruption, inflammation and edema formation, free radicals formation or neuronal death (Dietrich, Atkins et al. 2009; Tang and Yenari 2010) and all of them are ameliorated by hypothermia. Unravelling the exact endogenous neuroprotective effects underlying these phenomena could pave the way for specific enhancement of endogenous neuroprotection and therewith open the possibility of developing new strategies to protect the brain after an ischaemic insult.

2.4 Epigenetic Modifications

2.4.1 Epigenetic and post-translational modifications

The term `Epigenetics´ refers to DNA and chromatin modifications that persist from one cell division to the next despite a lack of change in the underlying DNA sequence. The `epigenome´ refers to the overall epigenetic state of a cell, and represents the long-sought-after molecular interfaces between the environment and the genome (Csoka and Szyf 2009). Changes in the epigenome throughout life are responsible not only for controlling normal development, adult homeostasis, and aging but also for mediating responses to injury. Recent studies have started to elucidate the key roles played by epigenetic mechanisms in the susceptibility to and the pathogenesis of complex diseases such as cancer and have demonstrated that identifying epigenetic biomarkers is important for risk stratification and molecular diagnosis (Mehler 2008). With epigenetic drugs, it is possible to reverse aberrant gene expression profiles associated with different disease states. Several epigenetic drugs targeting DNA methylation and histone deacetylation enzymes have been tested in clinical trials (Szyf 2009). Emerging evidence implicates a spectrum of epigenetic processes in the pathophysiology of stroke (Qureshi and Mehler 2010). Only recently it has been shown that

the development of tolerance to myocardial and cerebral ischaemia is also modulated by epigenetic DNA and histone modifications such as methylation and acetylation (Zhao, Cheng et al. 2007; Yildirim, Gertz et al. 2008). Yet there is a vast gap in knowledge regarding protein expression and post-translational regulation following ischaemic stroke. Post-translational modification is the enzymatic attachment of chemical groups, lipids, sugars, or polypeptides to a protein after its primary synthesis. These modifications are of critical importance because they can dictate protein folding, distribution, stability, activity and function. Post-translational modifications are also integral components of the signalling cascades that enable cells to efficiently and reversibly respond to extracellular stimuli (Wilkinson, Nakamura et al. 2010). Ischaemia suppresses protein synthesis and alters pathway signalling through post-translational modification (e.g. SUMOylation, phosphorylation, glycosylation, ubiquitinylation). Ubiquitination and SUMOylation are protein modifications that greatly impact protein turn-over and are associated with transient ischaemic stress (Vangilder, Huber et al. 2012). Stem cells that infiltrate a brain infarct are believed to synthesize and secrete growth and guidance factors that are protective and orchestrate tissue recovery following stroke. However, the epigenetic changes that occur in these infiltrating stem cells remain poorly understood (Yilmaz, Alexander et al. 2010). Understanding epigenetic mechanisms may be important for discovering more sensitive and specific biomarkers for risk, onset, and progression of stroke. Preliminary results suggest that agents targeting these pathways can regulate the deployment of stress responses that modulate neural cell viability and promote brain repair and functional reorganization (Szyf 2009).

2.4.2 The small ubiquitin-like modifier (SUMO) family

Small ubiquitin-like modifier (SUMO1-4) is a protein family with about 20% sequence identity with ubiquitin which binds to lysine residues of target proteins and modulates their activity, stability and subcellular localization (Gareau and Lima 2010). SUMO proteins are expressed ubiquitously throughout the eukaryotic kingdom. Some organisms, such as yeast, *Caenorhabditis elegans* and *Drosophila melanogaster*, have a single SUMO gene (Geiss-Friedlander and Melchior 2007). Other organisms, such as plants and vertebrates, have several SUMO genes. The human genome encodes four distinct SUMO proteins: SUMO1–

SUMO4. Of these, SUMO1–SUMO3 are expressed ubiquitously, whereas SUMO4 seems to be expressed mainly in the kidney, lymph nodes and spleen (Guo, Li et al. 2004). SUMO2 and SUMO3 proteins are closely related, with 95 % sequence identity, in their conjugatable form they only differ from one another by three N-terminal residues and together form a distinct subfamily known as SUMO2/3. Available antibodies cannot distinguish between these two SUMO paralogues in their mature forms. They are both relatively distinct from SUMO1, with about 50 % overlap of the amino acid sequence (Hay 2005). SUMO-4 seems to be unable to form covalent isopeptide bonds with substrate proteins due to a proline residue at position 90 which prevents its maturation to a conjugatable form. Nevertheless, recently SUMO4 was shown to interact with IκBα and inhibit NFκB transcriptional activity (Hwang, Won et al. 2012). Although all SUMO paralogues are conjugated to their substrate proteins by the same enymatic machinery they can modify distinct targets. Together, SUMO2 and SUMO3 constitute a greater percentage of total cellular protein modification than does SUMO1 (Saitoh and Hinchey 2000; Tatham, Jaffray et al. 2001). A large proportion of SUMO conjugation target proteins have proven to be transcription factors or other nuclear proteins involved in gene expression or DNA integrity (Gareau and Lima 2010). Any marked change in levels of SUMO conjugated proteins can therefore be expected to have a major impact on the fate of cells. SUMO conjugation has been shown to be activated in cultured cells exposed to various stress conditions including anoxic conditions, hypothermia, and hypoxia (Lee, Castri et al. 2009; Yang, Ma et al. 2009).

In the brain, both SUMO1 and SUMO2/3 conjugation were found to be strongly activated in hibernating animals during the torpor phase; it has therefore been suggested that this is a protective response shielding neurons from damage induced by low blood flow and substrate deprivation (Lee, Miyake et al. 2007). SUMO2/3 conjugation was also shown to be significantly activated during deep hypothermia (Yang, Ma et al. 2009). Hypothermia is effective in protecting the brain in a variety of clinical conditions, including resuscitation after cardiac arrest, and is considererd a promising therapy for stroke (van der Worp, Macleod et al. 2010). Furthermore, a significant increase in the levels of SUMO2/3 conjugated proteins has been found in brains of animals subjected to transient global or focal cerebral ischaemia (Yang, Sheng et al. 2008; Yang, Sheng et al. 2008). Along these lines, changes in the pattern of SUMO2/3 protein adducts along with SUMO1 protein adducts have

been reported after rat transient focal cerebral ischaemia and permanent focal cerebral ischaemia in NMRI mice (Cimarosti, Lindberg et al. 2008). The post-ischaemic pattern of SUMO2/3 conjugated proteins supports the assumption that elevated SUMO2/3 levels could represent a protective stress response: After transient focal cerebral ischaemia, the rise in levels of SUMO2/3 conjugated proteins was most pronounced in neurons of the penumbra, located at the border of the ischaemic territory, where various survival pathways are activated. Furthermore, a short, non-lethal duration of ischaemia was sufficient to activate this process. SUMO1 conjugation increased the resistance of primary neuronal cells to OGD, an *in vitro* model of ischaemia (Lee, Castri et al. 2009). OGD-induced cell death was more pronounced in neurons where SUMO1 expression was silenced, and cells over-expressing SUMO1 were more resistant to OGD. To date, no information is available as to whether SUMO2/3 conjugation is a protective stress response, although it is the conjugation pathway of this SUMO paralogue that is particularly activated after ischaemia (Yang, Sheng et al. 2008; Yang, Sheng et al. 2008). Because of its potential as a target to induce brain protection, it is of considerable interest to investigate the impact of SUMO2/3 conjugation on the fate of post-ischaemic neurons.

2.4.3 SUMOylation and de-SUMOylation, long-term effects of a highly dynamic process

SUMO (small ubiquitin-related modifier) is an 11 kD protein that can be covalently attached to lysine residues on target proteins via an enzymatic cascade analogous to the ubiquitin pathway. SUMOylation of the target protein requires an E1 (SUMO-activating), E2 (SUMO-specific conjugating, Ubc9), and, in most cases, E3 (SUMO ligase) enzymes. Following SUMO activation by the E1 enzyme, SUMO proteins are passed to the active cysteine of the sole SUMO-specific conjugating enzyme, Ubc9. Ubc9, either alone or in combination with a number of reported SUMO E3 enzymes, then catalyses conjugation of SUMO to the lysine residue in the target protein ((Wilkinson, Nakamura et al. 2010), see also Fig. 2).

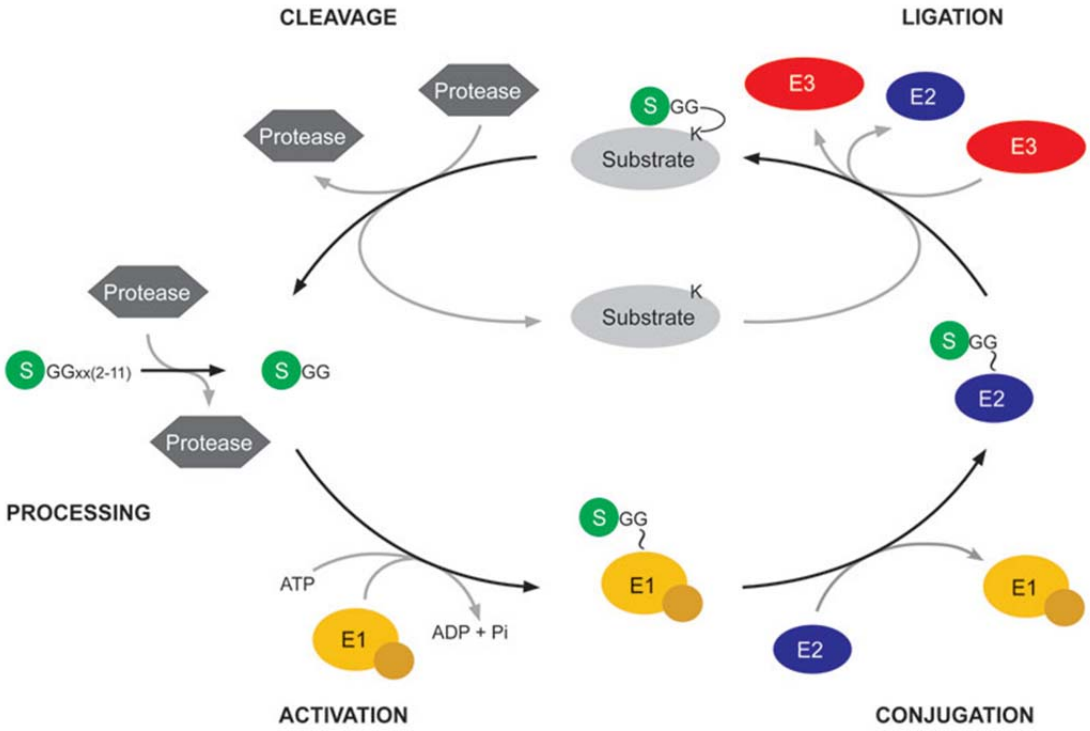

(Maderböck and Pichler 2010)

Fig 2: The circle of reversible SUMOylation. *Nascent SUMO (small ubiquitin-related modifier) needs to be proteolytically processed to reveal its C-terminal glycine-glycine (GG) motif. This is accomplished by SUMO-specific isopeptidases (sentrin-specific proteases; SENPs), which remove 4 C-terminal amino acids from SUMO1, 11 amino acids from SUMO2 and 2 amino acids from SUMO3. Mature SUMO is activated by the E1 heterodimer AOS1–UBA2 in an ATP-dependent reaction, which results in a thioester bond between the C-terminal glycine residue and cysteine (C) 173 in UBA2. SUMO is then transferred to the catalytic cysteine residue of the E2 enzyme Ubc9. Finally, an isopeptide bond is formed between the C-terminal glycine residue of SUMO and a lysine (K) residue in the substrate. This step is usually supported by an E3 ligase. SUMOylated targets serve as substrates for SENPs, which ensures the reversible and dynamic nature of SUMOylation (Geiss-Friedlander and Melchior 2007).*

SUMO conjugation often occurs at a consensus sequence in target proteins, designated ψKxD/E, where ψ is a large hydrophobic residue, K is the target lysine and D/E are acidic residues, i.e. aspartic or glutamic acids (Rodriguez, Dargemont et al. 2001; Sampson, Wang et al. 2001). The SUMOylation process is reversible due to the protease activity of deSUMOylating enzymes, the sentrin-specific proteases (SENPs). The balance between Ubc9-mediated conjugation and SENP-mediated deconjugation determines the SUMOylation state of a specific protein. Although modification appears to involve only a small proportion of a target protein, the effects can be dramatic and long-lasting (Geiss-Friedlander and Melchior 2007). The functional consequences of SUMO attachment vary depending on the substrate and the cell type and in many cases have yet to be elucidated (Meulmeester and Melchior 2008). The tumour suppressor protein p53, which plays a critical role in the differentiation and apoptosis of neurons and oligodendrocytes, is a known SUMO substrate (Wilkinson, Nakamura et al. 2010). SUMOylation of one of the MEF2 family members, MEF2A, strongly influences synapse formation through a phosphoregulated SUMO-acetyl switch (Shalizi, Gaudilliere et al. 2006), and SUMOylation seems to have direct effects on local protein synthesis in axons, which is critical for axonal regeneration and synaptic plasticity in adult neurons (Giuditta, Kaplan et al. 2002; van Niekerk, Willis et al. 2007). In addition to glutamate receptors, several other classes of neuronal membrane proteins have been reported to be SUMOylated, strongly implicating SUMOylation in the control of neuronal excitability, synaptic transmission and glucose transport (Martin, Wilkinson et al. 2007; Feligioni, Nishimune et al. 2009).

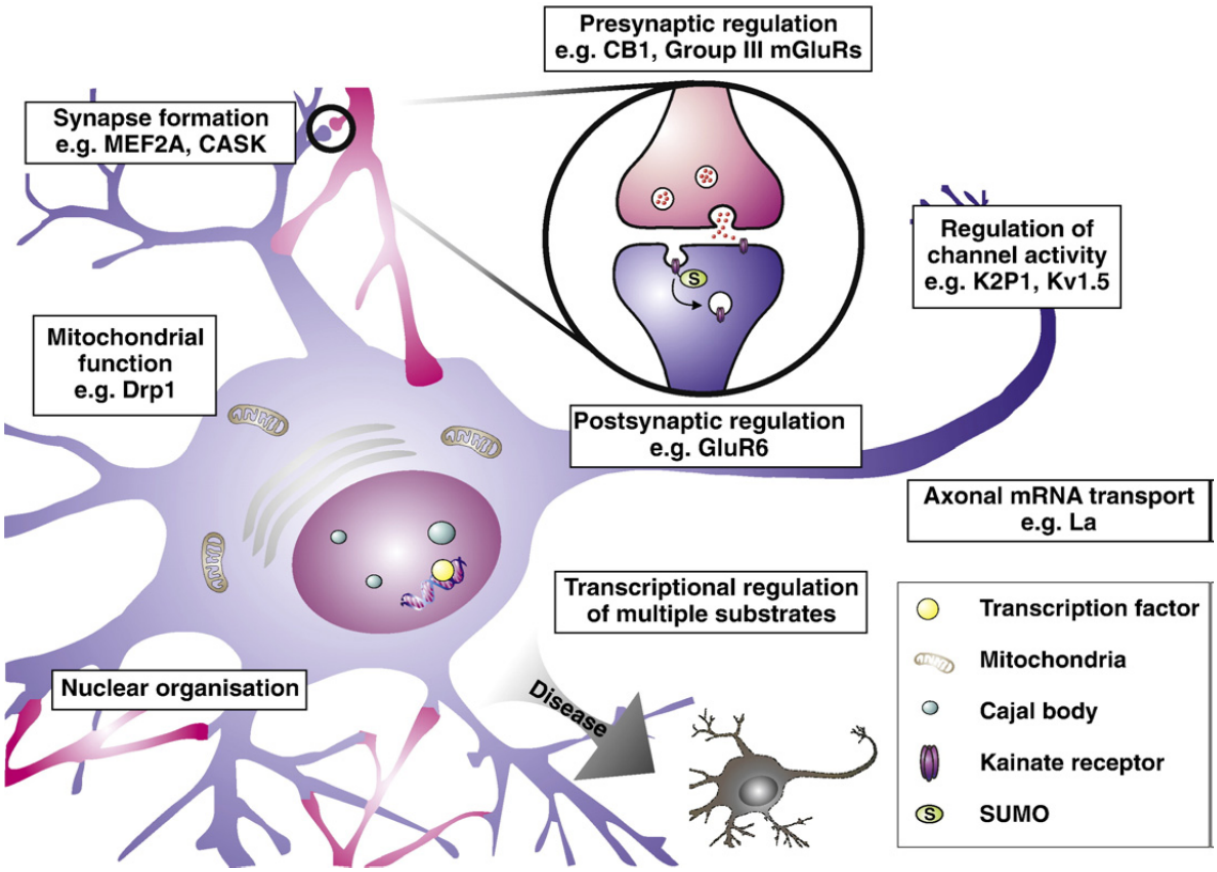

(Wilkinson, Nakamura et al. 2010)

Fig 3: SUMOylation and neuronal function. *SUMOylation has been implicated in the regulation of various aspects of neuronal function and morphology. Shown are a number of these processes, along with identified SUMO substrates involved. Drp1: Dynamin-related protein 1; MEF2A: Myocyte enhancer factor 2; CASK: calmodulin-dependent serine protein kinase; CB1: cannabinoid receptor1; mGluR: Metabotropic glutamate receptor; K2P1: subunit of K^+ channels; KV1.5: Homotetramers of alpha-pore subunits.*

2.4.4 SUMOylation as a neuroprotectant response in ischaemic stress?

While the SUMOylation of given substrates can be specifically regulated, global levels of SUMOylation in neurons can be modulated in an activity-dependent manner, potentially locating changes in protein SUMOylation at the hub of the coordination of neuronal signalling and response to ischaemic stress. A change in SUMO2/3 adducts could also be the key mechanism in explaining the neuroprotective effect during hypothermia in stroke

treatment. *In vivo* investigations have shown an induction of SUMO following hypothermia and stroke. Nevertheless it is unclear whether there is a causal link between increase in SUMO adducts and the protective effect observed during hypothermia, and whether neuronal survival and therewith the infarct volume development is dependent on SUMO2/3 conjugation. Expression of a neuronal specific microRNA directed against SUMO2/3 facilitates a reduction in protein expression similar to a pharmacological approach. Complete embryonic knockout of the gene has been proven to be lethal; therefore a knockdown strategy is appropriate for unraveling the direct effects of SUMO2/3ylation on neuronal survival after ischaemic stress *in vitro* and *in vivo*. Furthermore, as a rescue strategy, silently mutated SUMO2/3 can be introduced which carries the same protein information as normal SUMO2/3 but cannot be degraded by the microRNA. Up to now, an increase in total SUMO2/3 in brain lysates has been investigated, but neuron-specific investigation in the context of stroke has not been possible. Tools need to be developed to identify specific targets of SUMO2/3ylation in clearly defined brain regions and cell types at different time points and to investigate their meaning in stroke pathophysiology.

2.5 Hypotheses

In my Ph.D thesis project I tested the following hypotheses:

1) SUMO2/3ylation is induced in neurons in a stress-dependent manner.
2) SUMO2/3ylation protects neurons from OGD and glutamate stress *in vitro.*
3) SUMO2/3ylation is an endogenous neuroprotective mechanism in stroke *in vivo.*

The following working plan was applied to test the hypotheses:

1) Primary embryonic cortical neurons were stressed transiently through combined OGD to investigate SUMOylation patterns.
2) RNA interference was applied to investigate the effects of SUMO2/3 knock down on survival of primary embryonic cortical neurons before and after OGD. An *in vitro* model of adult neuronal cells was established to study the effects of Sumo2/3 microRNA transduction in glutamate excitotoxicity.

3) Sumo2/3 microRNA was applied *in vivo* in combination with MCAo to test for lesion volume development as well as behavioural differences.

   Transgenic mice were generated as a tool to investigate inducible and cell type-specific alterations in SUMO2/3 levels in different tissues and explore its effects on target proteins in different pathophysiological contexts.

3. Materials and Methods

3.1 Materials

3.1.1 Cell culture media and supplements

Product	Supplier
B27 Supplement	Gibco, Darmstadt, Germany
Collagen-G solution	Biochrom (Berlin, Germany)
D-(+)-glucose	Sigma (Taufkirchen, Germany)
Dulbecco´s Modified Eagle Medium (DMEM)	Gibco, Darmstadt, Germany
Dulbecco's phosphate-buffered saline (DPBS)	Biochrom (Berlin, Germany)
Foetal calf serum, Gold (FCS Gold)	PAA (Pasching, Austria)
Glucose	Carl Roth GmbH (Karlsruhe, Germany)
Glutamate	Sigma (Taufkirchen, Germany)
HEPES	PAA (Pasching, Austria)
Insulin (Insuman Rapid)	Sanofi Aventis, Berlin, Germany)
L-Glutamine	PAA (Pasching, Austria)
MEM non-essential amino acids	PAA (Pasching, Austria)
Modified Eagle's medium (MEM)	Biochrom (Berlin, Germany)
Neurobasal medium (NBM)	Gibco (Karlsruhe, Germany)
Penicillin/Streptomicin	PAA (Pasching, Austria)
Phosphate buffered saline (PBS)	PAA (Pasching, Austria)
Poly-L-Lysin (PLL)	Biochrom (Berlin, Germany)
Sodium pyruvate	PAA (Pasching, Austria)
Trypsin / EDTA	Biochrom (Berlin, Germany)

3.1.2 Chemicals

Product	Supplier
Acetic acid	Merck (Darmstadt, Germany)
Aceton	J. T. Baker (Deventer, Netherlands)
β-glycerophosphate	S. C. Biotech. (Heidelberg, Germany)
4',6-diamidino-2-phenylindole (DAPI)	Invitrogen (Darmstadt, Germany)
Ethylenediaminetetraacetic acid (EDTA)	Carl Roth (Karlsruhe, Germany)
Ethylene glycol tetraacetic acid (EGTA)	Carl Roth (Karlsruhe, Germany)
Eosin 1% in alcohol	Morphisto (Frankfurt am Main, Germany)
Eosin: 70% propanol containing 1% Eosin	Sigma-Aldrich, (München, Germany)
Ethanol	J. T. Baker (Deventer, Netherlands)
Formaldehyde solution (39%)	Merck (Darmstadt, Germany)
Hämalaun sauer nach Mayer	Carl Roth (Karlsruhe, Germany)
H_2O_2	Sigma-Aldrich (München, Germany)
LDH-standard	Greiner Diagnostic (Bahlingen, Germany)
Methanol	Carl Roth (Karlsruhe, Germany)
Methyl butane	Sigma-Aldrich (München, Germany)
Physiological natrium chloride solution (0.9%)	Fresenius (Bad Homburg, Germany)
Dodecyl sulphate (SDS)	Sigma-Aldrich (München, Germany)
Paraformaldehyde (PFA)	Sigma-Aldrich (München, Germany)
Propanol (90%)	Carl Roth (Karlsruhe, Germany)
Protease inhibitor cocktail I	Sigma-Aldrich (München, Germany)
Rotihistol	Carl Roth (Karlsruhe, Germany)
Triton X-100	Carl Roth (Karlsruhe, Germany)

3.1.3 Antibodies, reagents and kits

Product	Supplier
ABC-Elite-Kit Vectastain	Vector Laboratories (Peterborough, UK)
ApopTag® Red In Situ Kit	Millipore (Schwalbach, Germany)
CalPhos-Kit	Clontech (Saint-Germain, France)
CellTiter-Glo® Luminescent Cell Viability Assay	Promega (Mannheim, Germany)

3-3-Diaminobenzidine THC (DAB)	Sigma (Taufkirchen, Germany)
Anti-EGFP sc9996	S. C. Biotech. (Heidelberg, Germany)
Fluoromount G	Southern Biotech, Eching, Germany)
Anti-GAPDH	Millipore (Schwalbach, Germany)
Anti-NeuN antibody	Millipore (Schwalbach, Germany)
Invisorb Spin Tissue Mini Kit	Stratec (Berlin, Germany)
Normal goat serum (NGS)	Immunoresearch (Suffolk, UK)
Parafilm	Bemis packaging (Oshkosh, USA)
ProLong® Gold antifade reagent	Invitrogen (Eggenstein, Germany)
SUMO2/3 antibody	Invitrogen (Eggenstein, Germany)
Syringe 1ml in vivo	BD Biosciences (Heidelberg, Germany)
Microtubuli-associated protein 2 (MAP2)	Millipore (Hofheim, Germany)
Vitro clud	Langenbrinck (Emmendingen, Germany)

3.1.4 Tools and equipment

Product	**Supplier**
Cell culture flasks (175 mm^3)	Nunc (Langenselbold, Germany)
Cryostat Leica CM1950	Leica Biosystems (Wetzlar, Germany)
Falcon tube (15 ml)	BD Biosciences (Heidelberg, Germany)
Pyrex glass flask (25 ml)	VWR Int. (Darmstadt, Germany)
Hamilton syringe	Hamilton (Bonaduz, Switzerland)
Laser-Doppler Periflux System	Perimed (Järfälla, Sweden)
Lidocaine gel	Astra Zeneca GmbH (Wedel, Germany)
Luminometer Orion Microplate	Berthold (Bad Wildbad, Germany)
Microscope (IX81) with CellM software	Olympus (Hamburg, Germany)
Microscope slides (SuperFrost Plus)	Langenbrink (Emmendingen, Germany)
Microscopic stage (motorised)	Merzhäuser (Wetzlar, Germany)
Microtome MICROM HM 330	Thermo Scientific (Walldorf, Germany)
Microvascular clip	Fine science tools (Heidelberg, Germany)
Microscissors	Fine science tools (Heidelberg, Germany)
OGD chamber 'IN VIVO2 300'	Ruskinn (Pencoed, UK)

Opaque-walled 96-well plates	Nunc (Langenselbold, Germany)
Paraplast Plus Tissue embedding medium	Leica Biosystems (St Louis, USA)
Pasteur pipet	Neolab (Heidelberg, Germany)
PEG-it™ solution	SBI (Mountain View, USA)
PVDF filter (45 µm)	Carl Roth GmbH (Karlsruhe, Germany)
Pharmascan 7 Tesla rodent MRI scanner	Bruker BioSpin (Ettlingen, Germany)
Silk string usp 6/0	Suprana (Berlin, Germany)
Small animal stereotactic frame	Kopf Instruments (Tujunga, USA)
Superfrost Plus microscope slides	Langenbrink (Emmendingen, Germany).
Tissue embedding molds	Polysciences (Eppelheim, Germany)
Xantopren M Mucosa and Activator NF Optosil	Haereus Kulzer (Wehrheim, Germany)
Isoflurane	Abbot (Wiesbaden, Germany)
Isoflurane vaporizer	Drägerwerk AG (Lübeck, Germany)
Small Animal Monitoring & Gating System	SA Instruments (New York, USA)

3.1.5 Software

Product	Supplier
Analyse 5.0	AnalyseDirect, Inc. (Lenexa, USA)
GraphPad Prism	GraphPad (San Diego, USA)
Sigma stat	Systat Software (Erkrath, Germany)

3.2 Methods

3.2.1 *In vitro* model of embryonic primary cortical neurons: Lentivirus application and combined oxygen-glucose deprivation (OGD)

3.2.1.1 Preparation of primary cortical neurons and cell culture

Primary cortical neurons were obtained from mouse C57BL/6N embryos (E16) and cultured using neurobasal medium with B27 and L-Glutamine supplement.After the cerebral cortices had been dissected, they were incubated for 15 min in Trypsin/EDTA (0.05/0.02%) at 36.5 °C, washed twice in PBS and once with dissociation medium (MEM with 10% FCS Gold, 10 mM

HEPES, 44 mM glucose, 100 U/ml of penicillin plus streptomycin, 2 mM L-glutamine and insulin (3.5 µg/ml). The cells were separated by pipetting with a Pasteur pipet in dissociation medium, pelleted by centrifugation (210 x g for 2 min at 21 °C) and redissolved in starter medium (Neurobasal medium supplemented with B27 and 0.5 mM L-glutamine). Twenty-four well plates were coated with PLL and Collagen-G according to the following protocol: The wells were incubated with PLL (20 µg/ml) for 1 h at room temperature (RT), washed with PBS and incubated for 1 h in coating medium (dissociation medium with 0.03% collagen G) at 36.5 °C. Subsequently, the plates were washed twice with PBS and the primary cortical neurons were seeded at 325,000 cells per 24-well in 500 µl starter medium. The cells were kept in culture for 13 days *in vitro* (DIV) and supplemented with 500 µl of additional medium (NBM + B27) on DIV4, 7 and 10. Viral infections were carried out on DIV3 and combined OGD experiments on DIV12.

3.2.1.2 Generation and titration of lentiviral particles

Third-generation lentiviral particles were generated as described previously (Reich, Spering et al. 2011) with the following modification: microRNA delivery was driven by the synapsin promoter based on Addgene plasmid 27232 (Dittgen, Nimmerjahn et al. 2004). Target sequences and microRNA designs to interfere with SUMO2/3 and control microRNAs (LacZ and non-targeting 'scrambled') have been described recently (Yang and Paschen 2009).

Sequences of chained Sumo3 microRNA and Sumo2 microRNA including flanking regions:

Colour codes:

5´ miR155 flanking region
3´ miR155 flanking region
polylinker for oligo annealing
microRNA Sumo2
microRNA Sumo3

Sumo2 microRNA:

atcctggaggcttgctgaaggctgtatgctgtgatctgcctcattgacaaacgttttggccactgactgacgttt
gtcagaggcagatcacaggacacaaggcctgttactagcactcacatggaacaaatggcc

Sumo3 microRNA:

atcctggaggcttgctgaaggctgtatgctgaatcgaatctgcctcattgacgttttggccactgactgacgtca
atgacagattcgattcaggacacaaggcctgttactagcactcacatggaacaaatggcc

For generation of lentiviral particles, 293 Hek cells were plated out in 175 mm^3 flasks in 25 ml of culture medium (DMEM containing 10% FCS Gold, 100 U/ml of penicillin plus streptomycin, 1 mM sodium pyruvate, 0.5 mM L-glutamine, 1×MEM non-essential amino acids) on DIV1. The following day, 20 µg of the transfer vector of each microRNA construct was mixed with the two lentiviral packaging vectors psPAX (12.5 µg) and pMD2G (7.5 µg) in a 15 ml falcon tube. Distilled water was added to a final volume of 1250 µl, and subsequently 155 µl of 2 M Calcium solution were added to the mixture. While mixing on a vortexer, 1250 µl of 2 × HBS solution were added drop by drop. While the solution was allowed to incubate for 20 min at RT, the culture medium on the 293 Hek cells was exchanged and the transfection mixture was added. On DIV3, the culture medium was replaced and on DIV4 and DIV5 the supernatants were collected and kept on ice at 4 °C. On DIV5, the supernatants were pooled for each construct and centrifuged at 3000 × g for 15 min to remove cells and cell debris, then filtered through a 45 µm PVDF filter. The PEG-it™ solution was added 1:5. The solution was mixed well by pipetting up and down and put on a shaker at 4 °C for 72 h. The supernatant / PEG-it™ mixture was centrifuged at 1500 × g for 20 min at 4 °C, the supernatant was poured out and the pellet was centrifuged again for 5 min at 1500 × g. All traces of fluid were removed while care was taken not to disturb the precipitated lentiviral particles in the pellet. The pellets were redissolved in a 1:1000 volume of the original supernatant solution (50 µl for a starting volume of 50 ml) of PBS and stored in cryovials as 10 µl-aliquots at -80 °C. For titration of the lentiviral particles, primary cortical neurons were prepared as described above and seeded out on 24-well plates. A dilution series was carried out from 1 to 10^{-4} on DIV3, 500 µl of culture medium was added to the neurons on DIV4 and they were analysed on DIV7. Epifluorescent pictures were taken using the fluorescent reporter enhanced green fluorescent protein (EGFP) in combination with bright field images from the same predefined regions. The number of transduced cells per well was counted for 5 regions of interest (ROI) and the multiplicity of infection (MOI) was calculated for every virus.

3.2.1.3 The model of combined oxgen-glucose deprivation (OGD)

Neuronal cultures were subjected to combined oxygen and glucose deprivation as described previously (Harms, Albrecht et al. 2007). In brief, culture medium was removed from the primary neuronal cell cultures and collected. The cells were washed twice with PBS and placed in an OGD chamber 'IN VIVO2 300' with 5% CO_2/0.3% O_2 with a buffer free of glucose for 15, 45, or 75 min, respectively. After the respective OGD lengths, the plates were removed from the OGD chamber and the collected culture medium was mixed 1:1 with freshly made medium and added to the cultures. The cells were incubated for 0-24 h at 36.5 °C until analysed in the respective assays.

3.2.1.4 Adenosine triphosphat (ATP) assay

Adenosine triphosphate levels of neuronal cultures were quantified using the CellTiter-Glo® Luminescent Cell Viability Assay according to the manufacturer's instructions. After being subjected to 15, 45 or 75 min of OGD, respectively, the neuronal cultures were either incubated with 1:1 medium at 36.5 °C or directly analysed. To that end, they were washed in PBS and incubated in 100 µl of CellTiter-Glo® Buffer/ CellTiter-Glo® Substrate mixture and subsequently transferred to opaque-walled 96-well plates to avoid background luminescence. Luminescence of the different samples was recorded and analysed. Each data point was derived from whole-cell lysates of one 24-well and calculated as the ratio to cultures not subjected to OGD.

3.2.1.5 Lentivirus application and neuronal baseline survival

Transduction units (TU) and multiplicities of infection (MOI) were determined and calculated from serial dilutions in neuronal cultures using EGFP fluorescence as a reporter after 96 h and the MOIs were adjusted to 5. Transduction efficiencies used for the experiments were 95% or higher as evaluated by counting transmission as well as EGFP fluorescence images and using EGFP as a marker of equal transduction in western blotting. For the experiments,

neuronal cultures were transduced on DIV3 with equal amounts of virus. Eleven loci per 24-well were preselected and repeatedly analysed using an inverted IX81 microscope combined with CellM software and equipped with a motorized microscopic stage. Epifluorescence microscopic pictures of exactly the same loci were taken on DIV6, 9 and 12 using EGFP as a reporter for lentiviral gene delivery and microRNA expression. EGFP-positive cells were counted in a blinded manner and ratios calculated (DIV9/DIV6, DIV12/DIV9 and for final analysis DIV12/DIV6) to compare the effects of Sumo2/3 microRNA expression to control microRNA expression on baseline survival over 12 days *in vitro*. Each ROI initially contained 85 ± 10 cells (mean ± s.d. on DIV6).

3.2.1.6 Novel assessment strategy for neuronal survival after OGD

Additionally to the baseline survival analysis, a damage assessment strategy was developed to compare the effects of Sumo2/3 microRNA expression on survival and OGD-induced cell loss. The same predefined 11 ROIs as for the baseline survival analysis were evaluated just before (DIV12) and 24 h after OGD (DIV13), counting EGFP positive neurons in a blinded fashion. Ratios were calculated of surviving neurons after OGD compared to the baseline survival ratio DIV12/DIV6. In total, an average of 85 × 11 × 3 × 3 = 8,415 cells per condition (ROI × microRNAs × OGD durations) were analysed in triplicate (overall 25,245 neurons per condition). For visual display of neuronal survival in a particular ROI, emitted fluorescence was pseudocolored green (just before OGD) and red (24 h after OGD) and images were merged. The resulting yellow was indicative of surviving neurons.

3.2.1.7 Lactate dehydrogenase (LDH) assay

Lactate dehydrogenase activity (LDH) as a marker for the loss of cellular membrane integrity was measured in the supernatant and after total lysis of cells using 0.5% Triton-X for 20 min at RT.. Samples of 50 µl from the cell culture medium were repeatedly measured on days 6, 9, 12 (baseline) and 13 (after OGD) *in vitro* by means of a kinetic photometric assay (at 340 nm). The samples were pipetted into 96-well plates and mixed with 200 µl of β-NADH

solution (0.15 mg/ml in 1×LDH buffer). Measurement was started immediately after addition of the reaction substrate pyruvate (50 µl of 22.7 mM pyruvate-solution). Optical density was measured at 340 nm using a microplate reader, by 10 counts with 30 s intervals, followed by calculation of results using a LDH-standard.

3.2.1.8 Propidium iodide (PI) staining of dead cells

Cell viability was assessed after staining of naive cell cultures with propidium iodide (PI) to distinguish between living and dead cells (0.001 mg/mL for 5 min with subsequent rinsing) and five fluorescence images per well were taken using an inverted IX81 microscope. Viable neurons not incorporating PI (PI^-) were counted in overlays with transmission images and quantified as ratios versus all neurons as described previously (Harms, Albrecht et al. 2007).

3.2.1.9 Western immunoblotting

Neurons were harvested and total proteins were extracted with lysis buffer composed of b-glycerophosphate (50 mmol/L; pH7.4), 1 mmol/L EDTA, 1 mmol/L EGTA, 0.5 mmol/L Na_3VO_4, 1% Triton X-100, 2% sodium dodecyl sulphate (SDS), and the protease inhibitor cocktail I (1%), see also (Yang, Ma et al. 2009). The proteins were probed with a SUMO2/3-specific antibody (Invitrogen; 1:1,000), anti-GAPDH (anti-glyceraldehyde 3-phosphate dehydrogenase, Millipore; 1:75,000), and anti-EGFP (Santa Cruz Biotechnology, 1:1,000).

3.2.1.10 Immunocytochemistry

Cells were transduced with lentiviral particles on DIV3 and kept in culture as described. On DIV11, they were fixed with 4% paraformaldehyde (PFA) in phosphate buffered saline for 10 min at RT, washed twice in PBS, incubated for 1 h in blocking solution (10% milk powder in PBS) at RT and incubated with primary antibodies against microtubuli-associated protein 2 (MAP2, Millipore, Hofheim, Germany) and anti-EGFP (Santa Cruz Biotechnology, Heidelberg,

Germany) at 4 °C overnight. After 3 washing steps in PBS, secondary antibodies were applied in PBS for 1 h at RT. The neurons were washed again in PBS and mounted with ProLong® Gold antifade reagent containing the nuclear counterstain 4´,6-diamidino-2-phenylindole (DAPI).

3.2.1.11 Statistical analysis

Data are presented as dot blots and mean ± 95% confidence interval except for Figure 5, where mean ± standard deviation (s.d.) is presented. The number of experiments required to detect a standardized effect size ≥ 0.15 was calculated by a priori power analysis with the following assumptions: $\alpha = 0.05$, $\beta = 0.2$, mean: s.d.: 10% of the mean. The power was set therewith to $1 - \beta = 0.8$. Using GraphPad Prism, linear regression analysis or one-way and two-way repeated-measures ANOVA (analysis of variance) were carried out with Tukey's post hoc analysis. Two-way ANOVA followed by Tukey's post hoc tests were carried out where indicated. Experiments were performed in triplicate. P-values < 0.05 were considered statistically significant.

3.2.2 *In vitro* model of adult organotypic retina explant cultures: Lentivirus application and glutamate toxicity

3.2.2.1 Establishment of organotypical retina culture

Adult organotypic retina cultures were prepared from male Wistar rats (200 g). The animals were decapitated under deep isofluranee anaesthesia. The heads were washed in 70% ethanol and subsequently in double-distilled water. The eyes were removed and washed in 70% ethanol and rinsed twice in PBS. A first incision was made using a scalpel at the cornea-sclera junction followed by a circular cut with microscissors along the ora serrata. The eye was flipped open and cornea, lens and vitreaous body were removed. The retina was carefully dissected from sclera and retinal pigment epithelium and transferred into a 50 µl-drop of MEM culture medium containing 10% FCS, 0.8% glucose, 2 mM glutamine, 25 mM HEPES, 2% B-27 supplement, and penicillin/streptomycin 100 U/ml onto a sterile Petri dish.

The retina was smoothened and cut with a scalpel into 1-mm^2 rectangular fragments, approximately 20-25 per retina. All retinal slices were aspirated with culture medium using a plastic pipette and transferred into a 25 ml Pyrex glass flask a total volume of 3 ml medium. The flasks were placed on horizontal rollers in a dry incubator. The retinal slices were cultivated under constant rotation (60 rpm) at 36.5 °C for 7 days, up to 1 ml of culture medium was replaced every 24 h depending on the metabolism of the respective culture.

3.2.2.2 Lentiviral transduction in retina explant cultures

For lentiviral transduction of retina explant cultures, different protocols and time points of addition were tested out. For the experiments, the optimum was applied and lentiviral particles were added to the culture medium directly after preparation of the explant cultures, before they completely closed. Six animals were usually prepped within one day, so 12 groups were generated. Of these, 4 flasks were kept as controls, 4 flasks transduced with control microRNA expressing lentiviral particles and 4 flasks transduced with Sumo2/3 microRNA-expressing lentiviral particles. Two flasks of each group were kept in culture for 7 days before paraffin embedding, the two other flasks per group were challenged with glutamate damage on DIV6 and thereafter kept in culture for another 24 h. Culture medium was exchanged as for control sister cultures.

3.2.2.3 Glutamate damage in organotypical retina cultures

After DIV6, half of the above mentioned retinal explant cultures were challenged through adding 5 mM glutamate directly to the medium for 24 h as described in (Rzeczinski, Victorov et al. 2006).

3.2.2.4 Paraffin embedding and tissue processing of retina cultures

After incubation for 7 days, the retina cultures were aspirated from the flasks with a Pasteur pipette and transferred to a 15 ml falcon tube. Then, they were washed with PBS and fixated using Tellzesnicky/Davidsons fixative (70% of 96%-ethanol, 20% of 39%-formaldehyde and 10% of acetic acid for 15 min at RT. After incubating in 70% propanol containing 1% Eosin for 10 min at RT, the cultures were dehydrated for 30 min in 90% propanol and subsequently three times for 30 min in 99% propanol. Then, they were transferred into tissue embedding molds, the residual propanol was removed and paraffin (Paraplast Plus Tissue embedding medium) was added. The tissue embedding molds were incubated at 60 °C in an oven for 1 h, the paraffin was replaced and the cultures were incubated overnight at 60 °C. The next day, the retina fragments were orientated in one layer and the paraffin was allowed to harden overnight at RT. Eight-µm serial sections were cut on a MICROM HM 330 microtome, transferred into a water bath and mounted onto Superfrost Plus microscope slides.

3.2.2.5 Immunohistochemistry in paraffin embedded sections

For haematoxylin-eosin staining of the retina sections, the slides were incubated twice for 5 min in rotihistol and subsequently in 100%, 80% and 70% ethanol. They were rinsed in double-distilled water and incubated in hämalaun solution for 5 min, rinsed again in water and incubated in 1% eosin solution for 15 s. Then, the sections were dehydrated in 96% and 100% ethanol followed by two incubation steps in rotihistol for 5 min. Finally, the slides were mounted with vitro clud.

3.2.2.6 Analysis of cell loss in the retinal ganglion cell layer

Pyknotic cells of the retinal ganglion cell layer were identified in the H/E staining and counted in a blinded fashion.

3.2.3 *In vivo* models of cerebral ischaemia: Stereotactic lentivirus application and middle cerebral artery occlusion (MCAo)

All animal experiments were performed according to institutional and international guidelines. All surgical procedures were approved by the local authorities (G0213/07, G0200/07 and G0385/08).

3.2.3.1 Establishing the stereotactic lentivirus injection into the cortex

Using a small animal stereotactic frame combined with a mouse adapter, lentiviral particles were injected into the cortex of SV129 and C57BL6/N wildtype mice to downregulate SUMO2/3 expression in the penumbra region of experimental stroke. To that end, different injection strategies were investigated and analysed beforehand to find the optimal way of targeting the lateral cortex. Using a mouse brain atlas, stereotactic coordinates were predefined and tested *in vivo* for 3 injections per mouse into the putative penumbra region. A pointed Hamilton syringe (7001 N (ga 0,47/70 mm/pst2), 1 µl, P/N:80135/01, w/o 1367706, 19/09) was used to inject 1 µl of volume and to target a bigger area than with a blunted syringe. For 8 week old C57BL/6N mice, the following coordinates were tested for perpendicular injections:

1) Bregma -0.5 mm, lateral left 2.5 mm, depth 1 mm
2) Bregma -1.5 mm, lateral left 3 mm, depth 1 mm
3) Bregma -2.5 mm, lateral left 3.5 mm, depth 0.8 mm

For a more lateral distribution and a more exact positioning into the penumbra region, the following coordinates were tested on 8 week old SV129 mice with a 30° angle to the perpendicular line using a blunted syringe (7001 N (ga 0,47/70 mm/pst3), 1 µl, P/N:80100/02, w/o 1372469, 26/9):

1) Bregma 0 mm, lateral left 3 mm, depth 1 mm
2) Bregma -1 mm, lateral left 3 mm, depth 1 mm
3) Bregma -2 mm, lateral left 3.5 mm, depth 1 mm

The position of the injections was monitored in the T2 sequence of the magnetic resonance scans.

3.2.3.2 The model of MCAo

Middle cerebral artery occlusion was performed essentially as described (Endres, Meisel et al. 2000; Engel, Kolodziej et al. 2011). To prepare a filament for occlusion of the middle cerebral artery, a 8.0 nylon monofilament was cut into 12 mm long pieces and at least three quarters in length were covered homogenously with a mixture of Xantopren M Mucosa and Activator NF Optosil and dried overnight. For MCAo induction, mice were anaesthetized with 1.5% isofluranee and maintained with a vaporizer in 1.0% isofluranee in 70% N_2O and 30% O_2. During surgery, body temperature was maintained at 36.5 °C ± 0.5 °C using a feedback controlled heating pad. Mice were placed on the back and the skin and fur were disinfected. A midline neck incision was made and the soft tissues were pulled apart to expose the left common carotid artery (LCCA) without harming the vagal nerve. A ligature was placed around the LCCA with a 6.0 string. Further, the left external carotid artery (LECA) was ligated and a knot was placed around the left internal carotid artery (LICA) without closing it. After having gained a good view on the LICA and the left pterygopalatine artery (LPA), both arteries were clipped with a microvascular clip. With microscissors a small hole was cut in the LCCA before the bifurcation to the LECA and the LICA. The previously coated nylon monofilament was then introduced into the LCCA past the bifurcation into the LICA until it stopped at the clip. The clip was removed while the filament was further inserted into the LICA to occlude the origin of the LMCA in the circle of Willis. The third knot was closed around the LICA to keep the filament in position for the duration of the occlusion. The mice were put in a heating chamber and allowed to wake up for the time of occlusion, were then reanesthetized to withdraw the filament, the knot around the LICA and the suture were closed, putting all soft tissues back into place. For pain relief, Lidocaine gel was topically applied into the wound.

3.2.3.3 Neurological scoring of mice - determining functional deficits

Directly after the surgery, the animals were tested for neurological deficits according to (Bederson, Pitts et al. 1986), scoring from 0 (no observable deficit) to 3 (decreased resistance to lateral push, and forelimb flexion, circling). The grading was done by a researcher who was not aware of the experimental groups.

3.2.3.4 Behavioural testing

A blinded pole test was carried out as described in (Prinz, Laufs et al. 2008). The mice were habituated to the procedure the day before testing. They were placed head upwards near the top of a vertical rough-surfaced pole (diameter 1 cm, height 50 cm), then allowed to descend 5 times during one experimental session. The length of time each mouse needed to turn completely head downwards (`time-to-turn´) and the time each mouse needed to reach the floor with all 4 paws (`time-to-come-down´) was recorded. Results were expressed as the mean of 5 trials.

3.2.3.5 Magnetic resonance imaging (MRI) and data analysis

Magnetic resonance imaging was performed using a 7 Tesla rodent scanner (Pharmascan 70 / 16AS) with a 16 cm horizontal bore magnet and a 9 cm (inner diameter) shielded gradient with a H-resonance-frequency of 300 MHz and a maximum gradient strength of 300 mT/m. For imaging a ^{1}H-RF quadratur-volume resonator with an inner diameter of 20 mm was used. Data acquisition and image processing were carried out with the Bruker software Paravision 4.0. During the examinations mice were placed on a heated circulating water blanket to ensure constant body temperature of 37 °C. Anaesthesia was induced with 2.5% and maintained with 1.0–2.0% isofluranee delivered in an O_2/N_2O mixture (30/70%) via a facemask under constant ventilation monitoring. A T2-weighted 2D turbo spin-echo sequence and a T2*-weighted gradient echo sequence (FLASH) were used. Imaging parameters: for T2 TR/TE= 4059/36 ms, RARE factor 8, 4 averages); for T2*TR/TE = 619.7/7.2

ms, flip angle 30°, 1 average, triggered on respiration. 20 axial slices with a slice thickness of 0.5 mm, a field of view of 2.75x2.75 cm and a matrix of 256x256 were positioned over the brain excluding olfactory bulb. Data evaluation was performed with Analyse 5.0. For stroke volumetry the hyperintense areas of ischaemic tissue in T2-weighted images were assigned with a region of interest tool (ROI). This connects all pixels within a specified threshold range around the selected seed pixel and results in a 3D object map of the whole stroke region, which in turn makes a threshold-based segmentation possible. Further the total volume of the whole object map was automatically calculated.

3.2.3.6 Histological infarct volumetry

To assess infarct volumes after MCAo on a microscopic level, the mice were deeply anesthetised using isoflurane transcardially perfused with ice cold physiological natrium chloride solution (0.9% NaCl). The brains were removed and frozen in -40 °C cold methyl butane on dry ice and stored at -20 °C. They were cut on a cryostat in 20 µm thick sections and mounted onto SuperFrost Plus microscope slides. A NeuN-DAB staining was carried out. To that end, the sections were allowed to dry for 10 min at RT. They were then incubated in a precooled aceton-methanol mixture (1:1) at -20 °C, the mixture was allowed to evaporate for 10 min at RT and the slides were washed three times for 5 min in PBS. After endogenous peroxidases had been blocked by incubation in H_2O_2-solution (0.3% in PBS) for 20 min, the sections were rinsed three times for 5 min in PBS. Thereafter they were incubated in blocking solution (1% normal goat serum, 0.1% Trinton X-100 in PBS) for 30 min at RT and in the primary NeuN antibody (biotinylated, 1:100) at 4 °C overnight. The next day, the sections were rinsed three times for 5 min in PBS and incubated for 1 h in ABC-Elite-Kit solution, washed again three times for 5 min in PBS and DAB solution was applied for 10 min at RT. The reaction was stopped with double-distilled water, the sections were rinsed again in water and dehydrated in 70%, 80%, 96% and twice in 100% ethanol. After short incubation in rotihistol, the sections were mounted with vitro clud and allowed to dry for further analysis. Infarct volumetry was measured and calculated as described e.g. in Endres et al., 1997. In brief, 5 standardized infarct layers were analysed for stroke volumes, and direct and indirect infarct volumes were determined.

3.2.4 *In vivo* models of cerebral ischaemia: Intraarterial lentivirus application and MCAo

Middle cerebral artery occlusion was carried out as described above (3.2.3.2). At the timepoint of reperfusion, lentiviral particals encoding either for Sumo2/3 microRNA or control microRNA, both driven by the neuron-specific synapsin promoter, were injected into the left common carotid artery (LCCA). The ligature around the left internal carotid artery (LICA) and the suture were closed and Lidocain gel was applied for pain relief. Mice were placed in a heated cage for 2 h and brought back into the animal facility for observation and lentivirus incubation for 72 h, when they were analysed for lesion volume differences in T2-sequences in the MRI, as described above (3.2.3.5).

3.2.5 Generation of transgenic mice

3.2.5.1 Recombinase-mediated cassette exchange (RMCE), silent mutations and the Tandem-affinity purification (TAP) cassette

Using the Recombinase-mediated cassette exchange (RMCE) system, target sequences can be inserted into an endogenous genomically silent locus, the Rosa26 locus, to avoid off-target effects of integration. This can be achieved by the recombination of flanking attB sites from the targeting vector with attP sites of the Rosa-acceptor site in the embryonic stem cell (ESC) with the help of ζ-C31 integrase. We used the acceptor ESCs where a Rosa26 allele carries a splice acceptor in intron 1 followed by a phosphor glyerate kinase promoter driving a hygromycin selection marker which is flanked by attP sites (kindly provided by Prof. Dr. Ralf Kühn and described in Hitz et al., 2007). Two transgenic mouse models were generated:

1) Mouse model 1: A Cre-inducible and therefore cell-type specific insertion of **EGFP-Sumo2/3 microRNA** into the silent Rosa26-locus

2) Mouse model 2: A Cre-inducible and therefore cell-type specific insertion of **Sumo2/3 microRNA-*sumo2/3*$^{tm\#(silent\ mutation)}$ overexpression-T2A-EGFP**

3.2.5.2 Target vector designs

The cassette exchange donor vector pRMCE was assembled within the backbone of pBluescript containing a modified polylinker region as described in Hitz et al., 2007. We inserted a flip and excision cassette (FLEX) based on (Kano, Igarashi et al. 1998) with lox2272 and loxP sites on both sides of the target expression sequence to allow for inducible Cre-dependent (and therewith cell type specific) expression of the target sequence. The target sequence for mouse model 1 (MM1) was composed of EGFP-Sumo2/3 microRNA which was oriented inversely within the two flanking loxP/lox2272 sites of the FLEX cassette. Upon Cre-recombination, the insert is inverted and expressed in the tissue where Cre is active. Mouse model 1 was created to be able to investigate Sumo2/3 microRNA expression in a spatially and temporally controlled manner in different pathologies. The target sequence of mouse model 2 (MM2) was generated following the same principle as in MM1. In addition to the EGFP-Sumo2/3 microRNA sequence, a silently mutated form of SUMO2 and SUMO3 (SUMO2/3$^{tm\#(silent\ \ mutation)}$) was reintroduced to replace the endogenous proteins. The mutated forms of SUMO2 and SUMO3 were tagged with his- and HA-tags, respectively, and a tandem-affinity purification cassette was inserted to screen for SUMO2- and SUMO3-specific SUMOylation targets.

Original sequence of *sumo2* mus musculus with the target region of the silent mutation:

Atg gcc gac gag aaa ccc aag gaa gga gtc aag act gag aac aac gat cat att aat ttg aag gtg gcg gga cag gat ggt tct gtg gtg cag ttt aag att aag agg cat aca cca ctt agt aaa cta atg aaa gcc tat tgt gaa cgg cag ggt ttg tca atg agg cag atc aga ttc cgg ttt gat ggg cag cca atc aac gaa aca gac aca cct gca cag ttg gaa atg gag gat gaa gat acg att gat gtg ttc cag cag cag act gga ggt gtc tac tag

Original sequence:	silent mutation:
tcaatgagg	agcatgcgg

Original sequence of *sumo3* mus musculus with the target region of the silent mutation:

Atg tcg gaa gag aag ccc aag gag ggt gtg aag aca gag aat gac cac atc aac ctg aaa gtg gcg ggg cag gat ggc tcg gtg gta cag ttc agg atc aag agg cac acc cca ctg agc aag ctg atg aag gcc tac tgt gag agg cag ggc ttg tca atg agg cag att cga ttc cgg ttt gat gga caa cca atc aat gaa aca gac act cca gcc cag ctg gag atg gag gat gag gac acc att gat gta ttc cag cag cag aca gga gga tca gcc tcc cga ggg agc gtc ccc aca ccc aac cgt tgt cct gac ctg tgc tat

Original sequence:	silent mutation:
tcaatgagg	agcatgcgg

Due to the redundant genetic code, the original sequence and the silently mutated sequence lead to the same protein product. However, the silently mutated form is not degraded by the Sumo2/3 microRNA.

3.2.5.3 Electroporation of RMCE embryonic stem cells (ESCs) and screening for positive cassette exchange

The donor vectors were coelectroporated with a ζ-C31 integrase into mouse acceptor ES-cells, which were kindly provided by Ralf Kühn, followed by selection with G418 for 7 days as described in (Hitz, Wurst et al. 2007). Resistant colonies were isolated and analyzed for cassette exchange by PCR. DNA from ESCs was isolated to identify positive clones using the Invisorb Spin Tissue Mini Kit according to the manufacturer´s instructions. The following primers were used to screen for target insertion:

Primer pair 1:
GT1: PGK promoter: 5´ - CACGCTTCAAAAGCGCACGTCTG - 3´
GT2: Neo N-terminus: 5´- GTTGTGCCCAGTCATAGCCGAATAG - 3´
Primer pair 2:
GT6: Rosa26: 5´- TAAGCCTGCCCAGAAGACTC - 3´
GT20: EGFP-N1: 5´- AACTTCAGGGTCAGCTTGCCG – 3´

3.2.5.4 Generation of transgenic mice and genotyping

Positive ES cells containing the MM1 or the MM2 construct, respectively, were injected into acceptor blastocysts. For screening of transgenic mice, tail biopsies were cut and DNA was isolated using the Invisorb Spin Tissue Mini Kit according to the manufacturer´s instructions. The same primer pairs as those used for screening of ESCs were used to run polymerase chain reactions (PCR) for verification of integration:

Primer pair 1:
GT1: PGK promoter: 5´ - CACGCTTCAAAAGCGCACGTCTG - 3´
GT2: Neo N-terminus: 5´- GTTGTGCCCAGTCATAGCCGAATAG - 3´
Primer pair 2:
GT6: Rosa26: 5´- TAAGCCTGCCCAGAAGACTC - 3´
GT20: EGFP-N1: 5´- AACTTCAGGGTCAGCTTGCCG – 3´

3.2.5.5 Breeding

Chimeric mice were crossbred with C57BL/6N wildtype mice to control for germline transmission of the transgenes. In addition, backcrossing onto a C57BL/6N genetic background allows for clearly defined congenic backgrounds for proper comparison between transgenic mouse lines and wildtype littermates. Ten generations of backcrossing are necessary for ≥ 99% of homogenous background, which can be accelerated using speed congenics, where the proportion of C57BL/6N background is checked for each or for selected generations. Only the animals with the highest target background proportion are bred further. Nevertheless, for experiments it is always necessary to compare transgenic mice with wildtype littermates from the same generation.

4. Results

4.1 *In vitro* model of embryonic primary cortical neurons

4.1.1 SUMOylation and neuronal ischaemic injury

4.1.1.1 Adenosine triphosphat (ATP) is lost in neurons after OGD

To analyse the effects of SUMOylation on neuronal ischaemic injury we chose the model of combined OGD that mimics ischaemia-like stress *in vitro*. First, we quantified ATP levels in cell lysates of primary cortical neurons to characterize the extent of metabolic disturbance after 15, 45, 75 min of OGD. The ATP levels decreased to 73.2% ± 10.8%, 44.9% ± 2.0%, and 22.0% ± 2.1% of controls (mean ± s.d.), respectively. Over a period of 180 min ATP levels were measured repeatedly for the three durations of OGD. Oxygen–glucose deprivation intervals of 15 and 45 min led to recovery of ATP after 180 min of reoxygenation to 78.9% ± 3.3% and 73.7% ± 4.7% of control cultures. In contrast, 75 min of OGD led to poor recovery in ATP levels to 54.1% ± 17.5% after 180 min. To investigate if lentiviral transduction has an effect on the dynamics of ATP loss after OGD, primary neurons were transduced with control microRNA-expressing LVPs and were subjected to 75 min of OGD. The maximum ATP depletion at 0 min reoxygenation was unaltered after transduction with lentiviral particles expressing control microRNAs and the recovery observed to 43% ± 8.3% after 180 min was poor, similar to that observed in untransduced cultures (Fig 5). Furthermore, the extent of depletion and recovery was not influenced by Sumo2/3 microRNA expression (e.g., 60.5% ± 18.5% versus 60.4% ± 4.1% after 0 min of reoxygenation and 89.5% ± 7.5% versus 86.2% ± 4.5% after 180 min of reoxygenation, control microRNA versus Sumo2/3 microRNA; 45 min OGD; mean ± s.d.; n = 4 derived from two independent experiments).

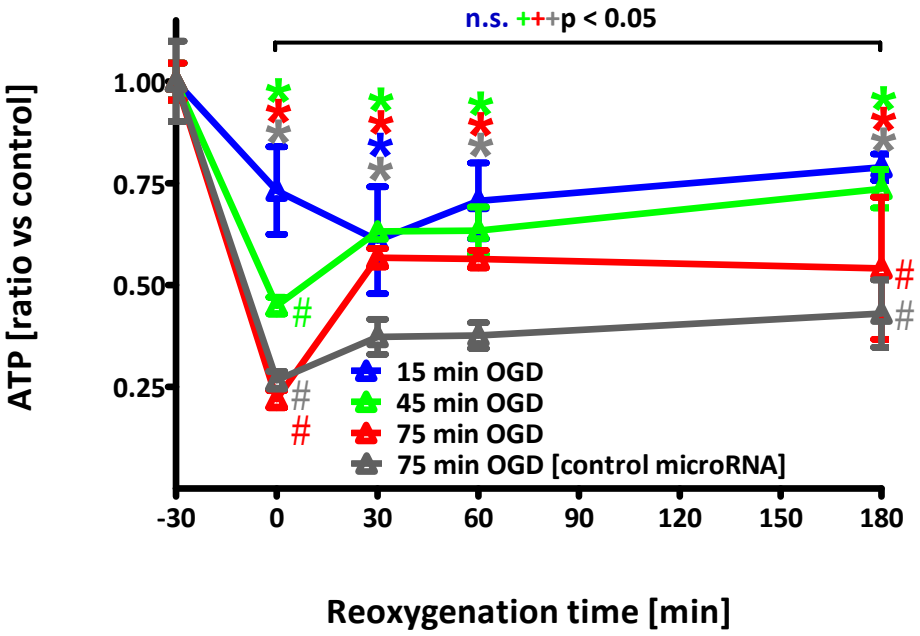

Fig 5: Characterization of ATP depletion and recovery after different durations of OGD. *ATP contents were analysed after 15, 45, and 75 min of OGD at different reoxygenation time points. Cultures with 75 min of OGD were compared with lentivirally transduced cultures (control microRNA). Data are presented as ratios versus controls and mean ± s.d.. Statistical analysis was performed for each length of OGD as one-way repeated-measures ANOVA (*p < 0.01 versus control). Interactions between duration of OGD and reoxygenation were analysed by a two-way repeated-measures ANOVA with* $F_{(1,\ 31)} = 39.5$ *(OGD duration), with* $F_{(1,\ 31)} = 59.2$ *(reoxygenation) and* $F_{(1,\ 31)} = 5.0$ *(duration × reoxygenation interaction), with p = 0.018 for interaction. The power of performed tests (α = 0.05) is 1 for the duration of OGD and reoxygenation and 0.7 for interaction. To isolate significant differences between groups, a Tukey post hoc analysis for multiple comparisons was performed. ATP recovery was significant for 15 and 45 min OGD (*p < 0.001; 180 min versus 0 min reoxygenation) and* $^{\#}p < 0.05$ *indicates the degree of ATP depletion referred to the duration of OGD (75 versus 45 min and 45 versus 15 min, respectively) either at 0 min or after 180 min recovery time. ATP depletion at 0 min reoxygenation and recovery at 180 min reoxygenation after 75 min of OGD did not differ significantly from that in cultures transduced with lentiviral particles to untransduced cultures. n = 4 for all conditions and timepoints.*

4.1.1.2 SUMO2/3 is induced upon OGD; its knockdown is neuronal specific and efficient

To interfere with the observed induction of SUMO2/3 after OGD, an RNA interference approach using microRNAs was applied. The Sumo2/3 microRNA was expressed under control of the synapsin promoter and compared over 12 days with expression of control microRNAs in primary mouse cortical neurons. The multiplicity of infection (MOI) was 50. Lentiviral transduction efficiencies were evaluated by comparing transmission images with EGFP fluorescence and counting EGFP-positive cells versus all cells in overlays. The transduction efficiencies were above 90%. Neuronal specificity of microRNA delivery along with EGFP as a reporter was driven by the synapsin promoter and evaluated by immunocytochemistry after paraformaldehyde (PFA) fixation on DIV12 with antibodies against EGFP, microtubuli-associated protein 2 (MAP2), and nuclear counterstain with 4',6-diamidino-2-phenylindole (DAPI). An overlay of EGFP- as well as Map2 fluorescence shows colocalization, reavealing that all microRNA expressing cells are neurons (Fig 6).

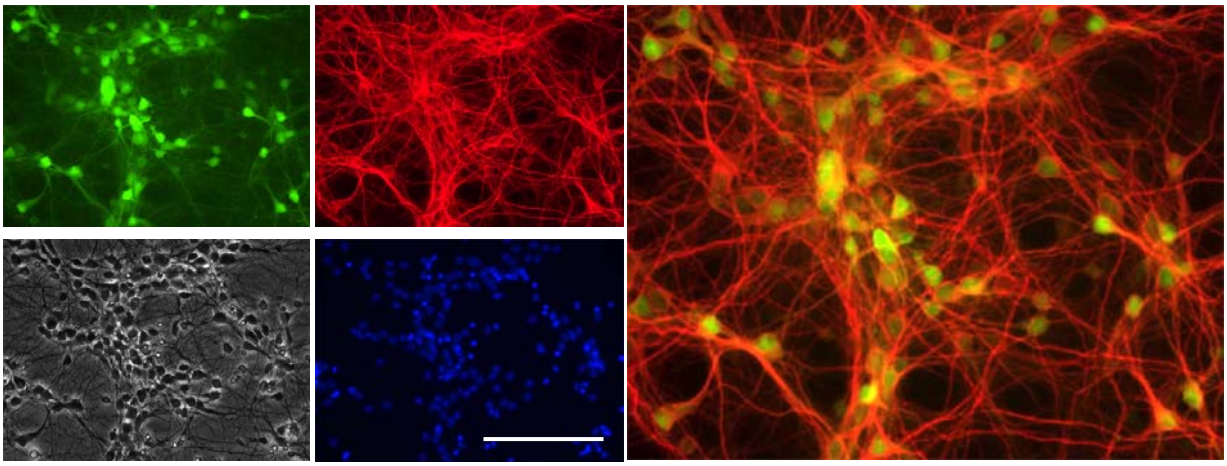

Fig 6: The synapsin promoter drives neuron-specific expression of microRNAs. *MicroRNAs were expressed over 12 days under the control of the synapsin promoter in primary mouse cortical neurons. Lentiviral transduction efficiencies were above 90% as analysed by comparing transmission images with EGFP fluorescence. Neuron specificity of microRNA delivery along with EGFP as a reporter was driven by the synapsin promoter and evaluated by immunocytochemistry with the marker for mature neurons microtubuli-associated protein 2 (Map2) along with the nuclear counterstain 4',6-diamidino-2-phenylindole (DAPI). The overlay shows EGFP-Map2 double-positive neurons. Scale bar=100 µm.*

To investigate induction of SUMO2/3 adducts and at the same time control for specific and efficient knockdown through Sumo2/3 microRNA, primary cortical neurons were transduced on DIV3 with either different control- or Sumo2/3 microRNAs. Protein lysates were analysed either without OGD (`baseline´) or after 45, 60 or 75 min of OGD and 3 h of reoxygenation (peak of SUMO2/3 protein adduction). Baseline cultures as well as cultures which had undergone 45 min of OGD were probed with antibodies against SUMO2/3, with GAPDH as a loading control and EGFP as an indicator for equal transduction efficiencies. Already at baseline SUMO2/3 adducts were observed, which might be due to a washing step which was carried out for control reasons at the time point of OGD, as SUMO2/3 induction is a very sensitive stress-induced system. However, in cultures subjected to 45 min of OGD, a further increase in SUMO2/3 adducts was observed. SUMO2/3 adducts as well as free SUMO2/3 were efficiently knocked down in both conditions when compared to control microRNA transduced cultures. There was no apparent difference in the EGFP expression pattern between groups, indicative of equal multiplicities of infection (Fig 7).

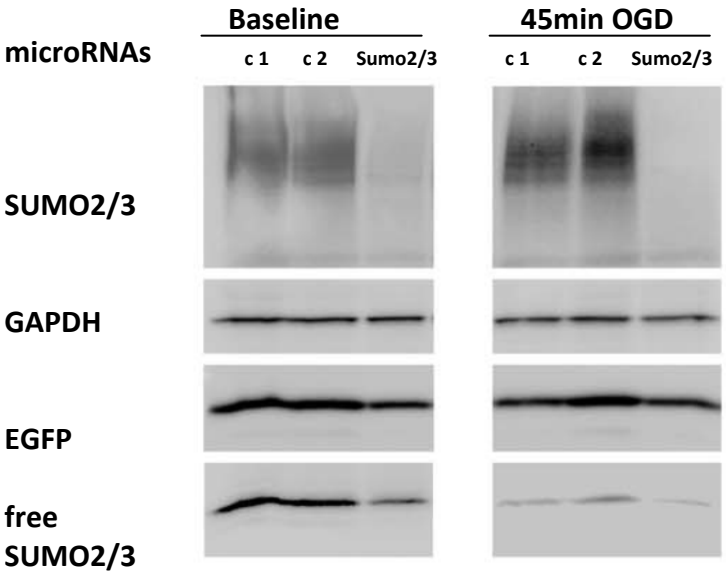

Fig 7: Knockdown of SUMO2/3 is efficient in primary cortical neurons. *Primary cortical neurons were transduced with lentiviral particles expressing either control- (c 1: control microRNA 1; c2: control microRNA 2) or Sumo2/3 microRNA on DIV3. On DIV10, they were either washed with PBS and incubated in medium another 3 h at 37 °C (Baseline), or subjected to 45 min of OGD. Protein lysates were harvested after 3 h of reoxygenation (peak of SUMO2/3 protein adduction) and analysed by Western immunoblotting with antibodies against SUMO2/3, with GAPDH as a loading control. EGFP expression corresponded to an equal MOI of lentiviral particles and concomitant microRNA expression. SUMO2/3 adducts as well as free SUMO2/3 were efficiently knocked down in both conditions if compared to control microRNA transduced cultures. The increase in SUMO2/3 protein adducts after OGD in control microRNA transfected neurons correlates inversely with the decrease of free SUMO2/3 protein. A representative blot is shown. Experiments were carried out in triplicate.*

Neuronal cultures which had undergone 60 or 75 min of OGD were also probed with antibodies against SUMO2/3, GAPDH and EGFP as before. Additionally, the same lysates were used for western immunoblotting using a SUMO1 antibody to investigate specificity of the Sumo2/3 microRNA. As shown in Fig 8, there was almost no cross-reaction between the two paralogues observed.

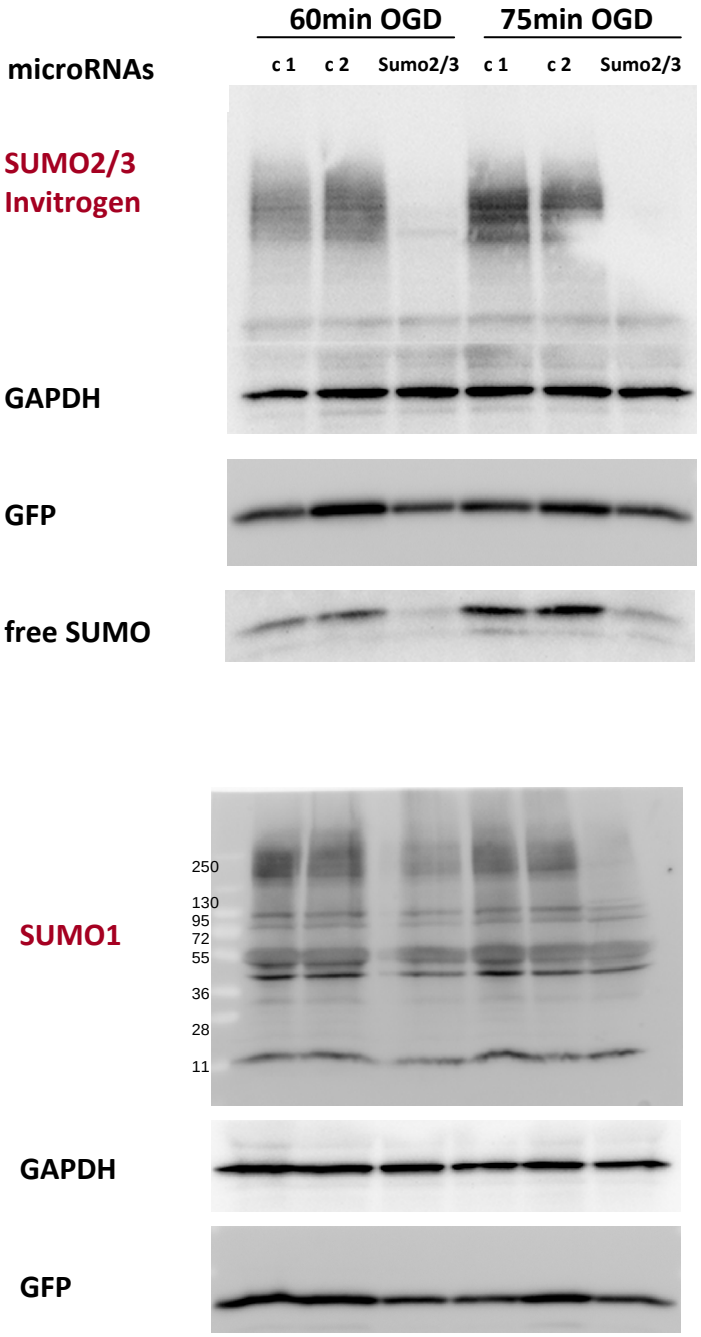

Fig 8: SUMO2/3 knockdown is specific. *Primary cortical neurons were transduced with lentiviral particles either expressing control- (c 1: control microRNA 1; c2: control microRNA 2) or Sumo2/3 microRNA on DIV3. On DIV10, they were subjected to 60 or 75 min of OGD, respectively. Protein lysates were harvested after 3 h of reoxygenation and analysed by Western immunoblotting with antibodies against SUMO2/3 for verification of knockdown efficiency, with GAPDH as a loading control, GFP as a transduction control and SUMO1 for investigation of the specificity of the SUMO2/3 knockdown. The SUMO2/3 protein adducts and free SUMO2/3 proteins were reduced after 60 and 75 min of OGD as a result of RNA interference. SUMO1 adducts stayed almost stable upon SUMO2/3 knockdown. A representative blot is shown. Experiments were carried out in triplicate.*

4.1.1.3 Neuron-specific expression of Sumo2/3 microRNA does not affect survival of cultured neurons

After having characterized OGD as a model as well as efficacy and specificity of SUMO2/3 knockdown in primary cortical neurons, a new cell survival assessment strategy was applied to investigate the effects of SUMO2/3 knockdown on baseline survival of neurons over 12 days *in vitro*. The Sumo2/3 microRNA was expressed under control of the synapsin promoter and compared with expression of control microRNAs in primary mouse cortical neurons. Lentiviral transduction efficiencies were above 90% as analysed by comparing transmission images with EGFP fluorescence and counting EGFP-positive cells. For analysis of neuronal survival over time, 11 ROIs per 24-well were preselected and analysed repeatedly over time. Surviving EGFP-positive cells were counted on DIV6, 9 and 12. The effects of Sumo2/3 microRNA on neuronal survival were investigated comparing the ratios between EGFP-positive cells on DIV9/6 and DIV12/9. There was no statistically significant difference between the groups. The expression of Sumo2/3 microRNAs in primary neuronal cultures did not lead to changes in vulnerability or viability in comparison with control microRNA-transduced neurons. Furthermore, even after prolonged periods of time in culture (DIV12/9), the survival ratios of both groups were comparable to those of the shorter life span (DIV9/6), see Fig 9.

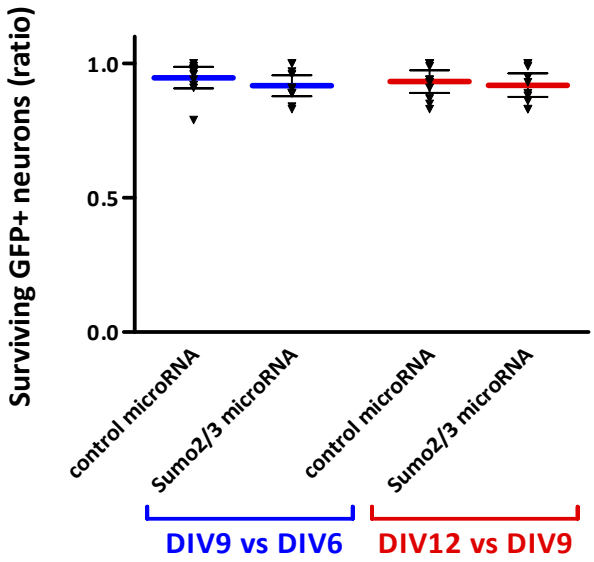

Fig 9: Sumo2/3 microRNA does not influence baseline survival of cultured neurons up to DIV12. *On DIV3, primary cortical neurons were lentivirally transduced to achieve Sumo2/3 or control microRNA expression. Microscopic pictures of EGFP fluorescence (indicative for microRNA delivery) were taken at DIV6, 9, and 12 as described in the materials and methods' section. EGFP-expressing neurons were counted and ratios were calculated for DIV9/6 (indicated in blue) and DIV12/9 (red) to evaluate cell survival over time. We assumed an effect size > 0.15 and performed a prospective power analysis with α = 0.05 and β = 0.20. There was no significant difference between groups in a two-way repeated-measures ANOVA followed by Tukey's post hoc analysis N = 3 for all timepoints and transduction conditions.*

4.1.1.4 Tolerance to OGD is lost in neurons after SUMO2/3 silencing

Next, we investigated the influence of SUMO2/3 silencing in neuronal cultures under stress. We therefore chose the model of OGD that mimics ischaemia-like stress *in vitro.* Primary cortical mouse neurons were transduced with control- or Sumo2/3 microRNA, respectively. They were analysed over time using different life-death assays. On DIV12, the cultures were subjected to either 15, 45, 60 or 75 min of OGD, respectively, and analysed 24 h later.

4.1.1.5 Survival is impaired following SUMO2/3 knockdown in OGD challenged primary cortical neurons

The same 11 ROIs per 24-well that were preselected for the baseline survival analysis were investigated just before and 24 h after different lengths of OGD. Extent of OGD-induced cell death was evaluated by calculating the ratios between the numbers of EGFP-positive neurons on DIV13/12 (directly before and 24 h after OGD) and compared with baseline cell counts as a ratio (DIV12/6). Oxygen–glucose deprivation intervals of 15 and 45 min did not result in any significant cell loss of neurons expressing control microRNA (Fig 12, as reflected by recovery of ATP levels, see 4.1.1.) In contrast, 75min of OGD led to a significant cell loss, with levels dropping to 54.3% ± 13.3% (Fig 10, and to poor recovery in ATP levels, see 4.1.1.). The RNA interference performed with neuron-specific Sumo2/3 microRNA resulted in a reduction in cell numbers to 40.3% ± 18.8% with an OGD interval of 15 min, an insult which did not harm neurons expressing control microRNA (Figure 10). With longer OGD duration, neurons expressing Sumo2/3 microRNA were even more susceptible to damage by OGD. Survival rates decreased to 28.1% ± 10.4% and 0.7% ± 1.5% for 45 and 75 min of OGD, respectively (Figure 12). Interactions between microRNA and OGD effects were analysed by a two-way repeated-measures ANOVA with $F_{(1,\ 67)} = 97.5$ (15 min OGD, panel A), with $F_{(1,\ 57)} = 157.4$ (45 min OGD, panel B) and $F_{(1,\ 41)} = 62.6$ (75 min OGD, panel C) with $P < 0.001$ for interaction. The power of the tests performed was 1 ($\alpha = 0.05$ and $\beta = 0.2$). To isolate significant differences between groups, a Tukey post hoc analysis for multiple comparisons was performed and p-values are indicated in the figures**.** All comparisons between neurons transduced with Sumo2/3/ or control microRNA yielded p-values < 0.001 for the interaction of microRNAs and OGD duration (Figure 10).

A.

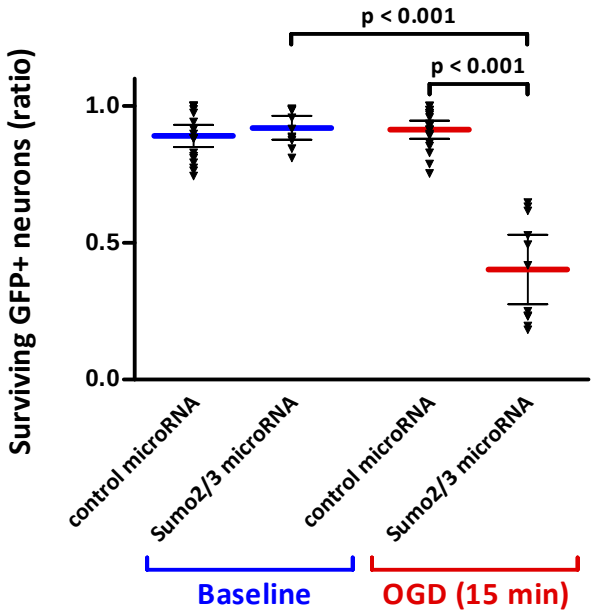
p < 0.001
p < 0.001
Surviving GFP+ neurons (ratio)
1.0
0.5
0.0
control microRNA
Sumo2/3 microRNA
control microRNA
Sumo2/3 microRNA
Baseline
OGD (15 min)

B.

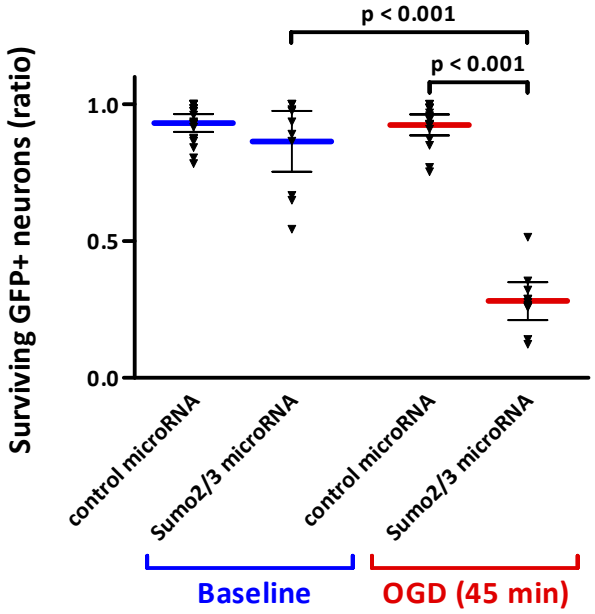
p < 0.001
p < 0.001
Surviving GFP+ neurons (ratio)
1.0
0.5
0.0
control microRNA
Sumo2/3 microRNA
control microRNA
Sumo2/3 microRNA
Baseline
OGD (45 min)

C.

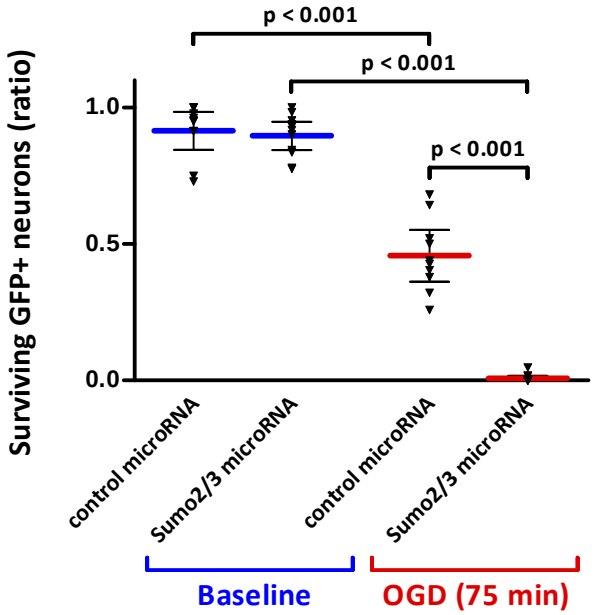

Fig 10: Tolerance to OGD is lost in neurons after SUMO2/3 silencing. *On DIV3, primary cortical neurons were lentivirally transduced to achieve Sumo2/3- or control microRNA expression. On DIV12, cultures were exposed to 15, 45, or 75 min of OGD resulting in no or significant damage of control microRNA expressing cultures. Predefined regions of interest were recorded using a semi-automated software algorithm, and the number of EGFP-expressing neurons per region was counted before and 24 h after OGD. Extent of OGD-induced cell death was evaluated by calculating the ratios between the numbers of EGFP-positive neurons on DIV 13/12 (directly before and 24 h after OGD) and compared with baseline cell counts as a ratio (DIV 12/6). Interaction between microRNA and OGD effects was analysed by a two-way repeated-measures ANOVA with* $F_{(1, 67)} = 97.5$ *(15 min OGD, panel A), with* $F_{(1, 57)} = 157.4$ *(45 min OGD, panel B) and* $F_{(1, 41)} = 62.6$ *(75 min OGD, panel C) with* $P < 0.001$ *for interaction. The power of the tests performed is 1 (*$\alpha=0.05$ *and* $\beta = 0.2$*). To isolate significant differences between groups, a Tukey post hoc analysis for multiple comparisons was performed and p-values are indicated in the figures. The loss of viable neurons depended heavily on the damage incurred (microRNA × OGD interaction, two-way ANOVA,* $P < 0.001$*). n = 3 for all conditions.*

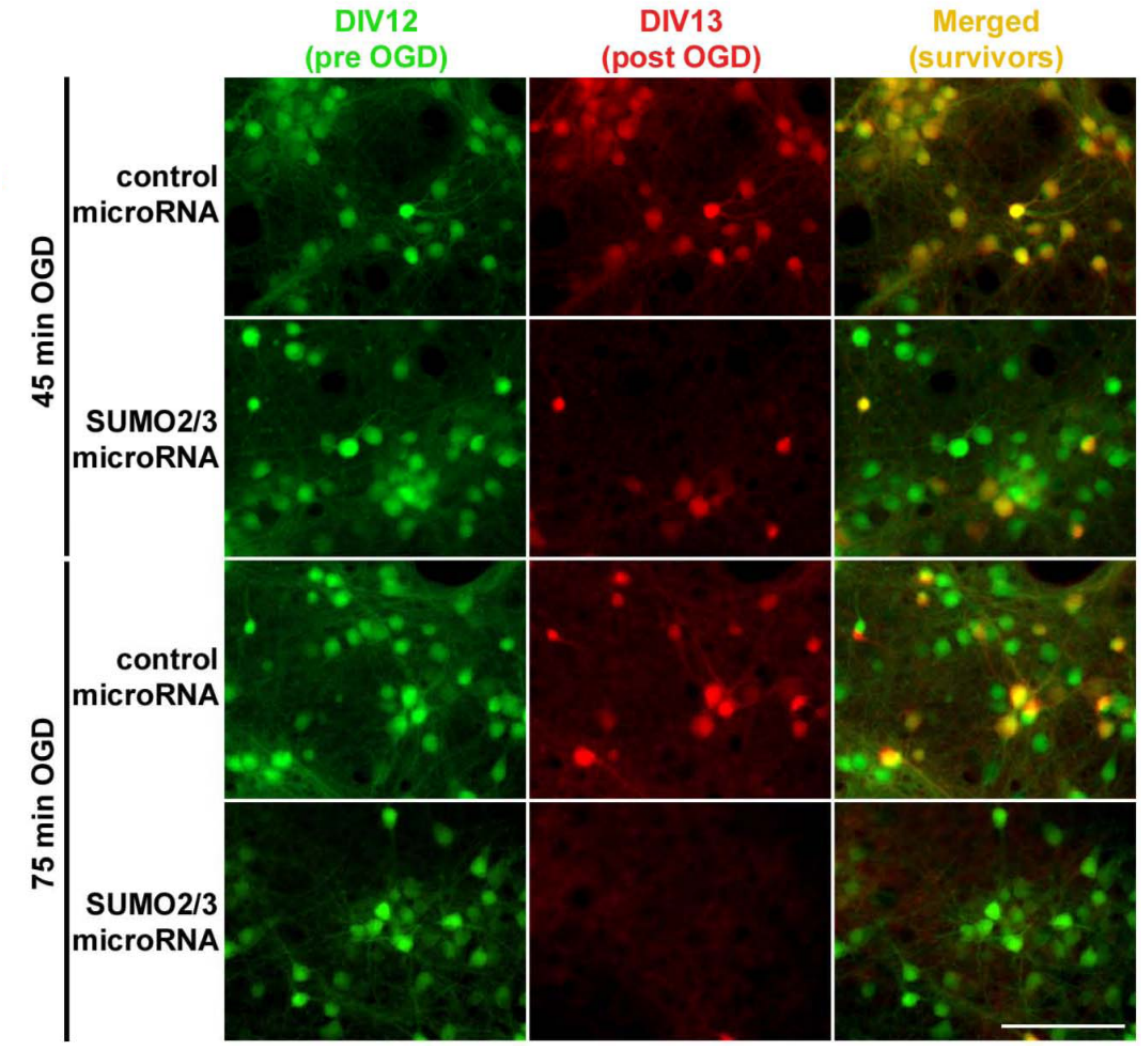

Fig 11: Effect of Sumo2/3 microRNA expression on neuronal survival after OGD. *To illustrate the effects of microRNA expression on the extent of OGD-induced cell death, digital images of EGFP expressing neurons were false colored before (green, left panel, DIV12) and 24 h after OGD (red, middle panel, DIV13). Merged yellow neurons are indicative for survival, green cells are indicative for lost neurons (right panel, merged pictures from DIV12 and 13). Scale bar = 100 µm.*

4.1.1.6 Lactate-dehydrogenase release is increased upon SUMO2/3 knockdown in combination with OGD

As an indirect marker for cell membrane disruption, LDH release into the medium of transduced primary cortical neurons was measured at baseline and 24h after 75min of OGD. In congruence with the cell count data, the LDH activity in the supernatant was significantly increased upon ischaemia-like stress after 24 h ($p < 0.001$ for OGD × microRNA interaction, Fig 12.

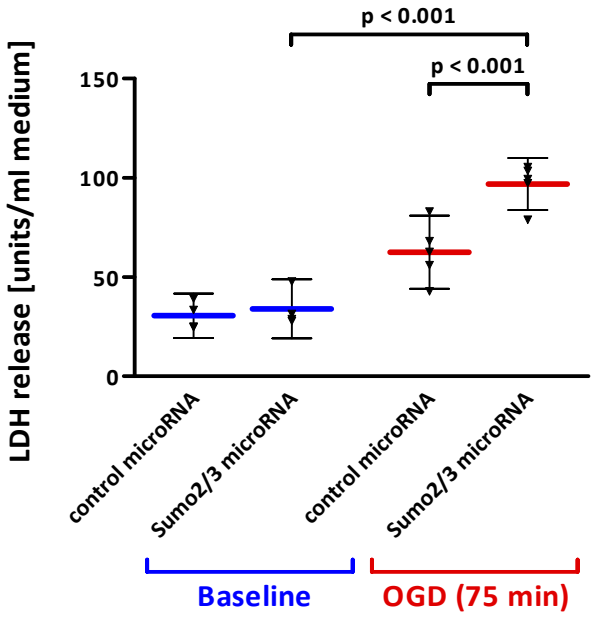

Fig 12: LDH release is significantly increased after OGD upon Sumo2/3 microRNA transduction. *The LDH assay measures the reduction in co-factor ß-NADH used in the LDH driven reaction at the excitation wave-length of 340 nm. Lactate-dehydrogenase release into the medium of transduced primary cortical neurons was measured at baseline and 24 h after 75 min of OGD and was significantly increased upon ischaemia-like stress after 24 h ($p < 0.001$ for OGD × microRNA interaction). N = 3 for all conditions.*

4.1.1.7 Inverse correlation of surviving neurons versus LDH release

To validate our new method for determining survival rates of neurons expressing the EGFP reporter along with the microRNAs, we plotted the normalized LDH release from these cultures (shown as a ratio to the maximum LDH release) to the ratio of EGFP-positive cells. This correlation was performed at baseline and after three different lengths of OGD exposure time in cultures transduced with control microRNA and analysed 24 h after OGD. The correlation that emerged is inverse (R^2 = 0.79, p = 0.007), signifying that the loss of GFP^+ neurons in predefined ROIs before and after 24h after OGD is accompanied by an increase in LDH activity in relation to the maximum activity achievable by total cell lysis in a given well.

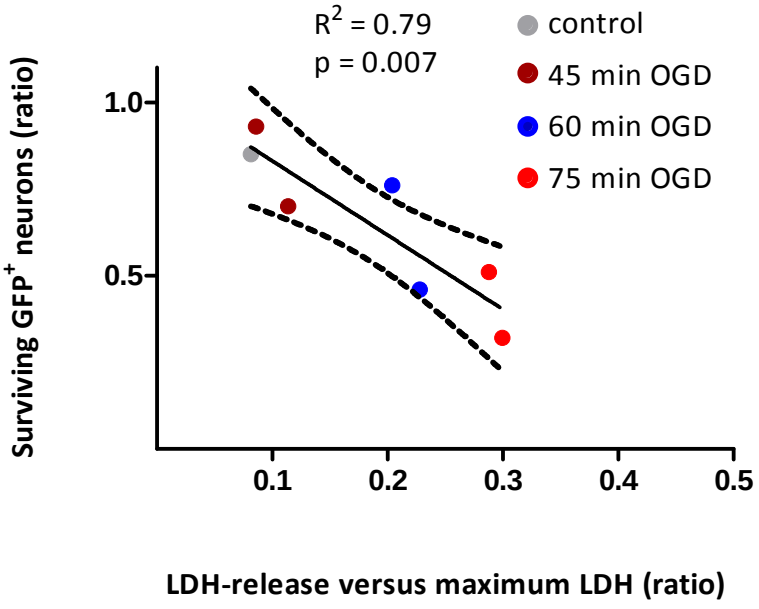

Fig 13: Method validation - Inverse correlation of GFP^+ neurons and LDH release. *Primary neuronal cultures were transduced with control microRNA and underwent different lengths of OGD exposure time. After 24 h, LDH release into the medium was measured for control cultures as well as three different OGD exposure times. From the same cultures the survival of GFP^+ neurons was assessed as shown in Figure 11. The mean values of the ratios (before and after OGD) per well were plotted against LDH activity (release per well/maximum LDH release). There is an inverse correlation of the loss of viability to the increase in normalized LDH release with $R^2 = 0.79$, $F_{(1, 7)} = 19.1$, $p = 0.007$.*

4.1.1.8 Propidium iodide incorporation is strongly enhanced upon SUMO2/3 knockdown in combination with OGD

As a third damage assessment strategy, propidium iodide incorporation was measured in control- as well as Sumo2/3 microRNA transduced neurons. The measurements were made 24 h after 75 min of OGD and compared to control sister cultures. Phase-contrast images were taken and merged to red fluorescence pictures of the same ROIs. Viable, PI-negative (PI^-) neurons were counted and expressed as a ratio to all neurons counted in transmission images. An OGD lasting 75 min led to a significantly greater decrease of viable PI^- neurons in the Sumo2/3 microRNA transduced group compared with the decrease seen in neurons subjected to OGD transduced with control microRNA (Figure 14).

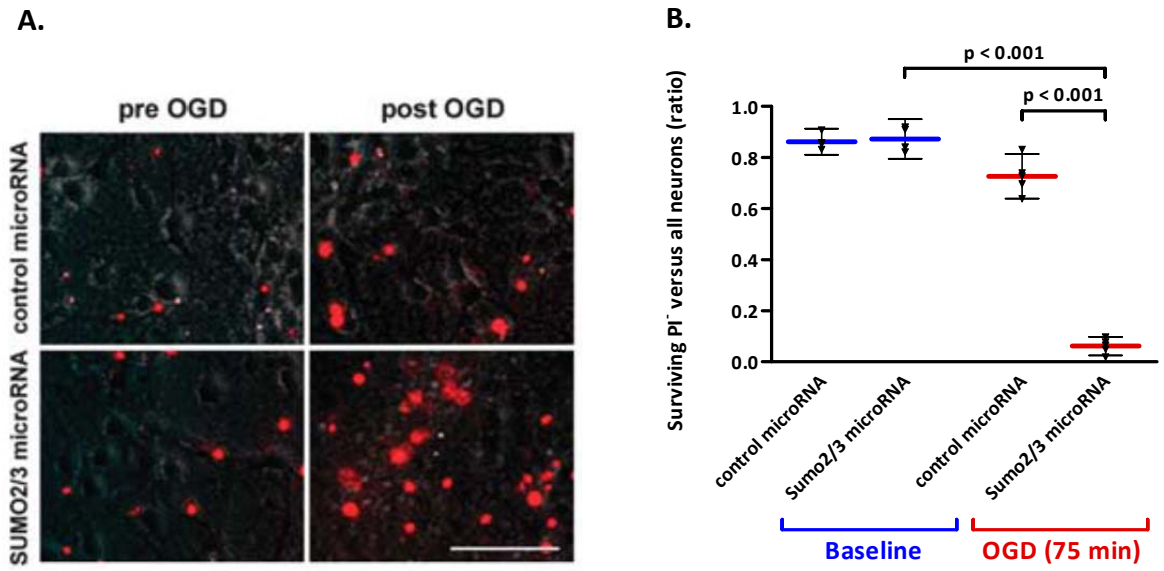

Fig 14: Propidium iodide incorporation is strongly enhanced upon SUMO2/3 knockdown in combination with OGD. *On DIV3, primary cortical neurons were lentivirally transduced to achieve Sumo2/3- or control microRNA expression. Propidium iodide (PI) was added 24 h after 75 min of OGD and phase-contrast images were merged to the red fluorescence channel. (Panel A) representative pictures illustrate PI incorporation after OGD or in the control sister cultures. (Panel B) Quantification of viable, PI-negative (PI^-) neurons as a ratio to all neurons counted in transmission images. Interactions between microRNA and OGD effects were analysed by a two-way ANOVA with $F_{(1, 17)} = 211.7$ with $p < 0.001$ for interaction followed by Tukey's post hoc analysis. The decrease in viable PI-negative neurons was severely enhanced in neurons tranduced with Sumo2/3 microRNA compared to the control group. N = 3 for all conditions.*

4.2 *In vitro* model of adult organotypic retina explant cultures

4.2.1 SUMOylation and glutamate toxicity

4.2.1.1 Sumo2/3 microRNA transduced neurons of the retinal ganglion cell layer show increased vulnerability to glutamate toxicity compared to controls

After having analysed the effects of SUMOylation on neuronal ischaemic injury *in vitro* in embryonic cultures, we went one step further and investigated the effects of SUMO2/3 knockdown in an *in vitro* model of adult neurons.Retina explant cultures were transduced with either control microRNA or Sumo2/3 microRNA expressing lentiviral particles. Sister cultures were used as controls. After cultivation for 6 days under constant rotation, half of the cultures from each group were challenged through adding 5 mM glutamate to the medium for 24 h. Pycnotic cells from the retinal ganglion cell layer (RGC) were counted in a haematoxylin-eosin staining on paraffin sections in groups with and without damage. The combination of SUMO2/3 knockdown and glutamate damage led to a significantly greater increase in pycnotic neurons in the RGC than that seen in control microRNA transduced groups. This model might mimick excitotoxicity and stress-related responses in a more physiological way than primary cortical neurons. As it has no artificial enlargement of the extracellular space, disruptions in the composition of the extracellular matrix directly lead to secondary damage in neighbouring cells. Therewith this reflects the *in vivo* situation in a more physiological way. Furthermore, since SUMO conjugation patterns are of impact on developmental processes, the study of adult neurons in an organotypical approach might predict better whether SUMO serves as an endogenous neuroprotective stress reponse in the mature brain. However, limitations of the model are unknown changes in the molecular pattern of retinal ganglion cells due to axotomy which might itself induce stress responses or adaption during preparation and culturing.

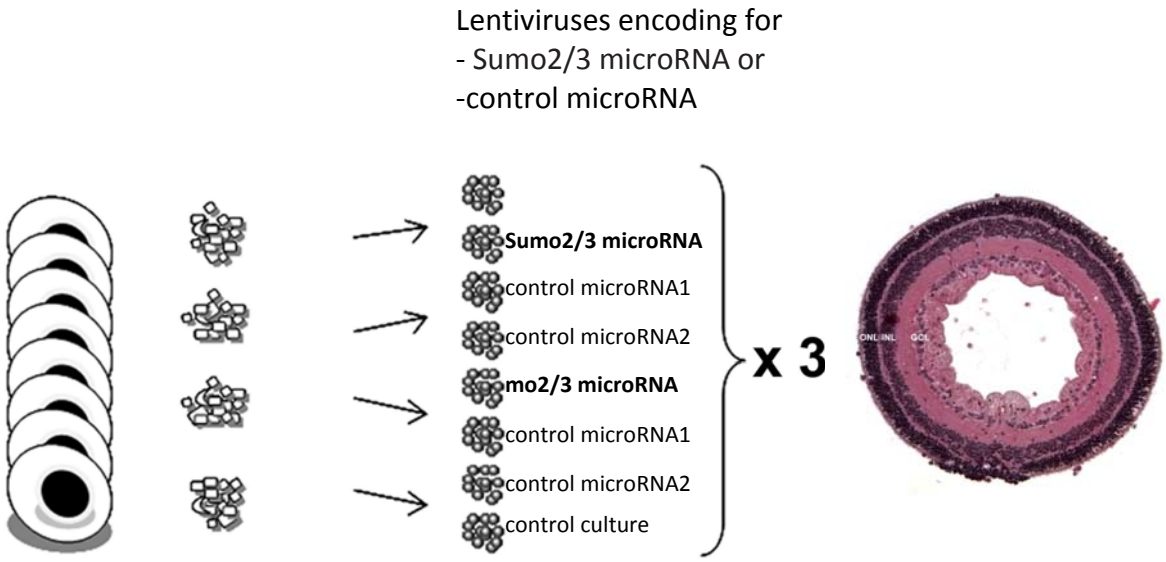

Fig 15: Schematic illustration of organotypic retina explant cultures. *Retina explant cultures were transduced with either control microRNA or Sumo2/3 microRNA expressing lentiviral particles and incubated as a rolling culture for 6 days. Then they were challenged through application of glutamate and fixated and embedded for eosin-haematoxylin staining and further analysis.*

A.

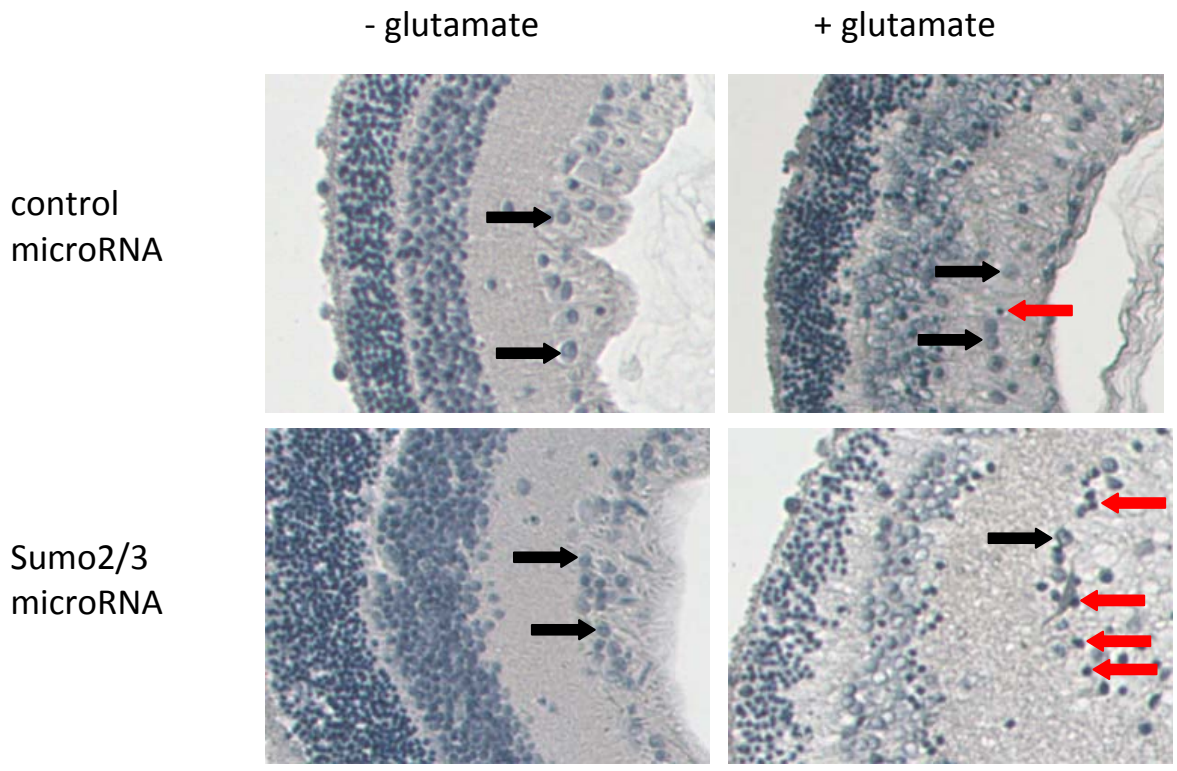

B.

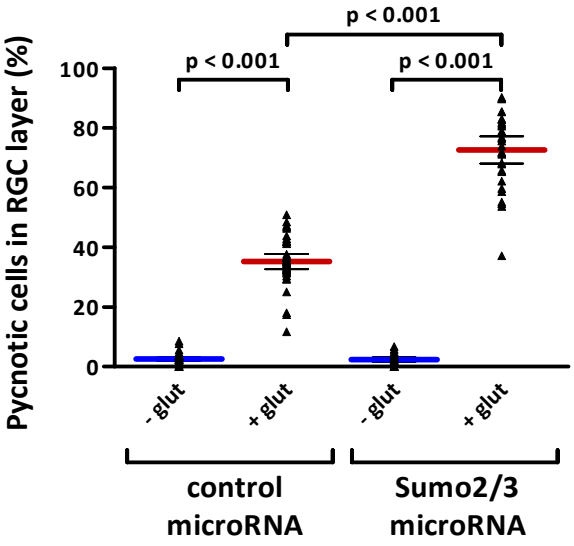

Fig 16: SUMO knockdown increases susceptibility to glutamate stress. *Primary organotypical retina cultures from Wistar rats were transduced with lentiviruses to achieve Sumo2/3 microRNA or control microRNA expression. On DIV6, they were challenged by the addition of 5 mM glutamate to the medium for 24 h. After paraffin embedding, 8 µm thin sections were cut and stained with haematoxylin-eosin.* ***A.*** *Pycnotic cells in the retinal ganglion cell layer (RGCL) were counted and expressed as a ratio to total cell numbers in the RCG (healthy RG cells: black arrows, pycnotic RG cells: red arrows).* ***B.*** *Interactions between microRNA and glutamate stress effects were analysed by a two-way ANOVA with* $F_{(1,141)}$ *with* $p < 0.001$ *for interaction followed by Tukey's post hoc analysis. Quantification revealed an increase in pycnotic cells after glutamate stress in the Sumo2/3 microRNA transduced group. N =3 for all conditions.*

4.3 *In vivo* models of cerebral ischaemia: SUMOylation and ischaemic brain injury

Following the experiments in cell culture as well as in organotypical explant cultures, *in vivo* experiments were carried out to assess the effects of SUMO2/3 knockdown in mice after stroke. To that end, different transduction methods were applied together with behavioural assessment and MRI *in vivo* imaging.

4.3.1 Stereotactic lentivirus application and MCAo

Lentiviral particles were injected into the cortex of SV129 wildtype mice to downregulate SUMO2/3 expression in the penumbra region of experimental stroke and compare it to control microRNA expression. After two weeks of incubation, a 30 min MCAo was carried out and behavioural outcome was assessed 2 and 4 days later in a pole test. Magnetic resonance imaging was carried out 3 and 10 days post stroke. Ten days after MCAo, the mice were sacrificed and brains were analysed in a NeuN-staining on cryosections to determine lesion volumes on a cellular level.

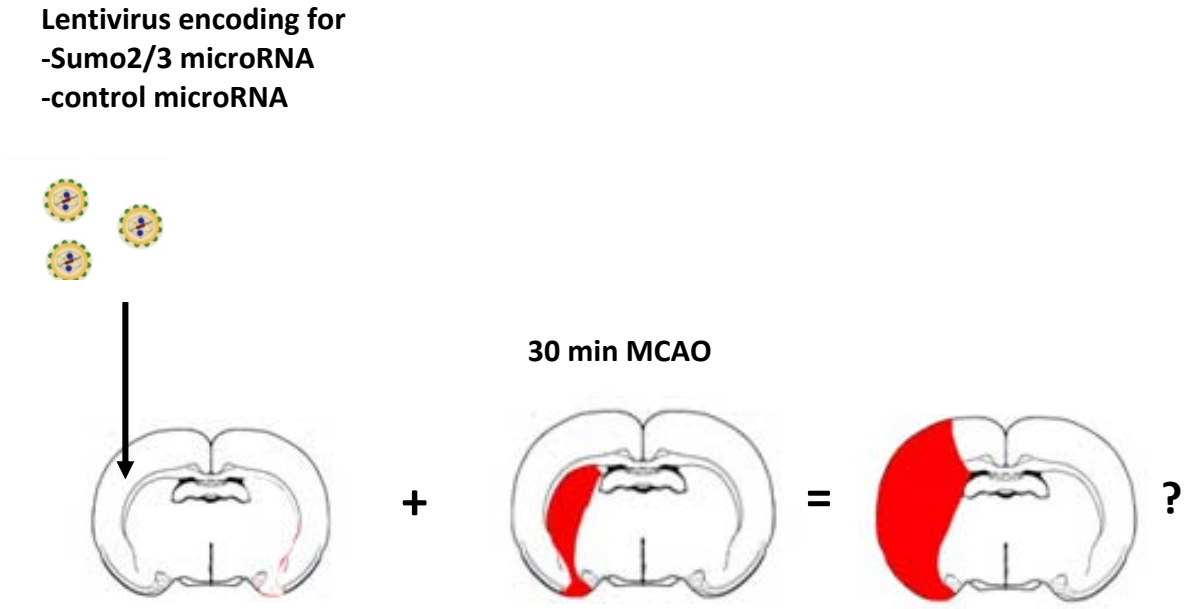

Fig 17: Experimental setup illustrating injection of lentiviral particles into the penumbra region followed by 30 min MCAo.

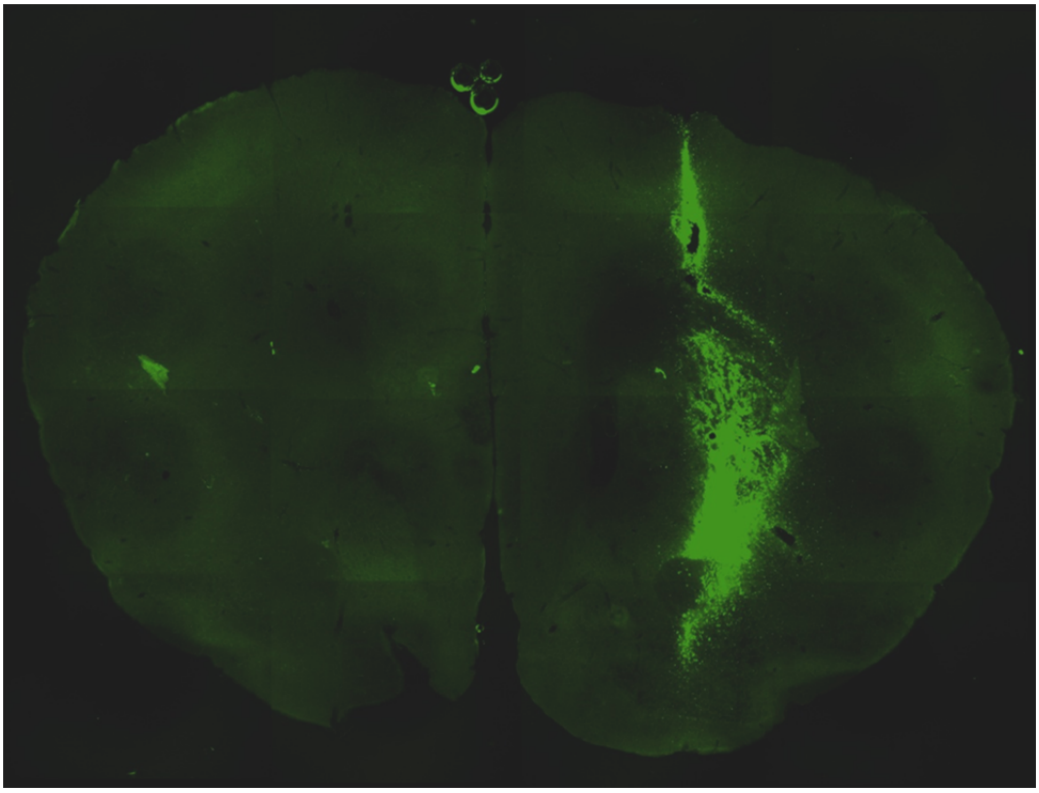

Fig 18: Exemplary image of transduction area of lentiviruses expressing EGFP, which were injected into the striatum of a wildtype mouse.

4.3.1.1 Mice with SUMO2/3 knockdown in the cortex do not show impaired behaviour in the pole test after stroke

Behavioural assessment of motor function after MCAo was analysed by a researcher not aware of the experimental groups. The time to turn and the time to come down in a pole test were slightly longer for the Sumo2/3 microRNA-injected group, however no significant difference was detected.

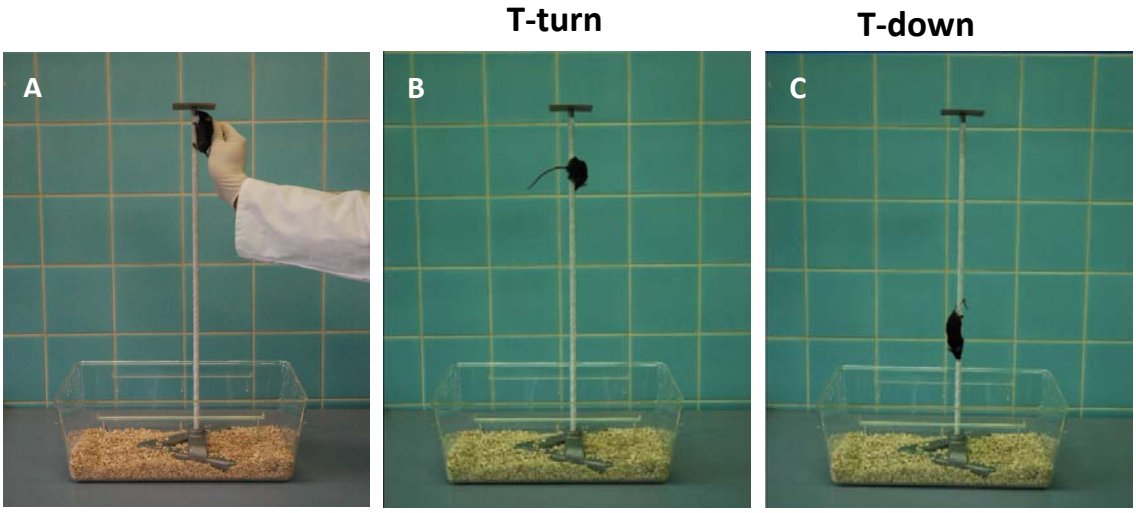

Fig 19: Illustration of the pole test procedure. A. *The mouse was placed head upwards near the top of the pole.* ***B.*** *The time it needed to turn completely head downward was recorded (T-turn).* ***C.*** *The time the animal needed to reach the ground with all 4 paws was recorded as T-down. Five trials were carried out per mouse, mean values of the 5 results were further analysed statistically. N = 16.*

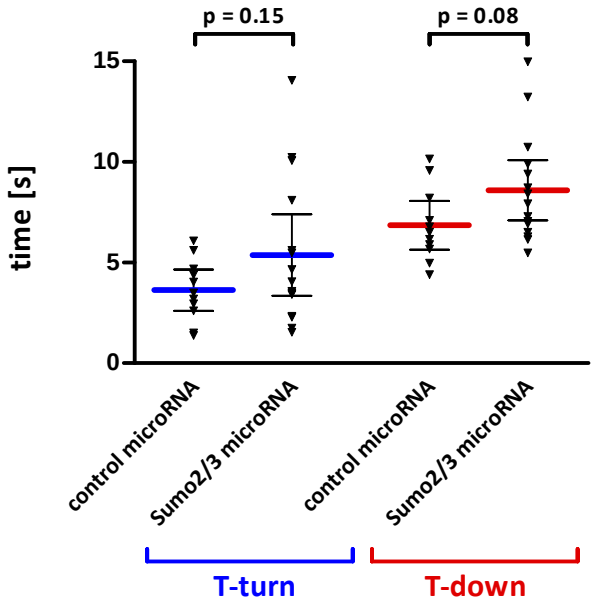

Fig 20: Pole test quantification reveals no impaired behaviour after SUMO2/3 knockdown in the cortex of ischaemic mice. *Mice were tested 2 and 4 days after MCAo for t-turn and t-down as illustrated in Figure 19. Five trials per mouse were carried out and the mean values of the results were statistically analysed. No statistical difference was detected, p = 0.08. n = 16.*

4.3.1.2 Magnetic resonance imaging volumetry is not altered, either 72h or 10d after MCAo

Magnetic resonance imaging was performed 72 h and 10 d after stroke using a 7 Tesla rodent scanner. Lesion volumetry was carried out 72 h after MCAo analysing the hyperintense areas of ischaemic tissue in T2-weighted images. As depicted in figure 21, no differences in infarct volumes between control microRNA and Sumo2/3 microRNA injected animals were detected.

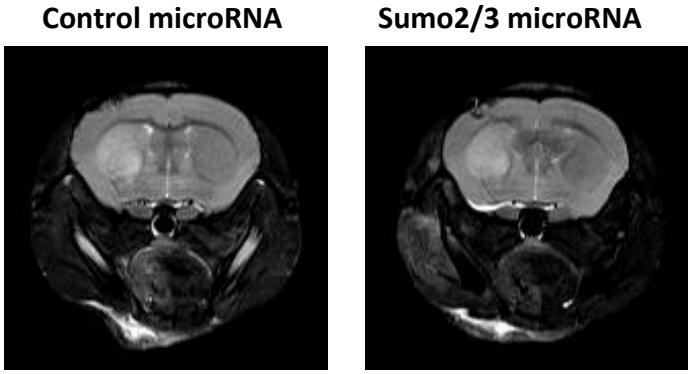

Fig 21: No differences in infarct volume were observed between Sumo2/3 microRNA and control microRNA injected mice. *As shown in these illustrative pictures, no infarct volume differences were detected due to Sumo2/3 microRNA expression, neither 72 h nor 10 d after MCAo.* ***A.*** *Control microRNA injected mice.* ***B.*** *Sumo2/3 microRNA injected mice. N = 16.*

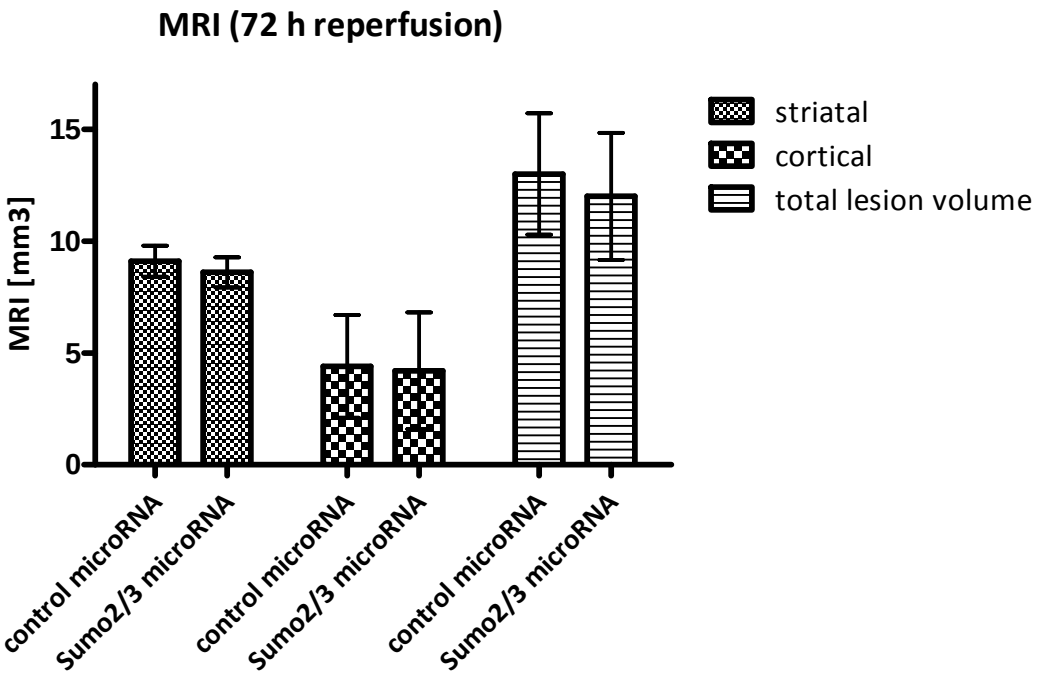

Fig 22: MRI lesion volume quantification does not show any macroscopic difference between groups. *Mice were analysed 72 h after MCAo for lesion volume differences in the hyperintense areas of ischaemic tissue in T2-weighted images. Striatal, cortical and total lesion volumes were measured and calculated using a threshold-based segmentation by connecting all pixels within a specified threshold range around the selected seed pixel to get a 3D object map of the whole stroke region. The total volume of the whole object map was automatically calculated. A two-way ANOVA was carried out followed by a Tukey post hoc analysis for multiple comparisons. There was no statistically significant difference between groups. N = 16.*

4.3.1.3 NeuN staining reveals no difference in infarct sizes between Sumo2/3- and control-microRNA transduced cortical neurons *in vivo*

Ten days after MCAo, mice were sacrificed and brains were cut in 20 µm coronal cryosections and stained for NeuN to analyse the extent of neuronal damage on a cellular level. Infarct volumes were analysed using the Olympus CellM software in 5 infarct levels and calculated as described. There were no differences detected in infarct volumetry between groups.

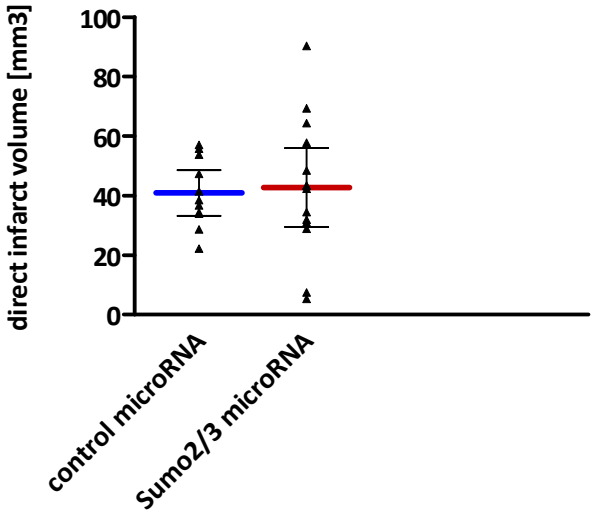

Fig 23: Direct infarct volumes are not altered upon Sumo2/3 microRNA transduction after MCAo. *A NeuN staining was carried out on coronal cryosections 10 days after MCAo. Analysed by a researcher not aware of the experimental groups, no difference in infarct sizes was observed on the cellular level. N = 16.*

4.3.2 Intraarterial lentivirus application and MCAo

4.3.2.1 Magnetic resonance imaging does not reveal short-term differences in infarct volumetry

Wildtype mice underwent 30 min of MCAo. Upon reperfusion, lentiviral particles encoding either for control microRNA or for Sumo2/3 microRNA and driven in both cases by the neuron-specific synapsin promoter were injected into the left common carotid artery (LCCA). Three days later, the mice were scanned with T2-weighted sequences in a 7 tesla MRI. Infarct sizes were determined as described above. There was no difference in infarct sizes observed between groups.

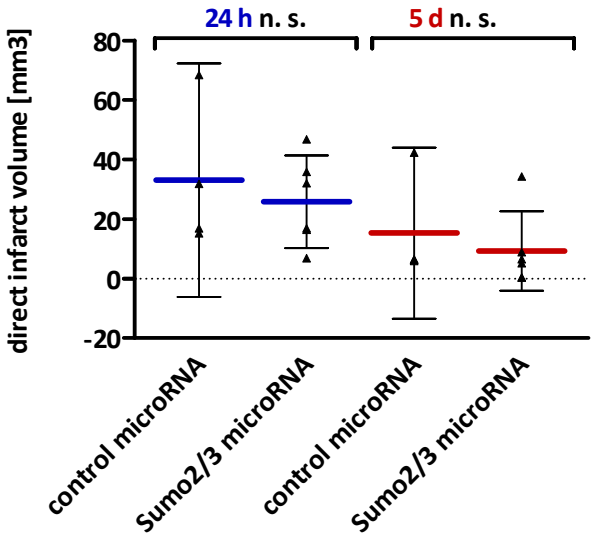

Fig 24: No lesion volume differences were detected after intraarterial Sumo2/3 compared to control microRNA injection followed by MCAo. *Mice were analysed 72 h after MCAo for lesion volume differences in the hyperintense areas of ischaemic tissue in T2-weighted images. Total lesion volumes were measured and calculated using a threshold-based segmentation by connecting all pixels within a specified threshold range around the selected seed pixel to get a 3D object map of the whole stroke region. The total volume of the whole object map was automatically calculated. A two-way ANOVA was carried out followed by a Tukey post hoc analysis for multiple comparisons. There was no statistically significant difference between groups. N = 16-17.*

4.4 Generation of transgenic mice

Two transgenic mouse models were generated as a tool to investigate the cell type-specific and inducible effects of SUMOylation in stroke and other relevant pathologies. To that end, targeted integration into the transcriptionally silent Rosa26 locus was facilitated. A tandem affinity purification cassette was introduced to screen for SUMO2- and SUMO3-specific target proteins. The expression cassettes were integrated in reverse orientation within a flip-and-exchange cassette to avoid developmental influences. The stop cassette within the inversely orientated cassette consists of an open reading frame v5-tag including a translational stop. This is followed by two transcriptional stops (polyA sequence) in reverse complement orientation to guarantee stable expression and processing of the polyA tail and to avoid gene trapping. Furthermore, an SV40 polyA sequence was added in forward orientation to make sure that without cre recombinase transcription of the microRNAs is stopped. Upon cross-breading with transgenic Cre recombinase expressing mouse lines, the expression cassette is inversed and transcribed in a tissue specific manner.

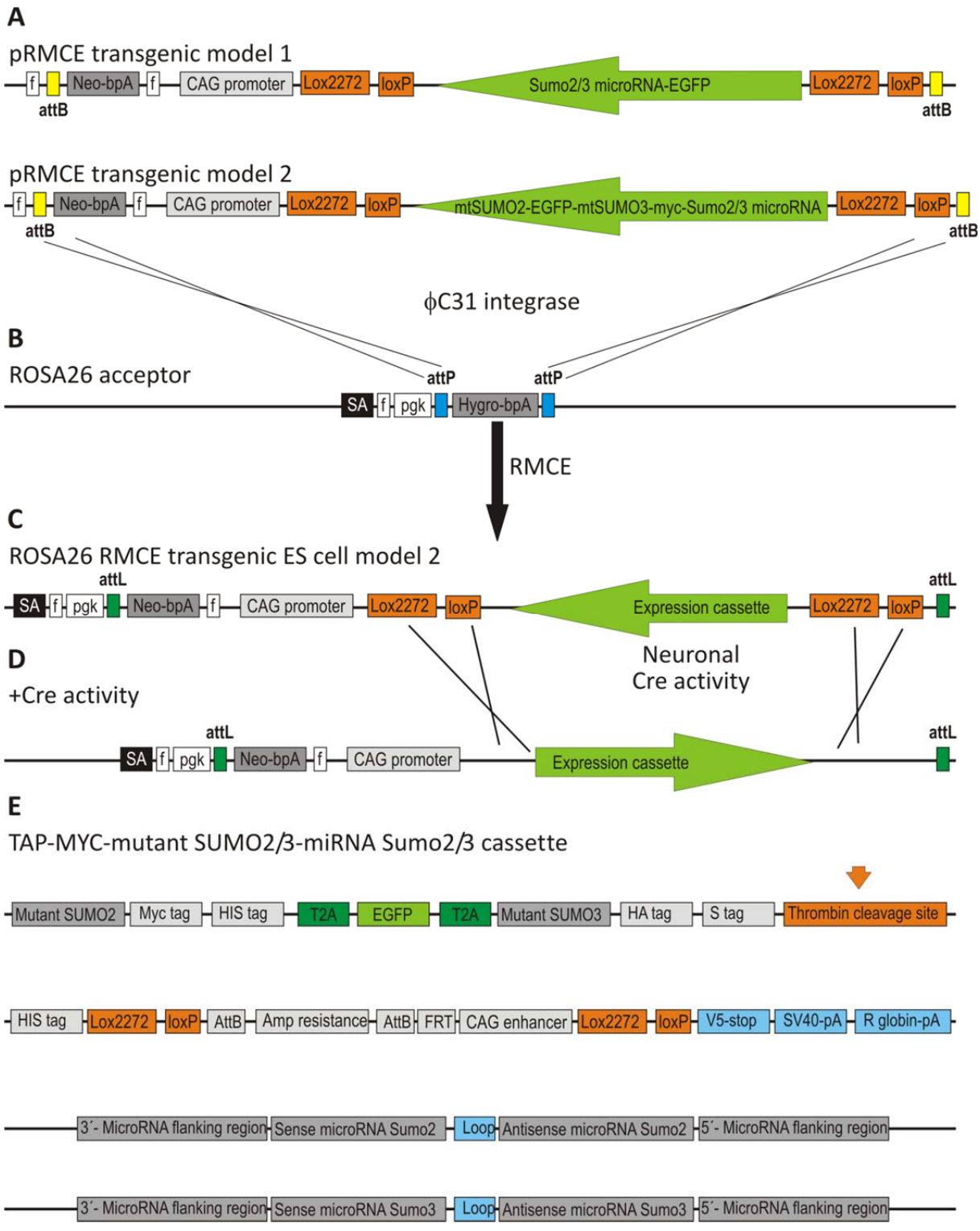

Fig 25: Schematic representation of mouse model generation. A. *MM1 and MM2 donor vectors. A neomycin cassette for selection is followed by the CAG promoter and the FLEX cassette of the respective mouse-model specific sequence. The whole sequence is flanked by attB sites which together with the attP sites from the Rosa26 acceptor facilitate integration.* ***B.*** *The Rosa26 acceptor consists of a PGK promoter-driven hygromycin resistance which is flanked by attP sites.* ***C. and D.*** *Through ζ C31 integrase, the attB sites of the donor vector recombine with the attP sites from the*

Rosa26 acceptor. Upon Cre activity, the expression cassette is irreversibly inversed, leading to stable expression of the transgenes. ***E.*** *Schematic representation of MM2-TAP- sumo2$^{tm\#(silent\ mutation)}$ - sumo3$^{tm\#(silent\ mutation)}$-Sumo2/3 microRNA. T2A: self-cleaving peptides.*

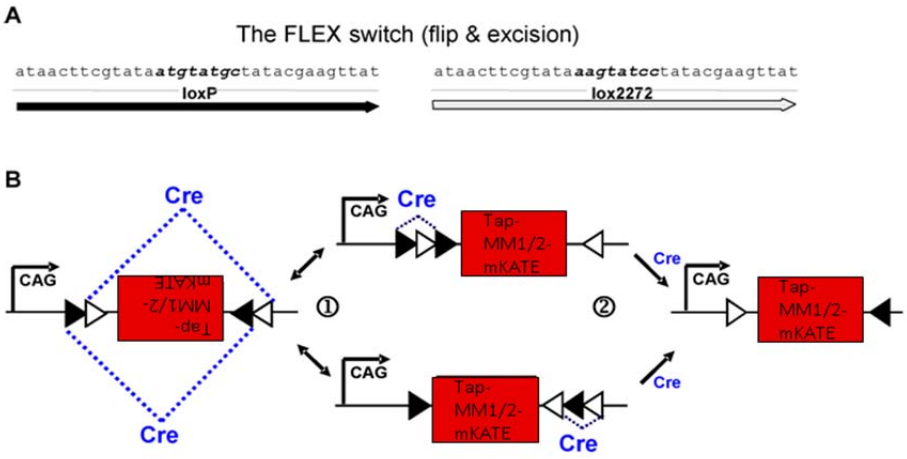

Fig 26: Principle of flip and excision cassette. *Upon induction with Cre recombinase, the insert between the loxP-los2272 cassette is inversed and gets transcribed.* ***A.*** *Sequence of loxP and lox2272 sites, respectively.* ***B.*** *Scheme of flip mechanism through Cre.*

4.4.1 *In vitro* testing

4.4.1.1 *In vitro* tests confirm functionality of targeting vectors for transgenic mouse model generation

The Sumo2/3 microRNA knockdown construct for generation of transgenic mouse model 1 (MM 1, inducible and neuronal specific expression of Sumo2/3 microRNA) has extensively been studied *in vitro* and *in vivo*. To confirm functionality of the targeting vector for mouse model 2 (inducible neuron-specific expression of mutant SUMO2 together with Sumo2/3 microRNA as a rescue of the microRNA-induced phenotype), a co-expression experiment was carried out. As expected, Sumo2/3 microRNA was unable to knock down the silently mutated form of SUMO2 (Fig 27, first lane, detected via HA-tag), but efficiently knocked down the unmodified SUMO2 protein (Fig 27, fourth lane, detected with a His tag). In contrast, when control microRNA was applied, SUMO2 protein was not downregulated (Fifth lane).

Simultaneous expression of Sumo2 microRNA and *sumo2*$^{tm\#(silent\ mutation)}$

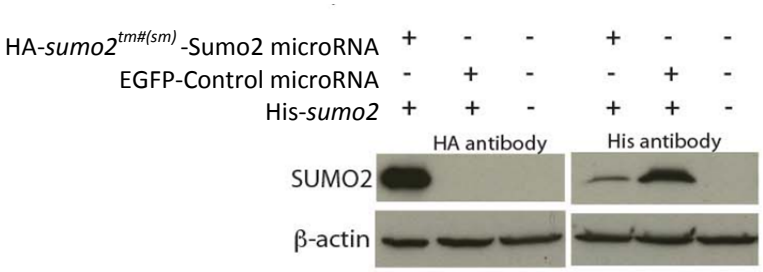

Fig 27: Proof-of-principle with targeting vectors for transgenic animal generation is positive. *Silently mutated SUMO2 was co-expressed with either Sumo2 microRNA or with control microRNA.β-actin served as a loading control. HA was used as a tag to indirectly show sumo2*$^{tm\#(silent\ mutation)}$ *expression; His was used as a tag for normal sumo2 expression. Sumo2 expression is inhibited through Sumo2-microRNA, sumo2*$^{tm\#(silent\ mutation)}$ *is still expressed.*

Induction of the TAP cassette was tested upon Cre-cotransfection. Western blot analysis showed expression of myc, which is part of the TAP cassette and indicates proper recombination of the system.

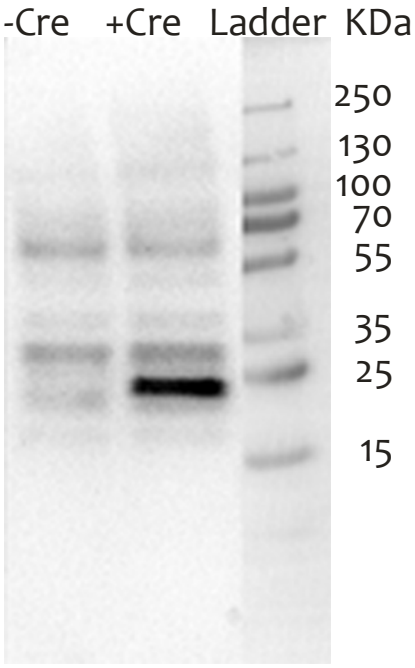

Fig 28: Western blot analysis confirms induction of TAP cassette. *293 Hek cells were transfected with the mouse-model-targeting vectors with or without Cre recombinase. Cell lysates were blotted against myc, which shows proper induction of the expression cassette.*

To investigate the self-cleaving capacity of T2A peptides, a transfection experiment was carried out in 293 Hek cells using a firefly-luciferase (FF) – T2A – EGFP – T2A – Puromycin sequence. Proper cleavage was verified in a western blot analysis.

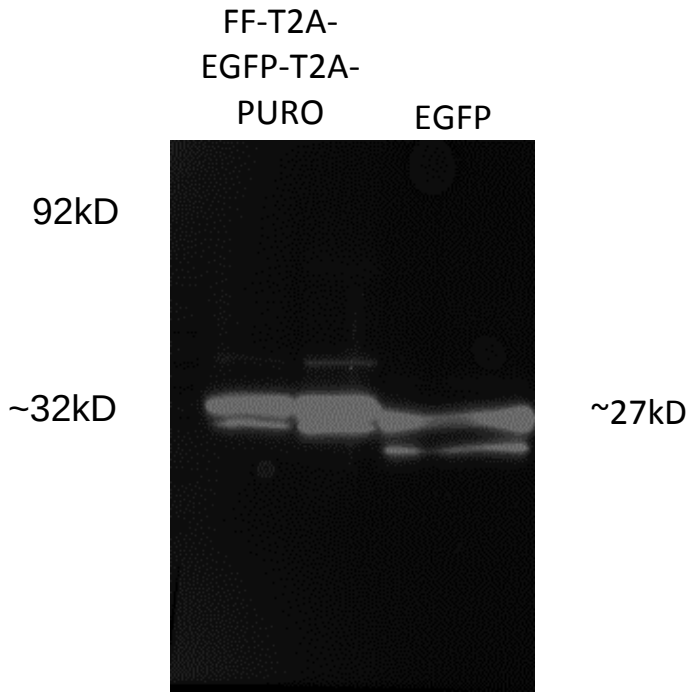

Fig 29: Functionality test of the self-cleaving peptide T2A in 293 Hek cells. *Detection of Luciferase-counts: 41 000 000 per 10 s. A luciferase-tagged T2A – EGFP – T2A – Puromycin sequence was transfected on Hek 293 cells. The cleaved EGFP – T2A could be detected at 32 kD whereas by comparison EGFP alone was detected at 27 kD. At 92 no band appeared, indicating that there was no uncleaved protein left.*

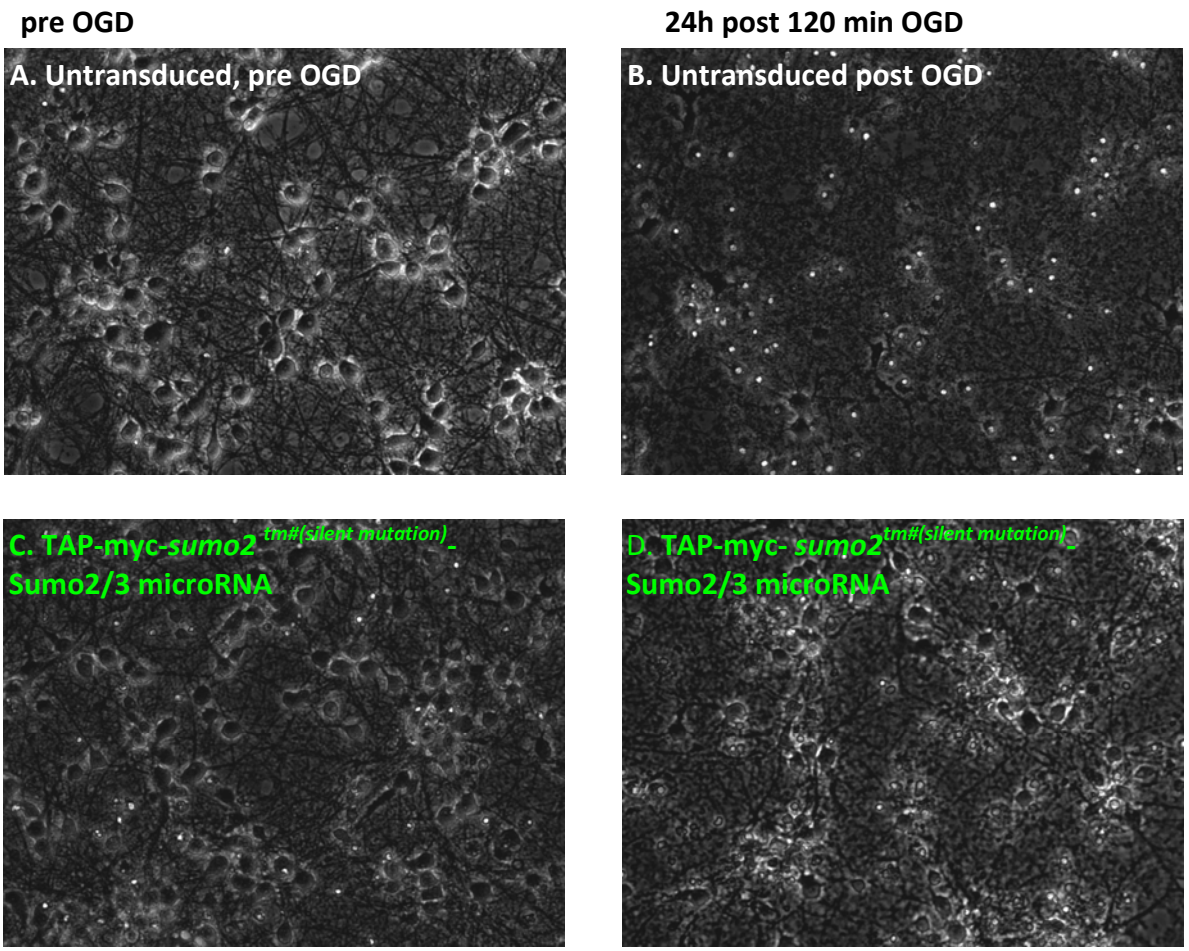

Fig 30: Proof of principle experiments in primary neuronal cell culture show rescue of OGD-induced damage with *sumo*$^{tm\#(silent\ mutation)}$ ***overexpression.*** *Primary cortical neurons were lentivirally transduced with a constitutive construct for myc-tagged sumo2*$^{tm\#(silent\ mutation)}$ *overexpression with concomitant Sumo2/3 microRNA and TAP expression. Neuronal cultures were subjected to damaging OGD.* ***A.*** *Untransduced neurons pre OGD show healthy primary cultures.* ***B.*** *Mock transduction post-OGD, most of the cells are lost.* ***C.*** *TAP-myc- sumo2*$^{tm\#(silent\ mutation)}$*-Sumo2/3 microRNA transduction pre-OGD shows healthy primary neurons.* ***D.*** *TAP-myc-sumo2*$^{tm\#(silent\ mutation)}$*-Sumo2/3 microRNA transduction post OGD. Neurons are in large parts rescued from OGD-induced cell loss.*

4.4.1.2 Embryonic stem cell (ESC) screening reveals positive clones

After performing electroporation of the MM1 or the MM2 targeting vector construct along with ζ-C31 Integrase for proper integration into the Rosa26-locus of the RMCE embryonic stem cells, we screened for positive clones using PCR.

4.4.2 *In vivo* results

4.4.2.1 Chimeric mice

Chimeric mice were born for both mouse models. In addition, MM2 was crossbred with C57BL6/N wildtype mice, and the litter was screened positively for germline transmission.

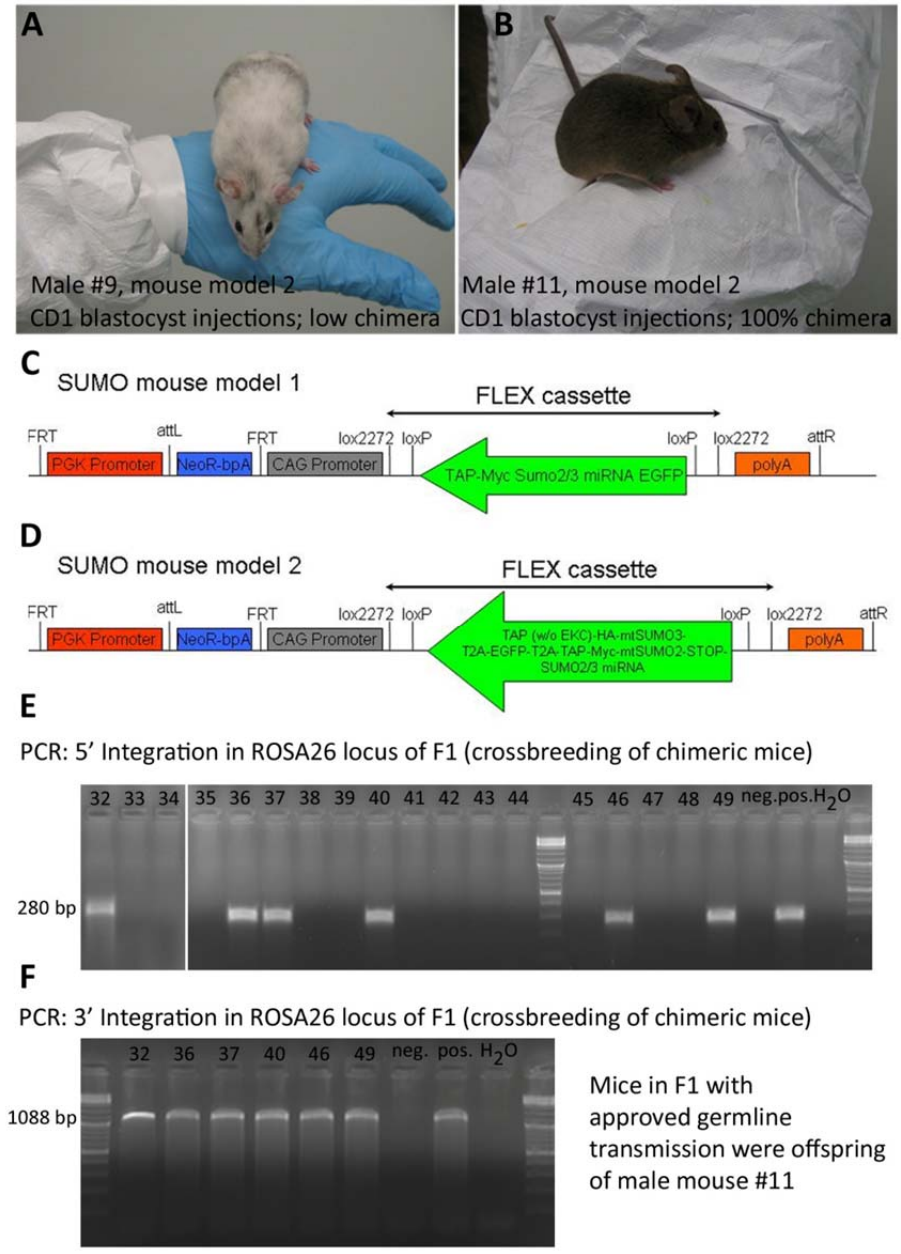

Fig 31: Chimeric mice and positive germline transmission of Mouse model 2*. Transgenic mice of MM2 with the highest chimerism were crossbread to C57BL6/N wildtype mice. Offspring of the male chimera No11 was analysed for integration into the Rosa26 locus. Analysis of the F1 generation revealed positive germline transmission.*

5. Discussion

The small-ubiquitin-like modifier (SUMO) was first discovered over a decade ago, and described by different groups. In 1996 a 12 kD protein, which is associated with the human RAD51 and RAD52 proteins, was discovered in a yeast-two-hybrid system and denoted as ubiquitin-like 1 (UBL1, (Shen, Pardington-Purtymun et al. 1996)). This relationship was later characterized in more detail. Recently, SUMO modification has implicated in the prevention of double-strand breaks and in the inhibition of recombination if replication stalls at DNA lesions, over all providing genome stability (Gali, Juhasz et al. 2012). It was described in the context of acute promyelocytic leukaemia in a human B-cell cDNA library screen and named PIC (Boddy, Howe et al. 1996). Gong et al characterized the interaction between sentrin and Ubc9 in the `sentrinization´ pathway. The requirements for interaction were specified as the ubiquitin domain and the C-terminal GG-residues of sentrin (Gong, Kamitani et al. 1997). Matunis et al described a novel ubiquitin-like modification which modulates the partitioning of Ran-GTPase-activating protein RanGAP1 between the cytosol and the nuclear pore complex. Ran is a nuclear Ras-like GTPase that is required for the bidirectional transport of proteins and ribonucleoproteins across the nuclear pore complex. Furthermore, the modified form of RanGAP1 was associated with the mitotic spindle apparatus during mitosis (Matunis, Coutavas et al. 1996). These studies showing covalent attachment demonstrated two important points: SUMO is a reversible protein modifier, and SUMOylation can alter the localization of the modified target by altering protein interactions. Whereas unmodified RanGAP1 is cytosolic, SUMOylated RanGAP1 localizes to the nuclear pore via interaction with the nucleoporin RanBP2 (also known as NUP358, (Geiss-Friedlander and Melchior 2007). One year later, it was determined that the posttranslational conjugation of RanGAP1 with SUMO-1 (for small ubiquitin-related modifier) requires ATP. SUMO1 was denoted as a novel protein of 101 amino acids that contains a low but significant homology to ubiquitin and appears to represent the prototype for a novel family of ubiquitin-related protein modifiers (Mahajan, Delphin et al. 1997). In 1997, a human homolog was also described, SMT3A (Lapenta, Chiurazzi et al. 1997) and it was suggested that at least two other proteins (HsSMT3a and HsSMT3b) exist in humans which are closely related to SUMO1 and together form a novel gene family (Saitoh, Pu et al. 1997). Since then, much research has been carried out on these newly discovered proteins, HsSMT3a and HsSMT3b, which were later denominated SUMO2

and SUMO3, respectively. SUMO-2/3 was described as conjugating poorly, if at all, to the Ran GTPase-activating protein RanGAP1, a major substrate of SUMO-1 (Saitoh and Hinchey 2000). Since then, research on the involvement of SUMO2/3 in different physiological and pathophysiological mechanisms in the body has exploded, particularly in regard to the brain. Furthermore, the quest for specific SUMO2/3-targets has won the interest of many researchers, and this work is still going on. In recent years, numerous publications demonstrated involvement of the SUMOylation pathway in different neuropathological conditions. SUMO2/3ylation was posited as a main molecular event facilitating survival of neurons in metabolically demanding circumstances such as hypothermia and hypoxia. Involvement of SUMO2/3ylation in survival of neurons after ischaemic stress, however, had not been thoroughly studied. The present work not only demonstrates a massive and rapid increase in SUMO2/3ylation of target proteins in neurons after an ischaemic insult, but it also evidences causal involvement of SUMO2/3ylation in neuroprotection following neuronal ischaemic injury. Here we show that upon down regulation of SUMO2/3 neurons are rapidly lost already after short ischaemic insults in mouse neurons and in retinal ganglion cells. We suggest that SUMO2/3ylation is an endogenous neuroprotective mechanism responding to ischaemic stress. Through the generation of transgenic mice we developed valuable tools to verify these findings in a temporally and spacially controllable manner and furthermore to screen stringently for tissue-specific and pathology-specific SUMOylation targets.

5.1 SUMOylation in neuronal ischaemic injury

SUMO conjugation has proved to be activated in cultured cells exposed to various stress conditions such as anoxic conditions, hypothermia, and hypoxia (Lee, Castri et al. 2009; Yang, Ma et al. 2009). In the present study, we investigated the function of SUMO2/3 induction after ischaemic stress. SUMO2/3 conjugation of target proteins was induced shortly after combined OGD, while at the same time free SUMO2/3 levels dropped in inverse proportion. It is known that within minutes after the onset of cerebral ischaemia, protein synthesis is inhibited at a threshold of about 0.55 ml/gm/min of CBF (Hossmann 1994). The stability, activity and and interactions of the proteins already present at the timepoint of ischaemic onset are therefore of significant importance. All three factors are influenced by

SUMOylation (Wilkinson, Nakamura et al. 2010). Possibly, SUMO2/3 is induced to protect neurons from ischaemic stress. To test this hypothesis, we applied neuron-specific RNA interference using Sumo2/3 microRNA. Blocking SUMO2/3 translation and thereby target protein conjugation did not interfere with viability of neurons cultured for up to 12 DIV. Cells were then exposed to ischaemia-like conditions to elucidate the role of SUMO2/3 protein conjugation in conferring resistance to experimental conditions of transient metabolic stress. The results provide strong evidence that neurons depend on SUMO2/3 conjugation to withstand ischaemia-like stress conditions. This finding was supported by diverse assays investigating neuronal integrity and survival. As a first step, we used transient OGD as a simplified model to investigate the role of SUMO2/3 conjugation in ischaemic stroke. As this approach does not involve cardiovascular and neurohumoral systems, we were able to focus on neuron-specific effects and conclude that metabolically compromised neurons activate a protective stress response to withstand stressful conditions. Importantly, RNA interference with SUMO2/3 did not alter the decrease and recovery of ATP per se in each degree of OGD. In addition, these data were not derived from a gain-of-function model with ectopic neuronal delivery of SUMO2/3 or ectopic delivery of the conjugation enzyme Ubc9, which might induce artificial SUMO protein adduction to target proteins, which are endogenously not conjugated. Only recently, our published findings (Datwyler, Lattig-Tunnemann et al. 2011) were indirectly confirmed in hippocampal neurons: Global SUMOylation levels were decreased by overexpression of the catalytic domain of SENP1 and therewith increased neuronal vulnerability to OGD-induced cell death. Surprisingly, the SUMO protease SENP-1, which removes SUMO from conjugated proteins, was also increased by OGD, suggesting that the neuronal response to OGD involves a complex interplay between SUMOylation and deSUMOylation (Cimarosti, Ashikaga et al. 2012). For many years, SUMO conjugation of target proteins was believed to be a predominantly nuclear process modifying transcription factors, nuclear pore proteins, and other nuclear proteins critical for genome integrity. Recently, many SUMO conjugation target proteins have been identified in neurons that are cytosolic or cell membrane proteins, and SUMO conjugation has been found to modulate neuronal calcium fluxes and neurotransmitter release (Martin, Nishimune et al. 2007; Feligioni, Nishimune et al. 2009). Several classes of neuronal membrane proteins have been reported to be SUMOylated, strongly implicating SUMOylation in the control of neuronal excitability, synaptic transmission and glucose transport (Martin, Wilkinson et al. 2007;

Feligioni, Nishimune et al. 2009). Our study allows the conclusion that physiologic levels of SUMO2/3 in neurons at the onset of ischaemic-like stress are neuroprotective. Furthermore, we speculate that development of an ischaemic penumbra after the first shortage in metabolites following decreased CBF could be contained through enhancement of this endogenous neuroprotective system through its impact on neuronal excitability and signal transmission.

5.2 SUMOylation in excitotoxic stress

Glutamate is the most predominant excitatory neurotransmitter in the mammalian CNS (Xiang, Dong et al. 2006) and is taken up into cells during the regulation of glutamate neurotransmission. Its concentration under normal conditions within the CNS varies amongst different structures: in the neuronal cytoplasm it is 10 mM, in the extracellular space 0.6 µm, in the synaptic cleft 20 nM, and in the synaptic terminal vesicles 100 mM (Albrecht, Hilgier et al. 2000). It plays a major role in the development of excitotoxicity following cerebral and retinal ischaemia. Excitatory amino acid transporters (EAATs) regulate uptake and release of glutamate into the cell or into the extracellular space. This process is sodium but not calcium-dependent. Dysfunction of EAATs is linked to the pathological development after ischaemia, and up-regulation of the transporters has been shown to be neuroprotective during an ischaemic insult (Chao, Fei et al. 2010). EAAT2, the major isoform found in the CNS, accounts for approximately 90 % of all EAATs within the brain and spinal chord and is expressed in neurons, astrocytes and non-astrocytic glial cells (Mennerick, Dhond et al. 1998; Schmitt, Asan et al. 2002). EAAT2 has been shown to be endogenously downregulated following stroke (Martin, Brambrink et al. 1997). Furthermore, Rao and co-workers showed that knockdown of EAAT2 exacerbates neuronal damage following MCAo (Rao, Bowen et al. 2001). In contrast, increasing the levels of EAAT2 has proven to be neuroprotective in ischaemic stress (Chu, Lee et al. 2007). In a mouse model of amyotrophic lateral sclerosis, a fragment of EAAT2 has been shown to be SUMOylated and therewith targeted to promyelocytic leukemia nuclear bodies (Gibb, Boston-Howes et al. 2007). However, the exact function of this altered targeting has not yet been fully understood. As up-regulation of EAAT2 and consequent increases in glutamate-uptake have been shown to be

neuroprotective during stroke, it can be speculated that SUMOylation could stabilise EAAT2 to provide neuroprotection. In the rat retina, SUMO E3 ligases have been shown to be expressed and to regulate SUMOylation of the metabotropic glutamate receptor GluR8b (Dutting, Schroder-Kress et al.). We show that knockdown of SUMO2/3 exacerbates glutamate excitotoxicity in the retinal ganglion cell layer (RGC). The combination of neuron-specific SUMO2/3 knockdown and glutamate damage led to a significantly greater increase in pycnotic neurons in the RGC than that seen in control microRNA transduced groups. We are aware of the unphysiologically high glutamate concentration used within the medium of the retina explant cultures, which is only half the concentration normally present in the neuronal cytoplasm, but which is high compared to the physiological concentration of the extracellular space of a neuron. However, up to now it is not clear whether glutamate toxicity also depends on the amount of glutamate receptors within a cell and whether or not the high glutamate concentration within the medium also reaches the ganglion cell layer of the retina culture. Our results are in line with the findings from the embryonic primary cortical neurons, showing that loss of SUMO2/3 leads to increased neuronal damage in the context of stress. As the RGC from the retina cultures consists of adult neuronal cells, these results provide evidence that SUMO2/3 could also prove to be neuroprotective in adult tissues.

5.3 SUMOylation in ischaemic brain injury

After transient global or focal ischaemia in rats, a significant increase in the levels of SUMO2/3-conjugated proteins was found (Yang, Sheng et al. 2008; Yang, Sheng et al. 2008). In a transient MCAo rat model with a striatal and a cortical infarction, increases in SUMOylation by both SUMO1 and SUMO2/3 were reported at 6 h and 24 h after stroke in the striatum. Interestingly, SUMO2/3ylation was also observed after 24 h in the hippocampus, which was not directly subjected to ischaemia but might be tissue at risk of developing secondary damage (Cimarosti, Lindberg et al. 2008). The post-ischaemic pattern of SUMO2/3-conjugated proteins after ischaemia supports the assumption that elevated SUMO2/3 levels could represent a protective stress response: After transient focal cerebral ischaemia, the rise in levels of SUMO2/3-conjugated proteins was most pronounced in

neurons of the penumbra located at the border of the ischaemic territory, where various survival pathways are activated. Furthermore, a short, non-lethal duration of ischaemia was sufficient to activate this process. We inhibited expression of SUMO2/3 in the ischaemic penumbra of mice through neuron-specific lentiviral delivery of Sumo2/3 microRNA. In the present study, transient MCAo was applied as a model with a stroke core developing within the striatum and a penumbra in the lateral cortex. We did not detect any differences in infarct sizes, neither in MRI imaging, nor on cellular levels. Furthermore, functional impairment in a pole test did not differ between groups. This could supposedly be due to restrictions in the models and complexity of the system. Due to variance in the ischemic model, successful targeting of the lentiviral particles into the putative penumbra region is not guaranteed. Furthermore, free diffusion of the lentiviral particles in the extracellular space is restricted due to the so called `partial volume effect´. Through secretion of glycoproteins into the extracellular matrix, free diffusion of proteins larger than 20 nm is limited, so that lentiviral particles with a diameter of approximately 100 nm cannot freely diffuse. In principle, transduction areas of approximately 500 nm in diameter were achieved earlier (See Fig 18), but this efficacy could potentially prove right for some tissues and wrong for others. We therefore suggest investigating the effects of SUMO2/3ylation in an inducible and tissue specific mouse model of targeted integration into a silent locus. Only recently, Lee and co-workers showed in Ubc9 transgenic mice that a global increase in SUMOylation levels is able to protect the brain against focal cerebral ischaemia. Ubc9 was expressed under the ubiquitous chicken β-actin promoter; this expression ranged from 2 to 30 times the endogenous level. The Ubc9 expression level correlated closely with global SUMO1 and SUMO2/3 conjugation up to a fivefold increase in Ubc9 levels. However, infarct sizes were inversely correlated with the Ubc9 expression levels for up to five fold (Lee, Mou et al. 2011). Given that this study was carried out in transgenic animals with indirectly elevated SUMO1 as well as SUMO2/3 levels in all tissues of the body, the observed effects in the brain could also be indirect. The answer to the question whether elevation of SUMO2 or SUMO3 levels within the brain or even neuron-specifically is beneficial, is still pending. To approach this question, we generated transgenic mouse models.

5.4 Transgenic mice as an efficient, inducible and specific tool to unravel the endogenous neuroprotective mechanisms of SUMOylation in brain ischaemia

The quest for *in vivo* studies considering the SUMOylation pathway as well as screening for specific targets in different pathophysiological contexts has enhanced research on transgenic mouse models. There are two conflicting studies regarding SUMO1 transgenic mice: Alkuraya and collegues showed that disruption of SUMO1 in mice caused embryonic lethality in homo- as well as heterozygous genomes, and SUMO1 haploinsufficiency induced a developmental craniofacial birth defect (cleft lip and palate) in mice and possibly also in humans (Alkuraya, Saadi et al. 2006). SUMO2/3 levels were not investigated in this study. The findings in humans were challenged by Almeida de Assis, as results gained from genotyping and subsequent single marker and haplotype association analyses from 413 non-syndromic cleft lip patients with or without cleft palate (NSCL/P) and 412 controls did not reveal a role for SUMO1 in the development of NSCL/P in Central European patients (de Assis, Nowak et al. 2011). A total of 17 tagging single-nucleotide polymorphisms (SNPs) were analysed in this study. This was confirmed in another patient study with 192 patients (Carta, Pauws et al. 2012). Zhang and co-workers in 2008 targeted the last three exons of murine SUMO1 by homologous recombination and reported predicted Mendelian ratios in genotypes of embryos and 21-day-old mice, and there were no defects in lip and palate development in $SUMO1^{+/-}$ or $SUMO1^{-/-}$ embryos. Mice of both sexes were reported to be viable and fertile. Although the authors reported no upregulation of SUMO2 and SUMO3 mRNAs in SUMO1 null mice, they suggested that most, if not all, SUMO1 functions are compensated for *in vivo* by SUMO2 and SUMO3 (Zhang, Mikkonen et al. 2008). However, embryonic stem cells had differently mixed genetic backgrounds in both studies, and the litters were analysed without backcrossing onto a pure background over 10 generations. The same mice from these two groups were later analysed and SUMO1 haploid and homozygous KO mutant mice were found to develop congenital heart disease. A reduced number of expected homozygous SUMO1 knockout newborn mice was observed. Also, $SUMO1^{-/-}$ mice exhibited a high postnatal mortality rate of 57% versus 22% for $SUMO1^{+/-}$ and 15% for wildtype mice ($p < 0.01$), and SUMO1 mutant mouse hearts exhibited dysregulation of genes critical for cell proliferation (Wang, Chen et al. 2011). Kim and collegues generated transgenic mice with cardiac-specific expression of SENP2, a SUMO-specific protease that

deconjugates SUMOylated proteins, to evaluate the impact of deSUMOylation on heart development and function. Overexpression of SENP2 resulted in premature death of mice with congenital heart disease, atrial septal defects and/or ventricular septal defects. Immunobiochemistry revealed diminished cardiomyocyte proliferation in SENP2 transgenic mouse hearts compared with wild type hearts. Surviving SENP2 transgenic mice showed growth retardation, and developed cardiomyopathy including impaired cardiac function (Kim, Chen et al. 2012). Cardiac-specific overexpression of the SUMO1 transgene reduced the incidence of cardiac structural phenotypes in the SUMOylation defective mice. Genomic ablation of SENP1 or SENP2 in mice also led to embryonic lethality (Cheng, Kang et al. 2007; Chiu, Asai et al. 2008; Kang, Qi et al. 2010). Taken together, these findings indicate the indispensability of a balanced SUMO pathway for proper cardiac development and function. Up to now it is not clear whether dysfunction of SUMO1 can be compensated *in vivo* and if so, to what extent. SUMOylation through SUMO1 has also been implicated in brain development through transcriptional activation of Pax-6 (Yan, Gong et al. 2010). So far, no reports on SUMO2/3 transgenic mice have been published. Former proteomic approaches and gene arrays after RNA interference with SUMO2/3 have identified a wide range of SUMOylated target proteins and transcriptional changes (Vertegaal, Ogg et al. 2004; Golebiowski, Matic et al. 2009; Yang and Paschen 2009). It is therefore likely that a total depletion of the free pool of SUMO2/3 does interfere with the ability of neurons to react to changes in the cellular environment in general and that an ensemble of required SUMO2/3-modifications will not be performed. However, all these studies have been carried out *in vitro* in non-neuronal cells. SUMO2/3 conventional knockout mice are not available and might have severe developmental defects, general phenotypic changes or even embryonic lethality. Apparently, the function of SUMO2/3 cannot be compensated for by SUMO1 in a ubiquitous transgenic context. It is therefore highly relevant to generate tissue-specific and inducible transgenic mouse models to investigate the function of SUMO2/3 *in vivo* in different pathophysiological contexts. Tissue specificity allows for analysis of the function of SUMOylation in different diseases, and inducibility circumvents embryonic lethality and allows for analysis of adult tissue, which is in many cases more relevant in the context of pathophysiologies. We applied recombinase-mediated cassette exchange to integrate Sumo2/3 microRNA into the genomically silent Rosa26-locus. Application of microRNAs produces a knockdown instead of complete knockout, which is similar to the action of a

pharmacon in humans and is a novel and innovative strategy to directly investigate neuroprotection *in vivo* in the context of stroke. The microRNA can be induced via Cre-recombinase in a tissue of choice, thus allowing the investigation of consequences of knockdown in different pathophysiological conditions. In our second mouse model, we reintroduced silently mutated ectopic SUMO2 and SUMO3, which cannot be degraded by the microRNAs. This approach leads to degradation of endogenous SUMO2/3 protein and in addition introduces ectopic SUMO2 and SUMO3 which are tagged with a tandem affinity purification cassette. This makes it possible to screen very stringently in a two-step extraction method through a His- and an S-tag for tissue-specific SUMOylation targets in an inducible manner. Specific purification of SUMO2 or SUMO3 targets can be achieved through a myc tag (SUMO2 adducts) and an HA tag (SUMO3 adducts). The second mouse model serves as a control for the microRNA-expressing mouse model, as the phenotype will be rescued. Additionally, targets of SUMOylation in different tissues can be identified *in vivo* and further investigated. In addition, it is of pivotal importance to screen for specific drugs that activate SUMO2/3 conjugation or inhibit the deconjugation of SUMO2/3 target proteins and modulate the fate of post-ischaemic neurons *in vivo* for preventive or therapeutic purposes. Furthermore, a combination of hypothermia and the effects of SUMO2/3 conjugation can be experimentally investigated. This can potentially lead to an enhancement of stroke treatment in patients.

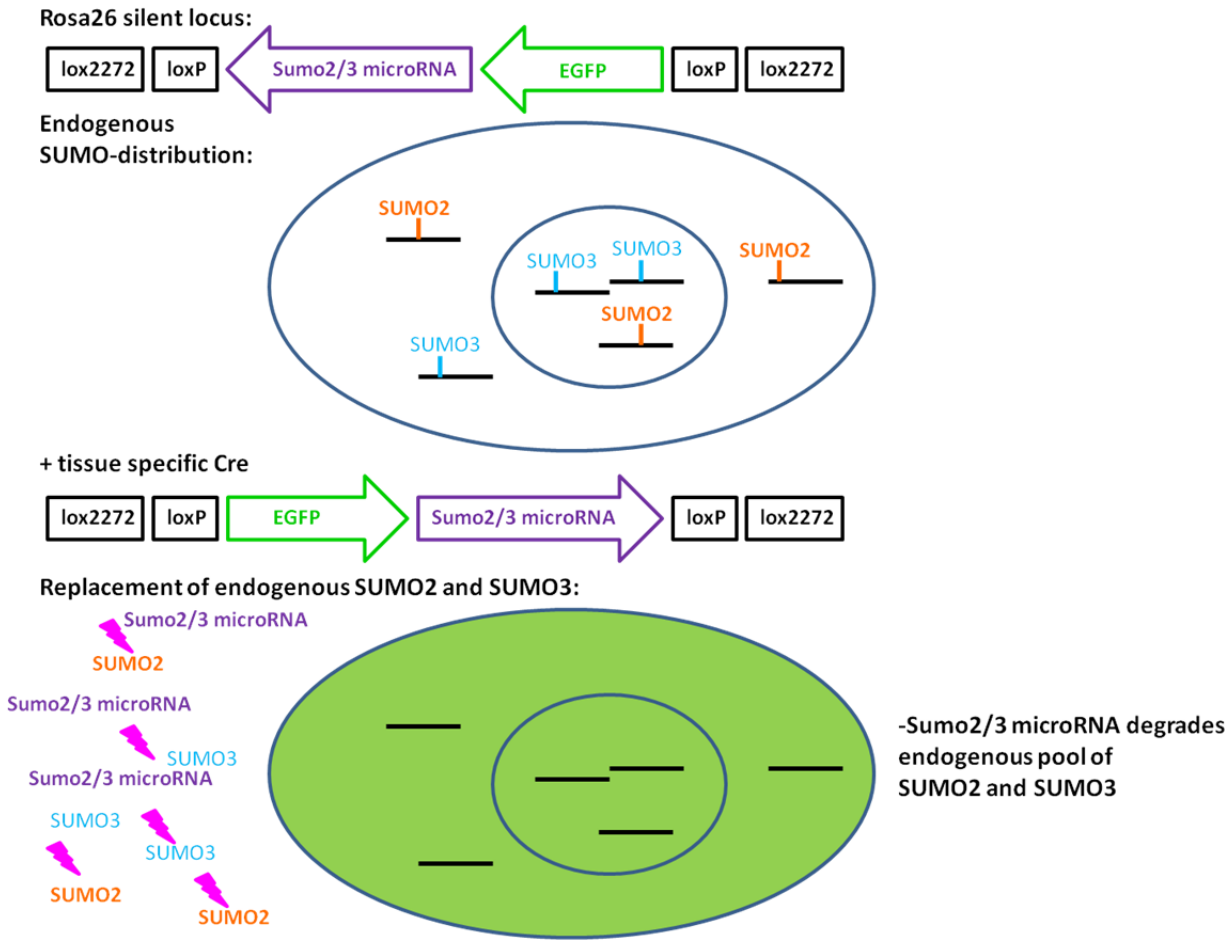

Fig 32: Schematic representation of the loss-of-function model (MM1): *The target sequence is integrated into the transcriptionally silent Rosa26 locus. Due to the inverse orientation within the FLEX cassette, the target sequence is not expressed without Cre recombinase and therewith off-target effects during development are avoided. Upon crossbreeding with Cre recombinant mouse lines, the expression cassette switches its orientation. Sumo2/3 microRNA degrades the endogenous SUMO2 and SUMO3 proteins in a tissue-specific manner.*

A:

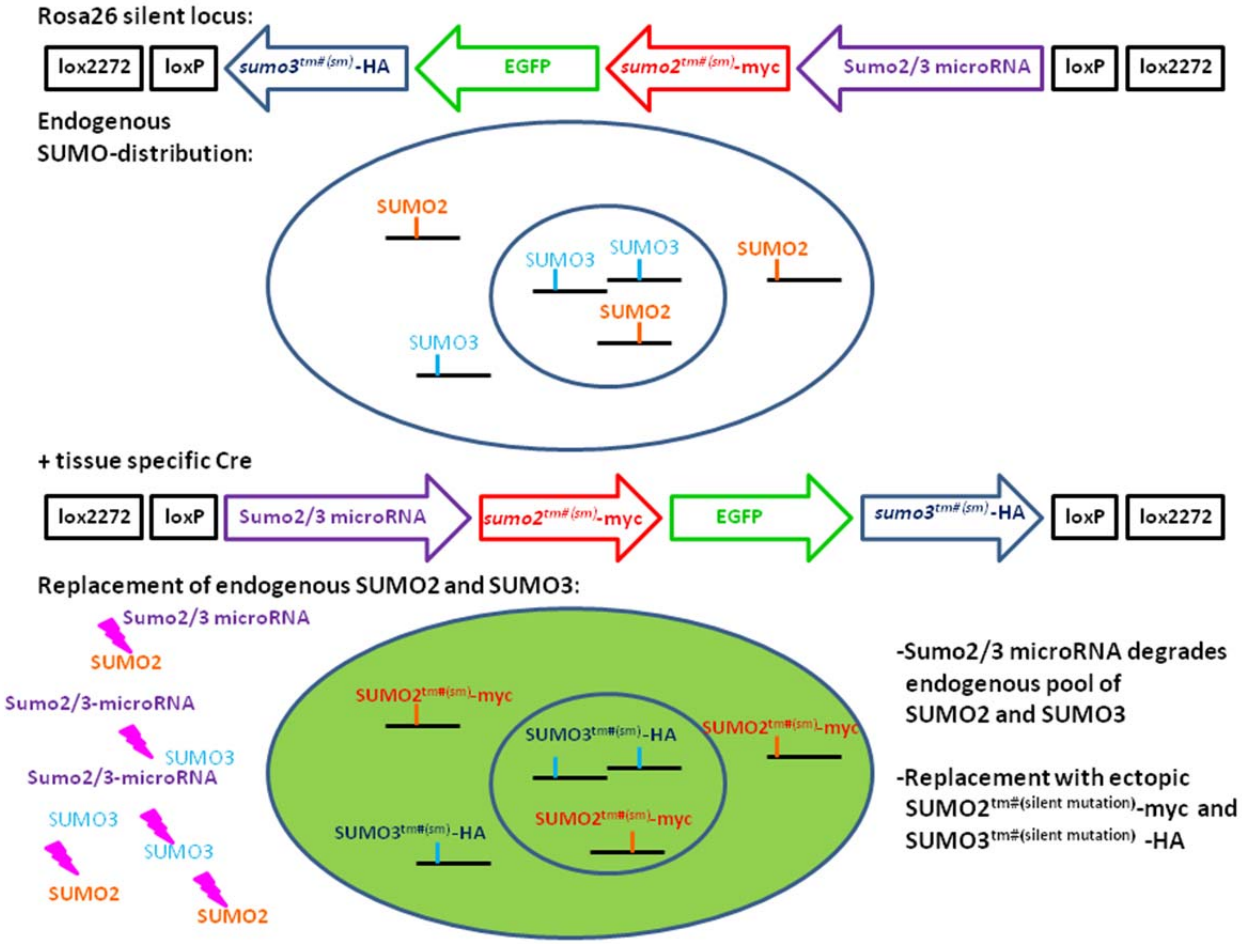
Rosa26 silent locus:
lox2272
loxP
sumo3tm#(sm)-HA
EGFP
sumo2tm#(sm)-myc
Sumo2/3 microRNA
loxP
lox2272
Endogenous
SUMO-distribution:
SUMO2
SUMO3
SUMO3
SUMO2
SUMO2
SUMO3
+ tissue specific Cre
lox2272
loxP
Sumo2/3 microRNA
sumo2tm#(sm)-myc
EGFP
sumo3tm#(sm)-HA
loxP
lox2272
Replacement of endogenous SUMO2 and SUMO3:
Sumo2/3 microRNA
SUMO2
Sumo2/3-microRNA
SUMO3
Sumo2/3-microRNA
SUMO3
SUMO3
SUMO2
SUMO2
SUMO2tm#(sm)-myc
SUMO3tm#(sm)-HA
SUMO2tm#(sm)-myc
SUMO3tm#(sm)-HA
SUMO2tm#(sm)-myc
-Sumo2/3 microRNA degrades endogenous pool of SUMO2 and SUMO3
-Replacement with ectopic SUMO2tm#(silent mutation)-myc and SUMO3tm#(silent mutation) -HA

B:

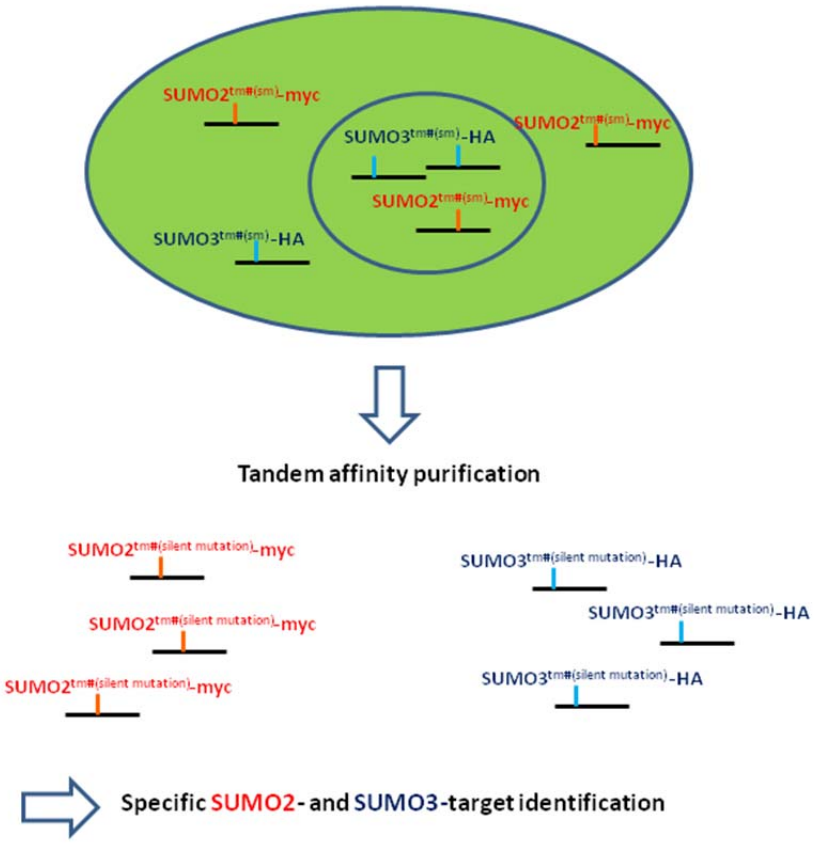

Fig 33: Schematic representation of the Sumo2/3 microRNA- *sumo2$^{tm\#(silent\ mutation)}$-* *sumo3$^{tm\#(silent\ mutation)}$-**TAP mouse model (MM2). A:** The target vector is integrated into the transcriptionally silent Rosa26 locus. Due to the inverse orientation within the FLEX cassette, the target sequence is not expressed without Cre recombinase and therewith off-target effects during development are avoided. Upon crossbreeding with Cre recombinant mouse lines, the expression cassette switches its orientation. Sumo2/3 microRNA degrades the endogenous SUMO2 and SUMO3 proteins in a tissue-specific manner. Within the same cells, silently mutated SUMO2 (SUMO2$^{tm\#(silent\ mutation)}$) and SUMO3 (SUMO3$^{tm\#(silent\ mutation)}$) proteins, which are separately tagged, replace the endogenous proteins. Due to the silent mutation they cannot be degraded by the microRNA. EGFP is expressed as a reporter within the same cells. **B:** SUMO2$^{tm\#(silent\ mutation)}$carries a myc tag and SUMO3$^{tm\#(silent\ mutation)}$ an HA tag. Both proteins covalently attach to their target proteins. Using tandem affinity purification, the SUMOylated proteins can be pulled down stringently with a two-step extraction method and His and S tags. Finally, they can be separated using the thrombin cleavage site, and specific SUMO2 and SUMO3 targets can be distinguished.

5.5 Transcriptional changes within the penumbra after stroke and target proteins of SUMOylation

Ischaemic stress in the brain causes acute and massive cell death in the targeted core area followed by a second phase of damage in the neighboring penumbra. Understanding transcriptional changes within the penumbra could lead to new strategies and provide therapeutic targets for rescuing this tissue at risk. We and others have shown that SUMO2/3ylation is induced after OGD as well as after transient global or focal cerebral ischaemia (Cimarosti, Lindberg et al. 2008; Yang, Sheng et al. 2008; Yang, Sheng et al. 2008; Datwyler, Lattig-Tunnemann et al. 2011). In our OGD model, induction happened fast and vulnerability of SUMO2/3-knockdown cultures was increased after very short stimuli, mimicking a penumbra-like status of the neurons, with light OGD and the potential for recovery and resuscitation. After transient focal cerebral ischaemia, the rise in levels of SUMO2/3 conjugated proteins was most pronounced in neurons of the penumbra, and a short duration of ischaemia was sufficient to activate this process (Yang, Sheng et al. 2008). This shows the potential involvement of SUMO2/3ylation in the protection of neurons within the penumbra after ischaemic stress. Yang and collegues also carried out a screen for SUMO3-conjugation target proteins in neuroblastoma B35 cells following OGD (Yang, Thompson et al. 2011). They applied stable isotope labeling with amino acids in cell culture (SILAC) to quantify OGD-induced changes in levels of specific SUMOylated proteins. Using HA-SUMO3 overexpression and transient OGD, 188 putative SUMO3-conjugated proteins, including numerous transcription factors and coregulators, and PIAS2 and PIAS4 SUMO ligases were identified. Twenty-two proteins were modulated more than 2-fold. For neurons to be rescued after an ischaemic insult, fast protection is of pivotal importance. Other endogenously protective systems such as ischaemic preconditioning have been shown to be gene expression-dependent. Furthermore, upon blood flow reduction within ischaemic tissue, protein synthesis is inhibited within minutes after the ischaemic insult at a flow rate threshold of approximately 0.55 ml/gm/min (Hossmann 1994). SUMOylatioin is a very fast process and is induced after cerebral ischaemia. Due to the constant free pool of SUMO2/3 within a neuron, relatively slow gene transcription is not primarily needed to enhance survival of neurons within an ischaemic penumbra. Potentially, this dynamic and endogenously neuroprotective effect facilitates the survival of neurons in tissue at metabolic

risk and could be further enhanced to achieve neuroprotection in patients. Screening for target proteins of SUMOylation has become the object of intense investigation and could lead to specific treatment strategies in stroke. Using our transgenic mouse models, we will set off to identify target proteins which are specific for neurons of the penumbra after induction of experimental stroke and reperfusion.

5.6 Normoxia, hypoxia and SUMOylation of the life-death master-switch HIF

Hypoxia is defined as a decrease in available oxygen reaching the tissues of the body. It is linked to the pathology of cancer, cardiovascular disease, and stroke. Cells under hypoxic stress either induce an adaptive response that includes increasing the rates of glycolysis and angiogenesis or undergo cell death by promoting apoptosis or necrosis The balance between adaptation and cell death is regulated by a family of transcription factors called the hypoxia inducible factors (HIF); especially the stability and transcriptional activity of the HIF1 α subunit are regulated (Lee, Roth et al. 2007). It has also been suggested that ischaemic tissue may recruit circulating stem cell progenitors regulated by hypoxia through differential expression of HIF1α (Chang, Shyu et al. 2007). VEGF and EPO, two primary HIF1 target genes, play a critical role in this process (Wick, Wick et al. 2002). EPO is a growth factor that has been studied for its hematopoietic regulatory function; however, recent studies have suggested a broader role for this hypoxia target gene. We have shown that recombinant human EPO protects retinal ganglion cells against excitotoxic cell death in an organotypical culture (Manuscript in preparation). It serves as a potent angio- and neuroprotective agent. In the context of stroke, Baranova and co-workers have shown that neuron-specific inactivation of HIF1 increases brain injury in a mouse model of transient focal cerebral ischaemia (Baranova, Miranda et al. 2007). More recently, HIF1 and its downstream genes EPO, VEGF and glucose transporter (Glut) have been shown to be upregulated in neurons and brain endothelial cells in an ischaemic stroke model of rats (Yan, Zhou et al. 2011). Inhibition of HIF1 and its downstream genes by 3-(5'-hydroxymethyl-2'-furyl)-1-benzylindazole (YC-1) significantly increased mortality and enlarged infarct volumes evaluated by MRI and histological stainings 24 h after stroke. Patients at risk of stroke-

induced hypoxia/reoxygenation injury might benefit from HIF1 activation to promote adaptive or neuroprotective effects. HIF1α is mainly regulated at the level of protein stability. In neurons and cardiomyocytes, HIF1α was shown to be SUMOylated (Shao, Zhang et al. 2004). RWD-SUMOylation enhancer (RSUME) has been found to stabilize HIF1α and to increase its transcriptional activity (Carbia-Nagashima, Gerez et al. 2007). RSUME is itself induced by hypoxia and enhances the activity of Ubc9, thereby resulting in the increased SUMOylation of several targets including HIF1α. In experimental brain death, drastic tissue hypoxia was described and found to be associated with augmented SUMOylation of HIF1α. SUMOylation of HIF1α stabilized and enriched HIF1α in the nuclear compartment and therewith enhanced transcriptional activitiy of HIF1α, preferentially during the pro-life phase of experimental brain death (Chan, Tsai et al. 2011). Although the variety of interactions between factors of the SUMOylation pathway and HIF1α have not yet been fully understood, SUMOylation takes part in stabilization of HIF1α and through this can enhance neuroprotective downstream signalling.

5.7 SUMOylation in mitochondrial DNA repair after stroke

Mitochondria play major roles in bioenergetics and cell death/survival signalling of the mammalian cell; they are 'gatekeepers of life and death'. In tissues with high energy consumption such as brain and heart, mitochondria comprise nearly half of the cell volume and produce 80–90% of the ATP. Over the last years major advances have been made in understanding the mitochondrial dysfunction following cerebral ischaemia and its contribution to tissue injury and cell death. ROS generated by mitochondrial electron transfer may damage mitochondrial DNA (mtDNA), in particular in the reperfusion phase after ischaemia. MtDNA repair ensures transcription of mRNA from intact genes. The maintenance of swift and effective mtDNA repair is therefore essential for postmitotic cells such as neurons and must be reversibly adapted to different energy states within a cell and to different pathophysiological conditions. The fact that SUMOylation can rapidly and reversibly change the properties, stability or localisation of target proteins without the need for *de novo* protein synthesis makes it an ideal regulator for finetuning DNA repair and damage response pathways (Ulrich 2012). SUMO modification has been implicated in diverse

aspects of DNA repair and genome stability (Hardeland, Steinacher et al. 2002; Steinacher and Schar 2005; Branzei, Sollier et al. 2006; Galanty, Belotserkovskaya et al. 2009; Morris, Boutell et al. 2009; Yang and Paschen 2009; Dou, Huang et al. 2011; Cremona, Sarangi et al. 2012; Gali, Juhasz et al. 2012; Hudson, Chiang et al. 2012).The SUMOylation pathway has also been implicated in maintaining mitochondrial morphology and function, as well as in the prevention of free radicals (Zunino, Schauss et al. 2007). Furthermore, it has recently been shown to play a role in vesicle transport between the mitochondria and peroxisomes (Braschi, Goyon et al. 2010). Mitochondrial base excision repair (BER) seems to be of particular significance in cerebral ischaemia and under conditions of oxidative stress. Cremona and co-workers found SUMOylation targets involved in BER in a biochemical screen in yeast (Cremona, Sarangi et al. 2012). Overexpression of SUMO1 induced the up-regulation of uracil DNA glycosylase (UDG or UNG) in hepG2 cells (Ma, Au et al. 2009). Further analysis of western blotting and RT-PCR indicated that the upregulation was mediated via changes at the translational level or post-translational modification. Uracil-DNA glycosylase is part of the base excision repair (BER) complex which repairs uracil as well as a broad variety of oxidative lesions in nuclear and mitochondrial DNA (Svilar, Goellner et al. 2011). Recently, it was shown that ung−/− mice develop increased lesion volumes after MCAo (Endres, Biniszkiewicz et al. 2004). There are two splice variants of UNG in humans and mice, namely UNG1 and UNG2. Brains of ung−/− mice show increased D1-deletion frequencies compared to wildtype littermates, pointing to a dysfunction linked to the preferentially mitochondrial splice variant UNG1 being responsible for the increased lesion volumes (Kronenberg, Gertz et al. 2011). We have shown (Datwyler et al., 2012, personal observation) that mitochondrial (UNG1) but not nuclear (UNG2) base excision repair is impaired following ischaemic stress. Neuronal specific lentiviral delivery of Ung1- and Ung1/2-specific microRNAs did not affect the viability of cortical neuronal cell cultures unless they were exposed to OGD. Ung1 microRNA-transduced cultures showed increased vulnerability in transient OGD lengths between 15 and 60 min with 24 h of reoxygenation. In a 75 min-OGD (loss of 50% of all control microRNA-transduced neurons), the survival rate for Ung1 microRNA transduced cultures dropped completely. In contrast, neurons with combined UNG1/2 knockdown did not differ from control microRNA cultures. We concluded that mitochondrial UNG1 induction is an endogenous neuroprotective stress response of the BER complex in mitochondria and we speculate that UNG2 has a negative impact on neuronal survival if UNG1 expression is

depleted. More data are needed to understand the impact of mitochondrial SUMO conjugation on BER. Overall, the variety of SUMO-mediated influences on DNA replication and repair reflects the flexibility by which neurons react to insults to their genetic information, and highlights the importance of SUMOylation and de-SUMOylation in this process.

5.8 Hypothermia treatment in stroke patients and the involvement of SUMOylation

In vivo investigations have shown an induction of SUMO in the brain following torpor, hypothermia and stroke. Potentially, this is an endogenous protective response shielding neurons from damage induced by low blood flow and substrate deprivation. Hypothermia is effective in protecting the brain in a variety of clinical conditions, including resuscitation after cardiac arrest (van der Worp, Macleod et al. 2010) and following stroke (Campos, Blanco et al. 2012). A major phase III clinical trial of mild hypothermia to treat stroke patients by cooling the brain has recently been initiated (Watson 2012). Hypothermia is associated with a reduction in oxygen consumption and glucose (Campos, Blanco et al. 2012). Saitoh and Hinchey found a large pool of free, non-conjugated SUMO2/3 as well as induction of the conjugation of SUMO2/3 to high molecular mass proteins when cells were subjected to protein-damaging stimuli such as acute temperature fluctuation (Saitoh and Hinchey 2000). We show that neurons exposed to combined OGD induce SUMO2/3ylation of target proteins endogenously. By inhibiting this endogenous response to ischaemic stress using lentiviral expression of Sumo2/3 microRNAs, we could show that resistance to combined OGD is dramatically lost if SUMO2/3ylation fails. As reduction of the metabolic rate and therewith of oxygen and glucose consumption is the most pronounced consequence of hypothermia, we speculate that SUMO2/3 induction is needed in this context to compensate for the hypothermia-induced reduction of the metabolic rate and therewith protect neurons. Further enhancing this endogenous neuroprotective response could not only lead to better protection of the brain during stroke treatment, but also prolong the time window in which curative hypothermia can be applied. As rewarming of the patients after hyperthermia is a crucial step and carrys the danger of increasing intracranial pressure, bleedings and recurring

stroke, additional protection especially during this phase would be of great benefit. Enhancing of SUMOylation can be achieved through different strategies. Either SUMO conjugation itself can be influenced, leading to an increase in SUMOylation of target proteins, or, alternatively, SUMO2/3 can be enriched by inhibition of the deconjugating isopeptidase SENP7, 6 or 3. Maturation of SUMO precursors is mediated through SENPs. SENP7, however, is mainly involved in deconjugation rather than maturation of SUMO2/3 and is thus a potential candidate for small inhibitor screening and enhancement of target protein SUMO2/3ylation. We initiated and together with SANOFI are currently investigating the potential of this approach in a screen.

Although there are a number of neuroprotectants in preclinical development, the use of 'synthetic' compounds in a potentially 'unphysiological' way (e.g. N-methyl-D-aspartate (NMDA) – receptor antagonists, (Dirnagl and Meisel 2008) has raised criticism and requests targeting of endogenous neuroprotective mechanisms of the brain itself. To this end, more basic research is needed to understand the exact pathways and diverse interactions between key players involved in neuroprotection under ischaemic and metabolic stress. So far, drugs targeting only one key mechanism of cerebral ischaemia have failed to improve outcome in clinical trials. One plausible reason for this failure might be the multiplicity of mechanisms involved in causing neuronal damage following stroke. Therefore, a novel approach for the development of neuroprotective drugs includes the evaluation of compounds with a multimodal mode of action (Sutherland, Minnerup et al. 2012). The SUMOylation pathway could potentially represent such a mechanism, which in combination with other strategies such as for example hypothermia or reperfusion enhancement might serve as an efficient therapeutic strategy for fighting stroke. More than 10 years after the first recommendations of the Stroke Therapy Academic Industry Roundtable (STAIR) were published, the ultimate proof that plain standardization of procedures in fact increases the rate of successful translation from bench to bedside in stroke research is still missing. Some critics even raise the provocative question of whether excessive methodological uniformity counteracts innovation and only prevents promising drug candidates from entering into clinical trials and renowned scientific journals (Mourand, Escuret et al. 2012). To gain fundamental insights into stroke pathophysiology, and for development of novel therapeutic strategies, different

models should be applied to elucidate relevant and robust endogenous neuroprotective effects in different contexts, as done in this study.

6. Conclusions

The most significant findings of my Ph.D thesis are the following:

1) SUMO2/3ylation of target proteins is increased following neuronal ischaemic injury, while free SUMO2/3 levels decrease. This finding is in line with the hypothesis that SUMOylation is induced upon stress.

2) RNA interference directed against SUMO2/3 has no impact on neuronal survival over 12 days. Upon ischaemic stress, vulnerability of Sumo2/3 microRNA-transduced neurons is increased compared to control microRNA-transduced neurons. This finding underlines the hypothesis that SUMOylation is an endogenous neuroprotective stress-response in embryonic cortical neurons. Knockdown of SUMO2/3 exacerbates glutamate excitotoxicity in the retinal ganglion cell layer (RGC), which is an *in vitro* model of adult neurons. These results provide evidence that SUMO2/3 could also prove to be neuroprotective in adult tissues. Given the diversity of pathologies in which the SUMOylation pathway is involved, SUMO2/3 activators or inhibitors of Sentrin-specific proteases such as SENP7 could reveal themselves as potent neuroprotective drugs.

3) *In vivo* application of Sumo2/3 microRNA did not lead to any changes after MCAo compared to the control microRNA injected group due to technical challenges. Therefore, using the Recombinase-Mediated Cassette Exchange technique for targeted integration into the transcriptionally silent Rosa26-locus of the genome, two efficient, inducible and cell-type specific transgenic mouse models were generated with

    i) Sumo2/3 microRNA expression to investigate specific RNA interference and function of SUMOylation in different pathologies *in vivo*.

ii) Sumo2/3 microRNA-SUMO2/3$^{tm\#(silent\ mutation)}$-TAP for rescue of the RNA interference phenotype and additionally, to efficiently and specifically screen for target proteins of SUMO2/3ylation and the pathways involved.

Altogether, these results suggest that SUMO2/3ylation is an endogenously induced neuroprotective mechanism and appears as an attractive novel treatment strategy for reducing brain injury following cerebral ischaemia. Given the current dearth of effective treatments for stroke, SUMO2/3 together with small inhibitors of SENP7 should be evaluated for their potential use for clinical trials in stroke patients. Based on the findings from this study, we initiated a small-inhibitor screen and are currently investigating it together with SANOFI to study the potential clinical implications of the SUMO2/3ylation pathway.

7. References

Albrecht, J., W. Hilgier, et al. (2000). "Extracellular concentrations of taurine, glutamate, and aspartate in the cerebral cortex of rats at the asymptomatic stage of thioacetamide-induced hepatic failure: modulation by ketamine anesthesia." Neurochem Res 25(11): 1497-502.

Alkuraya, F. S., I. Saadi, et al. (2006). "SUMO1 haploinsufficiency leads to cleft lip and palate." Science 313(5794): 1751.

Baranova, O., L. F. Miranda, et al. (2007). "Neuron-specific inactivation of the hypoxia inducible factor 1 alpha increases brain injury in a mouse model of transient focal cerebral ischemia." J Neurosci 27(23): 6320-32.

Bederson, J. B., L. H. Pitts, et al. (1986). "Rat middle cerebral artery occlusion: evaluation of the model and development of a neurologic examination." Stroke 17(3): 472-6.

Berger, C., W. R. Schabitz, et al. (2002). "Effects of hypothermia on excitatory amino acids and metabolism in stroke patients: a microdialysis study." Stroke 33(2): 519-24.

Boddy, M. N., K. Howe, et al. (1996). "PIC 1, a novel ubiquitin-like protein which interacts with the PML component of a multiprotein complex that is disrupted in acute promyelocytic leukaemia." Oncogene 13(5): 971-82.

Branzei, D., J. Sollier, et al. (2006). "Ubc9- and mms21-mediated sumoylation counteracts recombinogenic events at damaged replication forks." Cell 127(3): 509-22.

Braschi, E., V. Goyon, et al. (2010). "Vps35 mediates vesicle transport between the mitochondria and peroxisomes." Curr Biol 20(14): 1310-5.

Brethour, M. K., K. V. Nystrom, et al. (2012). "Controversies in acute stroke treatment." AACN Adv Crit Care 23(2): 158-72; quiz 173-4.

Campos, F., M. Blanco, et al. (2012). "Influence of temperature on ischemic brain: basic and clinical principles." Neurochem Int 60(5): 495-505.

Carbia-Nagashima, A., J. Gerez, et al. (2007). "RSUME, a small RWD-containing protein, enhances SUMO conjugation and stabilizes HIF-1alpha during hypoxia." Cell 131(2): 309-23.

Carta, E., E. Pauws, et al. (2012). "Investigation of SUMO pathway genes in the etiology of nonsyndromic cleft lip with or without cleft palate." Birth Defects Res A Clin Mol Teratol 94(6): 459-63.

Chan, J. Y., C. Y. Tsai, et al. (2011). "Sumoylation of hypoxia-inducible factor-1alpha ameliorates failure of brain stem cardiovascular regulation in experimental brain death." PLoS One 6(3): e17375.

Chang, Y. C., W. C. Shyu, et al. (2007). "Regenerative therapy for stroke." Cell Transplant 16(2): 171-81.

Chao, X. D., F. Fei, et al. (2010). "The role of excitatory amino acid transporters in cerebral ischemia." Neurochem Res 35(8): 1224-30.

Cheng, J., X. Kang, et al. (2007). "SUMO-specific protease 1 is essential for stabilization of HIF1alpha during hypoxia." Cell 131(3): 584-95.

Childs, C., T. Wieloch, et al. (2010). "Report of a consensus meeting on human brain temperature after severe traumatic brain injury: its measurement and management during pyrexia." Front Neurol 1: 146.

Chiu, S. Y., N. Asai, et al. (2008). "SUMO-specific protease 2 is essential for modulating p53-Mdm2 in development of trophoblast stem cell niches and lineages." PLoS Biol 6(12): e310.

Chu, K., S. T. Lee, et al. (2007). "Pharmacological Induction of Ischemic Tolerance by Glutamate Transporter-1 (EAAT2) Upregulation." Stroke 38(1): 177-82.

Cimarosti, H., E. Ashikaga, et al. (2012). "Enhanced SUMOylation and SENP-1 protein levels following oxygen and glucose deprivation in neurones." J Cereb Blood Flow Metab 32(1): 17-22.

Cimarosti, H., C. Lindberg, et al. (2008). "Increased protein SUMOylation following focal cerebral ischemia." Neuropharmacology 54(2): 280-9.

Cremona, C. A., P. Sarangi, et al. (2012). "Extensive DNA damage-induced sumoylation contributes to replication and repair and acts in addition to the mec1 checkpoint." Mol Cell 45(3): 422-32.

Csoka, A. B. and M. Szyf (2009). "Epigenetic side-effects of common pharmaceuticals: a potential new field in medicine and pharmacology." Med Hypotheses 73(5): 770-80.

Datwyler, A. L., G. Lattig-Tunnemann, et al. (2011). "SUMO2/3 conjugation is an endogenous neuroprotective mechanism." J Cereb Blood Flow Metab 31(11): 2152-9.

de Assis, N. A., S. Nowak, et al. (2011). "SUMO1 as a candidate gene for non-syndromic cleft lip with or without cleft palate: no evidence for the involvement of common or rare variants in Central European patients." Int J Pediatr Otorhinolaryngol 75(1): 49-52.

Dietrich, W. D., C. M. Atkins, et al. (2009). "Protection in animal models of brain and spinal cord injury with mild to moderate hypothermia." J Neurotrauma 26(3): 301-12.

Dirnagl, U., C. Iadecola, et al. (1999). "Pathobiology of ischaemic stroke: an integrated view." Trends Neurosci 22(9): 391-7.

Dirnagl, U. and A. Meisel (2008). "Endogenous neuroprotection: mitochondria as gateways to cerebral preconditioning?" Neuropharmacology 55(3): 334-44.

Dittgen, T., A. Nimmerjahn, et al. (2004). "Lentivirus-based genetic manipulations of cortical neurons and their optical and electrophysiological monitoring in vivo." Proc Natl Acad Sci U S A 101(52): 18206-11.

Dou, H., C. Huang, et al. (2011). "SUMOylation and de-SUMOylation in response to DNA damage." FEBS Lett 585(18): 2891-6.

Dutting, E., N. Schroder-Kress, et al. "SUMO E3 ligases are expressed in the retina and regulate SUMOylation of the metabotropic glutamate receptor 8b." Biochem J 435(2): 365-71.

Endres, M., D. Biniszkiewicz, et al. (2004). "Increased postischemic brain injury in mice deficient in uracil-DNA glycosylase." J Clin Invest 113(12): 1711-21.

Endres, M., A. Meisel, et al. (2000). "DNA methyltransferase contributes to delayed ischemic brain injury." J Neurosci 20(9): 3175-81.

Engel, O., S. Kolodziej, et al. (2011). "Modeling stroke in mice - middle cerebral artery occlusion with the filament model." J Vis Exp(47).

Erecinska, M., M. Thoresen, et al. (2003). "Effects of hypothermia on energy metabolism in Mammalian central nervous system." J Cereb Blood Flow Metab 23(5): 513-30.

Feligioni, M., A. Nishimune, et al. (2009). "Protein SUMOylation modulates calcium influx and glutamate release from presynaptic terminals." Eur J Neurosci 29(7): 1348-56.

Fisher, M. (2011). "New approaches to neuroprotective drug development." Stroke 42(1 Suppl): S24-7.

Galanty, Y., R. Belotserkovskaya, et al. (2009). "Mammalian SUMO E3-ligases PIAS1 and PIAS4 promote responses to DNA double-strand breaks." Nature 462(7275): 935-9.

Gali, H., S. Juhasz, et al. (2012). "Role of SUMO modification of human PCNA at stalled replication fork." Nucleic Acids Res 40(13): 6049-59.

Garcia, J. H., Y. Yoshida, et al. (1993). "Progression from ischemic injury to infarct following middle cerebral artery occlusion in the rat." Am J Pathol 142(2): 623-35.

Gareau, J. R. and C. D. Lima (2010). "The SUMO pathway: emerging mechanisms that shape specificity, conjugation and recognition." Nat Rev Mol Cell Biol 11(12): 861-71.

Geiss-Friedlander, R. and F. Melchior (2007). "Concepts in sumoylation: a decade on." Nat Rev Mol Cell Biol 8(12): 947-56.

Gibb, S. L., W. Boston-Howes, et al. (2007). "A caspase-3-cleaved fragment of the glial glutamate transporter EAAT2 is sumoylated and targeted to promyelocytic leukemia nuclear bodies in mutant SOD1-linked amyotrophic lateral sclerosis." J Biol Chem 282(44): 32480-90.

Ginsberg, M. D. (2003). "Adventures in the pathophysiology of brain ischemia: penumbra, gene expression, neuroprotection: the 2002 Thomas Willis Lecture." Stroke 34(1): 214-23.

Giuditta, A., B. B. Kaplan, et al. (2002). "Axonal and presynaptic protein synthesis: new insights into the biology of the neuron." Trends Neurosci 25(8): 400-4.

Globus, M. Y., O. Alonso, et al. (1995). "Glutamate release and free radical production following brain injury: effects of posttraumatic hypothermia." J Neurochem 65(4): 1704-11.

Golebiowski, F., I. Matic, et al. (2009). "System-wide changes to SUMO modifications in response to heat shock." Sci Signal 2(72): ra24.

Gong, L., T. Kamitani, et al. (1997). "Preferential interaction of sentrin with a ubiquitin-conjugating enzyme, Ubc9." J Biol Chem 272(45): 28198-201.

Guo, D., M. Li, et al. (2004). "A functional variant of SUMO4, a new I kappa B alpha modifier, is associated with type 1 diabetes." Nat Genet 36(8): 837-41.

Hacke, W., M. Kaste, et al. (2008). "Thrombolysis with alteplase 3 to 4.5 hours after acute ischemic stroke." N Engl J Med 359(13): 1317-29.

Hardeland, U., R. Steinacher, et al. (2002). "Modification of the human thymine-DNA glycosylase by ubiquitin-like proteins facilitates enzymatic turnover." EMBO J 21(6): 1456-64.

Harms, C., K. Albrecht, et al. (2007). "Phosphatidylinositol 3-Akt-kinase-dependent phosphorylation of p21(Waf1/Cip1) as a novel mechanism of neuroprotection by glucocorticoids." J Neurosci 27(17): 4562-71.

Harms, C., M. Lautenschlager, et al. (2001). "Differential mechanisms of neuroprotection by 17 beta-estradiol in apoptotic versus necrotic neurodegeneration." J Neurosci 21(8): 2600-9.

Hay, R. T. (2005). "SUMO: a history of modification." Mol Cell 18(1): 1-12.

Heiss, W. D., L. W. Kracht, et al. (2001). "Penumbral probability thresholds of cortical flumazenil binding and blood flow predicting tissue outcome in patients with cerebral ischaemia." Brain 124(Pt 1): 20-9.

Hitz, C., W. Wurst, et al. (2007). "Conditional brain-specific knockdown of MAPK using Cre/loxP regulated RNA interference." Nucleic Acids Res 35(12): e90.

Hoffmann, A., G. Zhu, et al. (2012). "Advanced neuroimaging in stroke patients: prediction of tissue fate and hemorrhagic transformation." Expert Rev Cardiovasc Ther 10(4): 515-24.

Hossmann, K. A. (1993). "Ischemia-mediated neuronal injury." Resuscitation 26(3): 225-35.

Hossmann, K. A. (1994). "Viability thresholds and the penumbra of focal ischemia." Ann Neurol 36(4): 557-65.

Hossmann, K. A. (2009). "Pathophysiological basis of translational stroke research." Folia Neuropathol 47(3): 213-27.

Hudgins, W. R. and J. H. Garcia (1970). "Transorbital approach to the middle cerebral artery of the squirrel monkey: a technique for experimental cerebral infarction applicable to ultrastructural studies." Stroke 1(2): 107-11.

Hudson, J. J., S. C. Chiang, et al. (2012). "SUMO modification of the neuroprotective protein TDP1 facilitates chromosomal single-strand break repair." Nat Commun 3: 733.

Hwang, K. W., T. J. Won, et al. (2012). "Erratum to ''Characterization of the regulatory roles of the SUMO." Diabetes Metab Res Rev 28(2): 196-202.

Kang, X., Y. Qi, et al. (2010). "SUMO-specific protease 2 is essential for suppression of polycomb group protein-mediated gene silencing during embryonic development." Mol Cell 38(2): 191-201.

Kano, M., H. Igarashi, et al. (1998). "Cre-loxP-mediated DNA flip-flop in mammalian cells leading to alternate expression of retrovirally transduced genes." Biochem Biophys Res Commun 248(3): 806-11.

Karaszewski, B., J. M. Wardlaw, et al. (2009). "Early brain temperature elevation and anaerobic metabolism in human acute ischaemic stroke." Brain 132(Pt 4): 955-64.

Kim, E. Y., L. Chen, et al. (2012). "Enhanced desumoylation in murine hearts by overexpressed SENP2 leads to congenital heart defects and cardiac dysfunction." J Mol Cell Cardiol 52(3): 638-49.

Kim, H. J., J. Yun, et al. (2011). "SUMO1 attenuates stress-induced ROS generation by inhibiting NADPH oxidase 2." Biochem Biophys Res Commun 410(3): 555-62.

Kronenberg, G., K. Gertz, et al. (2011). "Folate deficiency increases mtDNA and D-1 mtDNA deletion in aged brain of mice lacking uracil-DNA glycosylase." Exp Neurol 228(2): 253-8.

Lapenta, V., P. Chiurazzi, et al. (1997). "SMT3A, a human homologue of the S. cerevisiae SMT3 gene, maps to chromosome 21qter and defines a novel gene family." Genomics 40(2): 362-6.

Lee, K. A., R. A. Roth, et al. (2007). "Hypoxia, drug therapy and toxicity." Pharmacol Ther 113(2): 229-46.

Lee, Y. J., P. Castri, et al. (2009). "SUMOylation participates in induction of ischemic tolerance." J Neurochem 109(1): 257-67.

Lee, Y. J., S. Miyake, et al. (2007). "Protein SUMOylation is massively increased in hibernation torpor and is critical for the cytoprotection provided by ischemic preconditioning and hypothermia in SHSY5Y cells." J Cereb Blood Flow Metab 27(5): 950-62.

Lee, Y. J., Y. Mou, et al. (2011). "Elevated global SUMOylation in Ubc9 transgenic mice protects their brains against focal cerebral ischemic damage." PLoS One 6(10): e25852.

Ma, K. W., S. W. Au, et al. (2009). "Over-expression of SUMO-1 induces the up-regulation of heterogeneous nuclear ribonucleoprotein A2/B1 isoform B1 (hnRNP A2/B1 isoform B1) and uracil DNA glycosylase (UDG) in hepG2 cells." Cell Biochem Funct 27(4): 228-37.

Mahajan, R., C. Delphin, et al. (1997). "A small ubiquitin-related polypeptide involved in targeting RanGAP1 to nuclear pore complex protein RanBP2." Cell 88(1): 97-107.

Martin, L. J., A. M. Brambrink, et al. (1997). "Hypoxia-ischemia causes abnormalities in glutamate transporters and death of astroglia and neurons in newborn striatum." Ann Neurol 42(3): 335-48.

Martin, S., A. Nishimune, et al. (2007). "SUMOylation regulates kainate-receptor-mediated synaptic transmission." Nature 447(7142): 321-5.
Martin, S., K. A. Wilkinson, et al. (2007). "Emerging extranuclear roles of protein SUMOylation in neuronal function and dysfunction." Nat Rev Neurosci 8(12): 948-59.
Matunis, M. J., E. Coutavas, et al. (1996). "A novel ubiquitin-like modification modulates the partitioning of the Ran-GTPase-activating protein RanGAP1 between the cytosol and the nuclear pore complex." J Cell Biol 135(6 Pt 1): 1457-70.
McGee-Russell, S. M., A. W. Brown, et al. (1970). "A combined light and electron microscope study of early anoxic-ischaemic cell change in rat brain." Brain Res 20(2): 193-200.
Mehler, M. F. (2008). "Epigenetic principles and mechanisms underlying nervous system functions in health and disease." Prog Neurobiol 86(4): 305-41.
Mehta, S. L., N. Manhas, et al. (2007). "Molecular targets in cerebral ischemia for developing novel therapeutics." Brain Res Rev 54(1): 34-66.
Mennerick, S., R. P. Dhond, et al. (1998). "Neuronal expression of the glutamate transporter GLT-1 in hippocampal microcultures." J Neurosci 18(12): 4490-9.
Merrett, D. L., S. W. Kirkland, et al. (2010). "Synergistic effects of age and stress in a rodent model of stroke." Behav Brain Res 214(1): 55-9.
Messe, S. R., G. C. Fonarow, et al. (2012). "Use of tissue-type plasminogen activator before and after publication of the European Cooperative Acute Stroke Study III in Get With The Guidelines-Stroke." Circ Cardiovasc Qual Outcomes 5(3): 321-6.
Meulmeester, E. and F. Melchior (2008). "Cell biology: SUMO." Nature 452(7188): 709-11.
Minnerup, J. and W. R. Schabitz (2009). "Multifunctional actions of approved and candidate stroke drugs." Neurotherapeutics 6(1): 43-52.
Morris, J. R., C. Boutell, et al. (2009). "The SUMO modification pathway is involved in the BRCA1 response to genotoxic stress." Nature 462(7275): 886-90.
Mourand, I., E. Escuret, et al. (2012). "Feasibility of hypothermia beyond 3 weeks in severe ischemic stroke: an open pilot study using gamma-hydroxybutyrate." J Neurol Sci 316(1-2): 104-7.
NINS (1995). "Tissue plasminogen activator for acute ischemic stroke. The National Institute of Neurological Disorders and Stroke rt-PA Stroke Study Group." N Engl J Med 333(24): 1581-7.
Pandey, D., F. Chen, et al. (2011). "SUMO1 negatively regulates reactive oxygen species production from NADPH oxidases." Arterioscler Thromb Vasc Biol 31(7): 1634-42.
Polderman, K. H. and I. Herold (2009). "Therapeutic hypothermia and controlled normothermia in the intensive care unit: practical considerations, side effects, and cooling methods." Crit Care Med 37(3): 1101-20.
Prinz, V., U. Laufs, et al. (2008). "Intravenous rosuvastatin for acute stroke treatment: an animal study." Stroke 39(2): 433-8.
Qureshi, I. A. and M. F. Mehler (2010). "Emerging role of epigenetics in stroke: part 1: DNA methylation and chromatin modifications." Arch Neurol 67(11): 1316-22.
Rao, V. L., K. K. Bowen, et al. (2001). "Transient focal cerebral ischemia down-regulates glutamate transporters GLT-1 and EAAC1 expression in rat brain." Neurochem Res 26(5): 497-502.
Reich, A., C. Spering, et al. (2011). "Fas/CD95 regulatory protein Faim2 is neuroprotective after transient brain ischemia." J Neurosci 31(1): 225-33.
Rodriguez, M. S., C. Dargemont, et al. (2001). "SUMO-1 conjugation in vivo requires both a consensus modification motif and nuclear targeting." J Biol Chem 276(16): 12654-9.

Rzeczinski, S., I. V. Victorov, et al. (2006). "Roller culture of free-floating retinal slices: a new system of organotypic cultures of adult rat retina." Ophthalmic Res 38(5): 263-9.

Saitoh, H. and J. Hinchey (2000). "Functional heterogeneity of small ubiquitin-related protein modifiers SUMO-1 versus SUMO-2/3." J Biol Chem 275(9): 6252-8.

Saitoh, H., R. T. Pu, et al. (1997). "SUMO-1: wrestling with a new ubiquitin-related modifier." Trends Biochem Sci 22(10): 374-6.

Sampson, D. A., M. Wang, et al. (2001). "The small ubiquitin-like modifier-1 (SUMO-1) consensus sequence mediates Ubc9 binding and is essential for SUMO-1 modification." J Biol Chem 276(24): 21664-9.

Schmitt, A., E. Asan, et al. (2002). "A splice variant of glutamate transporter GLT1/EAAT2 expressed in neurons: cloning and localization in rat nervous system." Neuroscience 109(1): 45-61.

Shalizi, A., B. Gaudilliere, et al. (2006). "A calcium-regulated MEF2 sumoylation switch controls postsynaptic differentiation." Science 311(5763): 1012-7.

Shao, R., F. P. Zhang, et al. (2004). "Increase of SUMO-1 expression in response to hypoxia: direct interaction with HIF-1alpha in adult mouse brain and heart in vivo." FEBS Lett 569(1-3): 293-300.

Shen, Z., P. E. Pardington-Purtymun, et al. (1996). "UBL1, a human ubiquitin-like protein associating with human RAD51/RAD52 proteins." Genomics 36(2): 271-9.

Steinacher, R. and P. Schar (2005). "Functionality of human thymine DNA glycosylase requires SUMO-regulated changes in protein conformation." Curr Biol 15(7): 616-23.

Sundt, T. M., Jr. and A. G. Waltz (1966). "Experimental cerebral infarction: retro-orbital, extradural approach for occluding the middle cerebral artery." Mayo Clin Proc 41(3): 159-68.

Sutherland, B. A., J. Minnerup, et al. (2012). "Neuroprotection for ischaemic stroke: Translation from the bench to the bedside." Int J Stroke 7(5): 407-18.

Svilar, D., E. M. Goellner, et al. (2011). "Base excision repair and lesion-dependent subpathways for repair of oxidative DNA damage." Antioxid Redox Signal 14(12): 2491-507.

Szyf, M. (2009). "Epigenetics, DNA methylation, and chromatin modifying drugs." Annu Rev Pharmacol Toxicol 49: 243-63.

Tamura, A., D. I. Graham, et al. (1981). "Focal cerebral ischaemia in the rat: 1. Description of technique and early neuropathological consequences following middle cerebral artery occlusion." J Cereb Blood Flow Metab 1(1): 53-60.

Tang, X. N. and M. A. Yenari (2010). "Hypothermia as a cytoprotective strategy in ischemic tissue injury." Ageing Res Rev 9(1): 61-8.

Tatham, M. H., E. Jaffray, et al. (2001). "Polymeric chains of SUMO-2 and SUMO-3 are conjugated to protein substrates by SAE1/SAE2 and Ubc9." J Biol Chem 276(38): 35368-74.

Tong, D., M. J. Reeves, et al. (2012). "Times from symptom onset to hospital arrival in the get with the guidelines-stroke program 2002 to 2009: temporal trends and implications." Stroke 43(7): 1912-7.

Ulrich, H. D. (2012). "Ubiquitin and SUMO in DNA repair at a glance." J Cell Sci 125(Pt 2): 249-54.

van der Worp, H. B., M. R. Macleod, et al. (2010). "Therapeutic hypothermia for acute ischemic stroke: ready to start large randomized trials?" J Cereb Blood Flow Metab 30(6): 1079-93.

van der Worp, H. B., E. S. Sena, et al. (2007). "Hypothermia in animal models of acute ischaemic stroke: a systematic review and meta-analysis." Brain 130(Pt 12): 3063-74.
van Niekerk, E. A., D. E. Willis, et al. (2007). "Sumoylation in axons triggers retrograde transport of the RNA-binding protein La." Proc Natl Acad Sci U S A 104(31): 12913-8.
Vangilder, R. L., J. D. Huber, et al. (2012). "The transcriptome of cerebral ischemia." Brain Res Bull 88(4): 313-9.
Vertegaal, A. C., S. C. Ogg, et al. (2004). "A proteomic study of SUMO-2 target proteins." J Biol Chem 279(32): 33791-8.
Wahlgren, N., N. Ahmed, et al. (2008). "Thrombolysis with alteplase 3-4.5 h after acute ischaemic stroke (SITS-ISTR): an observational study." Lancet 372(9646): 1303-9.
Wang, C. X., A. Stroink, et al. (2009). "Hyperthermia exacerbates ischaemic brain injury." Int J Stroke 4(4): 274-84.
Wang, J., L. Chen, et al. (2011). "Defective sumoylation pathway directs congenital heart disease." Birth Defects Res A Clin Mol Teratol 91(6): 468-76.
Watson, R. (2012). "European research is launched into hypothermia stroke treatment." BMJ 344: e2215.
White, M. G., L. E. Luca, et al. (2007). "Cellular mechanisms of neuronal damage from hyperthermia." Prog Brain Res 162: 347-71.
Wick, A., W. Wick, et al. (2002). "Neuroprotection by hypoxic preconditioning requires sequential activation of vascular endothelial growth factor receptor and Akt." J Neurosci 22(15): 6401-7.
Wilkinson, K. A., Y. Nakamura, et al. (2010). "Targets and consequences of protein SUMOylation in neurons." Brain Res Rev 64(1): 195-212.
Xiang, Y. Y., H. Dong, et al. (2006). "Versican G3 domain regulates neurite growth and synaptic transmission of hippocampal neurons by activation of epidermal growth factor receptor." J Biol Chem 281(28): 19358-68.
Yan, J., B. Zhou, et al. (2011). "Differential effects of HIF-1 inhibition by YC-1 on the overall outcome and blood-brain barrier damage in a rat model of ischemic stroke." PLoS One 6(11): e27798.
Yan, Q., L. Gong, et al. (2010). "Sumoylation activates the transcriptional activity of Pax-6, an important transcription factor for eye and brain development." Proc Natl Acad Sci U S A 107(49): 21034-9.
Yang, W., Q. Ma, et al. (2009). "Deep hypothermia markedly activates the small ubiquitin-like modifier conjugation pathway; implications for the fate of cells exposed to transient deep hypothermic cardiopulmonary bypass." J Cereb Blood Flow Metab 29(5): 886-90.
Yang, W. and W. Paschen (2009). "Gene expression and cell growth are modified by silencing SUMO2 and SUMO3 expression." Biochem Biophys Res Commun 382(1): 215-8.
Yang, W., H. Sheng, et al. (2008). "Transient focal cerebral ischemia induces a dramatic activation of small ubiquitin-like modifier conjugation." J Cereb Blood Flow Metab 28(5): 892-6.
Yang, W., H. Sheng, et al. (2008). "Transient global cerebral ischemia induces a massive increase in protein sumoylation." J Cereb Blood Flow Metab 28(2): 269-79.
Yang, W., J. W. Thompson, et al. (2011). "Analysis of oxygen/glucose-deprivation-induced changes in SUMO3 conjugation using SILAC-based quantitative proteomics." J Proteome Res 11(2): 1108-17.
Yenari, M., K. Kitagawa, et al. (2008). "Metabolic downregulation: a key to successful neuroprotection?" Stroke 39(10): 2910-7.

Yildirim, F., K. Gertz, et al. (2008). "Inhibition of histone deacetylation protects wildtype but not gelsolin-deficient mice from ischemic brain injury." Exp Neurol 210(2): 531-42.
Yilmaz, G., J. S. Alexander, et al. (2010). "Induction of neuro-protective/regenerative genes in stem cells infiltrating post-ischemic brain tissue." Exp Transl Stroke Med 2(1): 11.
Yilmaz, U. and W. Reith (2012). "[Treatment of acute ischemic stroke]." Radiologe 52(4): 375-83; quiz 384-5.
Zhang, F. P., L. Mikkonen, et al. (2008). "Sumo-1 function is dispensable in normal mouse development." Mol Cell Biol 28(17): 5381-90.
Zhao, T. C., G. Cheng, et al. (2007). "Inhibition of histone deacetylases triggers pharmacologic preconditioning effects against myocardial ischemic injury." Cardiovasc Res 76(3): 473-81.
Zunino, R., A. Schauss, et al. (2007). "The SUMO protease SENP5 is required to maintain mitochondrial morphology and function." J Cell Sci 120(Pt 7): 1178-88.

8. Publications and presentations

8.1 Publications

SUMO2/3 conjugation is an endogenous neuroprotective mechanism.

Dätwyler Anna Lena, Lättig-Tünnemann G**,** Yang W**,** Paschen W**,** Lee SL**,** Dirnagl U**,** Endres M**,** Harms C.

J Cereb Blood Flow Metab. 2011 Nov;31(11):2152-9. doi: 10.1038/jcbfm.2011.112.

Epub 2011 Aug 24.

Certain types of iron oxide nanoparticles are not suited to passively target inflammatory cells that infiltrate the brain in response to stroke.

Dätwyler Anna Lena*, Harms C*, Lindquist R, Schellenberger E, Mueller S, Schütz G, Roohi F, Ide A, Harms U, Endres M, Dirnagl U, Farr T.

*Equally contributing

In revision

Apoptosis repressor with CARD domain interacts with DAXX: a novel therapeutic approach in focal cerebral ischemia in mice.

Donath Stefan*, An Junfeng*, Lee Sabrina Lin Lin, Gertz Karen, **Dätwyler Anna Lena**, Harms Ulrike, Müller Susanne, Lättig-Tünnemann Gisela, Balkaya Mustafa, Kronenberg Golo, Endres Matthias*, Harms Christoph*

*Equally contributing

Pre submission

8. 2 Presentations

The roles of Uracil-DNA gylcosylase 1 and 2 in endogenous neuroprotection and DNA repair

Dätwyler Anna Lena, Hoffmann C, Endres M., and Harms C

Poster presentation at Berlin Brain Days 2011, Berlin, Germany

Monitoring of glioma invasion and inflammation in vivo using combined multimodal near infrared and magnetic resonance imaging

Dätwyler Anna Lena, Harms U, Müller S, Akyüz L, Meisel C, Lindquist R, Piper S, Klohs J, Steinbrink J, Schellenberger E, Czabanka A, Dirnagl U, Taupitz M, Endres M, Harms C

Poster presentation at Society of Neuroscience Meeting 2011, Washington DC, USA

SUMOylation in neurons – strategies to cope with stress

Dätwyler Anna Lena, Lättig G, Yang W, Paschen W, Dirnagl U, Endres M, Harms C

Poster presentation at Brain Conference 2011, Barcelona, Spain

Monitoring of glioma invasion and inflammation in vivo using combined multimodal near infrared and magnetic resonance imaging

Dätwyler, Anna Lena, Harms U, Müller S, Akyüz L, Meisel C, Lindquist R, Piper S, Klohs J, Steinbrink J, Schellenberger E, Czabanka M, Bayerl S, Vajkoczy P, Wunder A, Dirnagl U, Taupitz M, Endres M, Harms C

Poster presentation at Brain tumor meeting 2011, Berlin, Germany

Elucidating the function of SUMO2/3 in neurons after ischemic stress

Dätwyler Anna Lena, Lättig G, Kunz A, Yang W, Paschen W, Dirnagl U, Endres M, and Harms C

Poster presentation at Berlin Brain days 2010, Berlin, Germany

Impact of apoptosis repressor with caspase recruitment domain (ARC) protein delivery on stroke outcome

Lee SLL, Lättig G, Gertz K, Kronenberg G, Harms U, Balkaya M, **A. L. Dätwyler**, J. An, S. Donath, M. Endres, C. Harms

Poster presentation at Society of Neuroscience Meeting 2010, San Diego, USA

Generation of two transgenic mouse models for the identification of neuronal SUMOylation targets after stroke

Anna Lena Dätwyler, G. Michel, G. Lättig, U. Dirnagl, W. Paschen, M. Endres, and C. Harms

Poster presentation at Berlin Brain days 2009, Berlin, Germany

E2F4-dependent target genes determine neuronal damage after focal cerebral ischemia

D. Huebner, R. Kanski, **Anna Lena Dätwyler**, S. L. L. Lee, K. Gertz, U. P. Lindauer, M. Endres, C. Harms

Poster presentation at Society of Neuroscience Meeting 2009, Chicago, USA

9. Further projects

Mitochondrial Uracil-DNA glycosylase1 but not nuclear Uracil-DNA glycosylase2 is endogenously neuroprotective in combined oxygen-glucose deprivation.

Datwyler AL, Hoffmann CJ, Kronenberg G, Sobol RW, Endres M, Harms C.

Challenges towards imaging blood borne macrophage infiltration into ischaemic tissue.

Harms C *, **Datwyler AL***, Lindquist R, Schellenberger E, Mueller S, Dirnagl U, Farr T

***Equally contributing**

Monitoring of glioma invasion and inflammation in vivo using combined multimodal near infrared and magnetic resonance imaging

Datwyler AL*, Harms U*, U.; Müller, S.; Akyüz, L.; Meisel, C.; Lindquist, R.; Piper, S.; Klohs, J.; Steinbrink, J.; Schellenberger, E.; Czabanka, A.; Dirnagl, U.; Taupitz, M.; Endres, M.,Harms, C.

***Equally contributing**

Modulation of angiogenesis and neuroprotection by erythropoietin in the ganglion cell layer of long-term organotypic cultures of adult rat retina

Thein E, Freyer D, **Datwyler AL**, Kronenberg G, Endres M, Dirnagl U, Harms C.

Neuronal de novo Orc1 transcription contributes to cell death without aberrant cell cycle re-entry after ischemia

Denise Hübner, Christian hoffmann, **Anna Lena Datwyler**, Regina Kanski, Karen Gertz, Golo Kronenberg, Gisela Lattig-Tunnemann, Bert Maier, Ulrike Harms, Manfred Gossen Ulrich Dirnagl, Matthias Endres, Christoph Harms

Simvastatin protects against glutamate toxicity in adult rat organotypic retinal cultures

Thein E, Freyer D, Rosenstein S, **Datwyler AL**, Kronenberg G, Przesdzing I, Dirnagl U, Endres M**,** Harms C

10. Curriculum vitae

Mein Lebenslauf wird aus datenschutzrechtlichen Gründen in der elektronischen Version meiner Arbeit nicht veröffentlicht.

11. Eidesstaatliche Erklärung

Ich, Anna Lena Dätwyler, erkläre, dass ich die vorgelegte Dissertation mit dem Thema: `SUMOylation is an endogenous neuroprotective mechanism in stroke´ selbst verfasst und keine anderen als die angegebenen Quellen und Hilfsmittel benutzt, ohne die (unzulässige) Hilfe Dritter verfasst und auch in Teilen keine Kopien anderer Arbeiten dargestellt habe.

Berlin, den 6. August 2012

Anna Lena Dätwyler